UNIVERSITY OF CALIFORNIA, SAN DIEGO

Significance of microscale interactions in bacterial ecology and carbon biogeochemistry in the ocean

A Dissertation submitted in partial satisfaction of the

requirements for the degree Doctor of Philosophy

in

Marine Biology

by

Francesca Malfatti

Committee in charge:

Professor Farooq Azam, Chair
Professor Lihini I. Aluwihare
Professor Douglas H. Bartlett
Professor Peter J. S. Franks
Professor Milton H. Saier

2009

The Dissertation of Francesca Malfatti is approved, and it is acceptable in quality and form for publication on microfilm

---

Chair

University of California, San Diego

2009

DEDICATION

To my family always present and to Andrea at my side.

EPIGRAPH

Cogito ergo sum.

René Descartes, Principles of Philosophy (1644), Part 1, article 7

Alea iacta est.

Gaius Suetonius Tranquillus reporting Julius Ceasar'words (49 BC)

TABLE OF CONTENTS

LIST OF FIGURES

LIST OF TABLES

ACKNOWLEDGEMENTS

I would like to sincerely and deeply thank my PhD advisor Farooq Azam.

Farooq has put his care, energy, time, patience, and dedication in shaping me as a scientist. He has always trusted me and my "hidden potentials". He has allowed me to harvest science and knowledge in many different projects around the world. He helped me become who I am now (hopefully with the less possible "lost in translation" mistakes).

I would like to thank my committee, Douglas Bartlett, Lihini Aluwihare, Peter Franks and Milton Saier for their support and critical advice in my student career.

Thanks to the Azam lab present and past: Ty Samo, Steve Smriga, Byron Pedler, Xavier Mayali, Krystal Ripien, Jessica Ward, Johnny Nguyen, Melissa Garren and Anne-Claire Baudoux. The Azam lab has been for me a great training school, a family and a place to cheer together. Melissa Garren, Anne-Claire Baudoux, Patricia Lucas-Elio, Huda Mahmoud, Hoang Nhan, Ty Samo, Steve Smriga, Byron Pedler, Stacy Kaltenbach, Wendy Strangman, Molly Ewen, ChuiWei Bong, Jasodhara Ray, Maura Manganelli, Emiley Eloe and Karen Osborn are irreplaceable persons of my human SIO life.

MB-division Business Staff and SIO Graduate Office have helped me constantly and allowed me to focus on the research making my bureaucratic life easier.

My USA and International friends have shared their energy and joy with me.

My parents Edda and Ferruccio have constantly supplied their love to me and they have done everything for me.

I would like to thank my partner Andrea for his love and care. He dedicated a lot of

his time and energy in supporting the exploration of myself and helping me in becoming a joyful and more balanced human being.

I would like to thank Maura Manganelli, Haili Wang, Greg Mitchell, Ty Samo and Farooq Azam for the great opportunity to collaborate with them. These tight and intense interactions have resulted in three research papers all of them submitted for publication; they are included in this dissertation.

The text in Chapter II, in full, is a reprint of the material, as it appears in 'Nature Review of Microbiology' 5 (10): 782-791: Azam, F., Malfatti, F. (2007). Microbial structuring of marine ecosystems.

The text in Chapter III has been submitted to Plos One: Manganelli, M.*, Malfatti, F.*, Samo, T.J., Mitchell, B.G., Wang, H., Azam, F. - Major role of microbes in carbon fluxes during the austral winter in the southern Drake Passage. * These authors contributed equally to the paper. Submitted to Plos One.

The text in Chapter IV had been submitted to ISME Journal: Malfatti, F., Samo, T.J., Azam, F., - Ecological and biogeochemical considerations of in situ morphology and biovolume of marine bacteria studied by Atomic Force Microscopy.

The text in Chapter V has been submitted to Aquatic Microbial Ecology: Malfatti, F., Azam, F. - Atomic Force Microscopy reveals microscale networks and apparent symbioses among pelagic marine bacteria.

This work was funded by National Science Foundation and Gordon and Betty Moore Foundation to Professor Farooq Azam.

VITA

Born in Trieste Italy

1999 B. A. (Biology), University of Trieste, Italy

2000-2002 Research Technician at the Marine Biology Laboratory, Trieste Italy (renamed as: OGS, Biology Section)

2009 Ph.D., University of California San Diego

PUBLICATIONS

Zutic, Z., Svetlicic, V., Radic, T., Malfatti, F., Degobbis, D., Azam, F. (2004). Controlled ecosystem carbon flow experiment in the northern Adriatic Sea. Periodicum Biologorum. 106:1-6

Worden, A.Z., Seidel, M., Smriga, S., Wick, A., Malfatti, F., Bartlett, D., Azam, F. (2006). Trophic regulation of *Vibrio cholerae* in coastal marine waters. Environ. Microbiol. 8:21-29

Azam, F., Malfatti, F. (2007). Microbial structuring of marine ecosystems. Nat. Rev. Microbiol. 5: 782-791

Samo, T.J., Malfatti, F., Azam, F. (2008). A new class of transparent organic particles in seawater visualized by a novel fluorescence approach. Aquatic Microbial Ecol. 53: 307-321

Submitted publications:

Manganelli, M.*, Malfatti, F.*, Samo, T.J., Mitchell, B.G., Wang, H., Azam, F. - Major role of microbes in carbon fluxes during the austral winter in the southern Drake Passage. * These authors contributed equally to the paper. Submitted to Plos One.

Malfatti, F., Samo, T.J., Azam, F., - Ecological and biogeochemical considerations of in situ morphology and biovolume of marine bacteria studied by Atomic Force Microscopy. Submitted to ISME Journal.

Malfatti, F., Azam, F. - Atomic Force Microscopy reveals microscale networks and apparent symbioses among pelagic marine bacteria. Submitted to Aquatic Microbial Ecology.

ABSTRACT OF THE DISSERTATION

Significance of microscale interactions in bacterial ecology and carbon biogeochemistry in the ocean

by

Francesca Malfatti

Doctor of Philosophy in Marine Biology

University of California, San Diego 2009

Professor Farooq Azam, Chair

Marine bacteria are important players in regulating the pelagic ecosystem structure and functioning and in biogeochemical cycles of carbon, nitrogen, phosphorus and other bio-elements in the ocean. Although a major role of bacteria in ecosystem function and carbon cycle is well established we still know little about the underlying *in situ* mechanisms. A fundamental problem concerns the nature and the strength of

coupling between bacteria and organic matter. Individual bacteria in seawater must exert their actions on organic matter—mostly polymeric and particulate--at the microscale, e.g. with cell-surface associated hydrolytic enzymes, to create hotspots of growth substrates. Microscale microbial ecology in the pelagic ocean is currently little explored.

The general premise of this research is that microscale imaging of *in situ* interactions, along with ecosystem-level studies of bacteria-mediated carbon cycling, will help constrain hypotheses on the underlying mechanisms and their biogeochemical consequences. Atomic Force Microscopy, epifluorescence microscopy, radiotracers approaches and molecular techniques were used to generate an integrated basis to answer specific questions on nanoscale to microscale ecology of marine bacteria and their implications for ocean-basin-scale-carbon biogeochemistry.

Field studies during the summer and winter in the Southern Ocean indicated that the degree of coupling between phytoplankton production and bacteria carbon demand is critically important for ecosystem functioning during the long austral winter when primary production is negligible. We discovered that in the austral winter, in the Drake Passage, a significant amount of dissolved organic carbon produced during the summer supports an active microbial loop with important consequences for ecosystem functioning, carbon cycling and climate.

Atomic Force Microscopy combined with Epifluorescence Microscopy enabled us to discover bacteria-bacteria and bacteria-*Synechococcus* associations—putative symbioses-- in the pelagic ocean. This has implications for primary productivity and nutrient cycling. Further, at the nanometer to micrometer scale a substantial fraction of

bacteria generally considered free-living were interconnected within organic matrixes forming bacterial networks suggesting potential for concerted metabolisms and biogeochemical activities as well as a role in marine aggregation. Finally, imaging of live pelagic bacteria by Atomic Force Microscopy provided insights on cell volumes based on measured height unbiased by fixation and drying. The new measurements provide a more reliable basis for quantifying bacteria-mediated carbon fluxes and the role of bacteria in pelagic marine ecosystems.

I

Introduction

I

Introduction

Our perception of the role of bacteria in the ocean has drastically changed in the last three decades, with the development of the notion that bacteria are important players in the ocean's biogeochemical cycles and pelagic foodweb (reviewed in: Azam and Malfatti, 2007). Microbes are highly abundant and comprise an enormous biodiversity. They generally dominate the oceanic biomass and metabolic activity. Typically, one milliliter of seawater contains 10^{6} heterotrophic bacteria, 10^{7} viruses, $10^{3\text{-}4}$ protozoa, $10^{2\text{-}3}$ algal cells (in coastal, non-bloom water) and 1/10 of a zooplankton (Azam and Malfatti, 2007). Heterotrophic microbes channel ~ 50% of primary production (Fuhrman and Azam, 1982) into the microbial loop *via* dissolved organic matter. Since primary production consists mainly of polymers and particles, it is of interest to ask: how do the obligate osmotrophic heterotrophic bacteria (and Archaea) compete so well with particle eating animals to dominate the fate of the fixed carbon (Azam et al., 1995)? And how do they play such broad roles in the ocean ecosystems? These questions require studies that address not only the players and the rates of processes they mediate but also the mechanisms they use for their ecosystem functions.

Until 1977 the ecosystem role of bacteria in the ocean was considered negligible. This was reflected in models of ecosystem function, fisheries and pollutant transfer. The

development of a method of counting bacteria by epifluorescence microscopy (Hobbie, 1977) and methods for bacterial production (Hagstrom et al., 1979; Fuhrman and Azam, 1980) greatly changed this view by showing that heterotrophic bacteria were a major biomass and carbon pool and were responsible for a large fraction of the pelagic metabolism. They were estimated to use ~1/2 but a highly variable fraction of carbon fixed into organic matter by the primary producers.

Because of the recognition of the large role of bacteria in the ocean's ecosystems and carbon cycle there has been great interest in microbial oceanography. During the last 20 years there have been amazing discoveries of the genetic diversity and potential for functional diversity of bacteria and Archaea and their roles in marine ecosystems. Particularly exciting discoveries have been made through the use of molecular, genomic and metagenomic approaches. For instance, archaea were discovered as highly abundant microbes throughout the world ocean and especially at depth (Fuhrman et al., 1992; DeLong, 1992). Complete genome sequencing of >100 marine isolates of bacteria as well as ocean metagenomics (Venter et al., 2004, Yooseph et al., 2007) have revolutionized microbial oceanography.

All the above discoveries have been very exciting also because they are being used to ask whether they can help us to answer questions of the lives of bacteria *in the sea*. However, despite the developing knowledge and advances in microbial oceanography the main stream of research is not considering the system scale at which bacteria interact with the organic matter, namely the micrometer scale of the seawater. What mechanisms

underlie the biogeochemical activities of bacteria? There is a fundamental need to integrate microscale structure of organic matter field and bacteria metabolism at the microscale in order to understand how bacteria mediate biogeochemical changes in the ocean. So, although genomics can tell us many important aspects and provide many clues regarding *in situ* functions of bacteria understanding the ecology of bacteria also requires direct analysis of the ocean organic matter at the scale where bacteria interact with it.

This is a very complex and exciting problem. The study of bacterial interactions with the organic matter requires that we understand the interactions of many co-existing taxa that are using an *extremely complex* organic matter pool, most (>90%) of which is 100s to 1000s of years old (Williams and Druffel, 1987; Bauer et al., 1992). The remaining <10% is the usable. While directly usable substrates such amino acids and sugars are present and their fluxes are fast (10-100 hours turnover times) most of the dissolved organic matter (DOM) pool composed of a great diversity of types of molecules, polymers and colloids. Phytoplankton and autotrophic bacteria are main producers of organic matter in the ocean, and are sources of DOM. The various mechanisms of DOM introduction into seawater include phytoplankton exudation, cell autolysis, viral attack, grazing, excretion, and particles solubilization *via* enzymatic hydrolysis. In the three-dimensional matrix there are "hotspots" of concentration and activity. In this scenario, "organic matter sources" sustain structured nutrient fields, regions in which there are steep gradients of bacterial utilizable dissolved organic matter.

In the classical view, marine organic matter has been operationally defined as

dissolved (DOM) or particulate (POM) based on filtration, creating a clear-cut confinement of DOM and POM pools in the ocean. The recent view perceives the organic matter in the ocean as a continuum of sizes, structures and chemical moieties (Azam et al., 1993). The organic matter field ranges from colloids and gel particles (1-1000 nm) up to micro- (1100 μm) and macro-aggregates (≥ 1 mm) (Koike et al., 1990; Wells and Goldberg, 1992; Chin et al., 1998; Zutic and Svetlicic, 2000; Alldredge et al., 1993; Long and Azam, 1996; Verdugo et al., 2004, Samo et al.,2008). Bacteria, viruses, protozoa and phytoplankton are embedded in the continuum, in dynamic interaction with it, creating and maintaining physical and chemical heterogeneity *via* their *in situ* biochemistry (Azam et al., 1993).

As bacteria exert their biochemical activities to convert the organic matter into usable molecules they also shape the organic matter continuum actively through their metabolic interactions with it (Azam et al., 1993; Verdugo et al., 2004). However, the nature and ecosystem consequences of interactions of bacteria with organic matter are only beginning to be understood. These ideas are changing how we approach the study of bacteria-organic-matter interactions and their biogeochemical consequences; how the heterogeneous organic matter hot and cold spots might provide microniches for the adaptive behaviors of different taxa and support the observed high bacterial diversity in the ocean.

Many important questions need to be addressed about *in situ* bacterial biogeochemistry and adaptive behaviors at the microscale level. Although we know that

bacterial action at the microscale level influences biogeochemical cycles of the ocean (Smith et al., 1992, Bidle and Azam, 1999), we are still largely ignorant of how microscale influences bacteria growth, behavior and response to nutrient fields. In order to understand and predict the role of microbes in organic matter cycling in the ocean, it is necessary to examine *in situ* biochemical interactions between bacteria and organic matter at the relevant scale.

This dissertation addresses ocean basin scale bacteria-mediated carbon fluxes as well as explores the nanometer to micrometer scale bacteria-organic-matter interactions using Atomic Force Microscopy. Following a review and synthesis of the knowledge and ideas on microbial oceanography and microscale biogeochemistry (Chapter II) the research findings are organized in three chapters (Chapters III, IV and V) followed by summary and directions for future research (Chapter VI).

Chapter II highlights the importance of thinking about microbial oceanographic processes in terms of microbial biology at the microscale and further advocates the need to find ways to extrapolate microscale processes to ocean basin scale and global ocean scale biogeochemistry. It further suggest that understanding the mechanisms of microscale interactions should help discover basic principles useful in large scale effect of microbial activity biogeochemistry. The chapter points to the need for new methods and novel approaches in the initial phase of the development of microscale biogeochemistry.

Chapter III presents the results of a field study conducted in the Southern Ocean during summer (2004) and winter (2006). The aim was to understand the strength and variability of bacteria-organic-matter coupling in dramatically different productivity regimes in austral summer and winter. Further, the study compared two contiguously occurring iron deplete and comparatively iron-replete regions. An important finding was that while the microbial loop was a significant carbon flow pathway during summer there was still accumulation of slow-to-degrade dissolved organic matter; its use by bacteria and Archaea during the long, dark winter supported continued bacteria production to sustain an active microbial loop during the winter. Thus, in the winter, when primary production was greatly reduced *Bacteria* and *Archaea* were the major producer of biogenic particles at the expenses of dissolved organic carbon drawdown. This study has implications for food web structure and carbon cycling in a part of the world ocean that is particularly important in future scenarios of climate change.

Chapter IV expands on the AFM-based interrogation of pelagic marine bacteria to address the long-standing problem of bacterial volume and size-frequency distribution—critical parameters in bacterial ecophysiology and role in food web and carbon cycling. Their typically diminutive size has been a challenge to gain information on size and morphology dependent parameters such as growth and carbon content. Exhaustive AFM imaging was combined with imaging by epifluorescence microscopy (EFM) using current protocols as well as two new epifluorescence protocols developed in this study. AFM

allowed three-dimensional imaging of live bacteria in seawater environment. This study provides a reliable basis for bacteria volume determination as well as shows that previous studies may have significantly underestimated bacterial volume and bacterial carbon pool in the ocean. Further, AFM-based bacteria height measurements provide insights into *in situ* physiology, live-dead bacteria, and in situ phage-bacteria interactions. This paper refines the methodology for quantifying bacteria-mediated carbon fluxes and the role of bacteria in marine ecosystems as well as suggests the potential of AFM for individual cell physiological interrogations in the natural marine assemblages.

Chapter V reports the discovery of the nanoscale to microscale association of "free-living" marine bacteria with other heterotrophic bacteria and *Synechococcus* cells in the pelagic ocean. Using Atomic Force Microscopy we made the surprising discovery that a substantial, and variable, fraction (30%-43%) of "free-living" bacteria and *Synechococcus* cells in samples from California coastal and open ocean environments were intimately associated with other bacteria at the nm-μm scale. These putative pelagic symbioses have implications for oceanic productivity and nutrient and carbon cycling and the significance of microscale interactions for the ecology of pelagic heterotrophic bacteria and *Synechococcus*. Furthermore, we discovered that a substantial fraction of marine bacteria previously thought to be "free living" occurred interconnected in microscale networks. These findings change how we think about the free-living and particle attached bacteria in the ocean and they have implications for carbon cycling, bacteria-phytoplankton coupling and grazing- and phage-induced mortality at the microscale level.

Chapter VI summaries the dissertation and suggest future research directions

LITERATURE CITED

Alldredge, Passow, Logan - 1993 The abundance and significance of a class of large, transparent organic particles in the ocean. Deep-Sea Res., Part 1, Oceanogr. Res. Pap. 40:1131–1140

Azam, Smith, Steward, Hagström - 1993 Bacteria-organic matter coupling and its significance for oceanographic carbon cycling. Microb. Ecol. 28:167–179

Azam, Smith, Long, Steward - 1995 Bacteria in oceanic carbon cycling as a molecular problem. In In NATO ASI vol. G38 Particle Molecular Ecology in Aquatic Microbes ed. I. Joint. Springer-Verlag Berlin Heidelberg pp.39-54

Azam, Malfatti 2007 Microbial structuring of marine ecosystem. Nature Rev. Microbiol. 5(10):782-791

Bauer, Williams, Druffel -1992- ^{14}C activity of dissolved organic carbon fractions in the north-central Pacific and Sargasso Sea. Nature 357, 667 - 670

Bidle, Azam - 1999 Accelerated dissolution of diatom silica by marine bacterial assemblages. Nature 397: 508-512

Chin, Orellana, Verdugo - 1998 Spontaneous assembly of marine dissolved organic matter into polymer gels. Nature 391:568–572

Fuhrman, Azam - 1982 Thymidine incorporation as a measure of heterotrophic bacterioplankton production in marine surface waters: evaluation and field results. Mar Biol. 66 :109–120

Hagström, Larsson, Horstedt, Normark - 1979 Frequency of dividing cells, a new approach to the determination of bacterial growth rates in aquatic environments. Appl. Environ. Microbiol. 37:805–812

Hobbie, Daley, Jasper - 1977 Use of the nucleopore filters for counting bacteria by fluorescence microscopy. Appl. Environ. Microbiol. 33:1225-1228

Koike, Hara, Terauchi, Kogure - 1990 Role of sub-micrometer particles in the ocean, Nature 345:242–244

Long, Azam - 1996 Abundant protein-containing particles in the sea. AME 10:213-22

Samo, Malfatti, Azam - 2008 A new class of transparent organic particles in seawater visualized by a novel fluorescence approach. AME 53:307-321

Smith, Simon, Alldredge, Azam - 1992 Intense hydrolytic enzyme activity on marine aggregates and implications for rapid particle dissolution. Nature 359:139-142

Venter, Remington, Heidelberg, Halpern, Rusch,.Eisen, Wu, Paulsen, Nelson, Nelson, Fouts, Levy, Knap, Lomas, Nealson, White, Peterson, Hoffman, Parsons, Baden-Tillson, Pfannkoch, Rogers, Smith. 2004. Environmental genome shotgun sequencing of the Sargasso Sea. Science304:66–74

Verdugo, Alldredge, Azam, Kirchman, Passow, Santschi - 2004 The oceanic gel phase: a bridge in the DOMPOM continuum. Mar. Chem. 92:67-85

Wells, Goldberg - 1992 Occurrence of small colloids in seawater, Nature 353:342–344

Williams, Druffel - 1987 Radiocarbon in dissolved organic matter in the central North Pacific Ocean. Nature 330, 246 - 248

Yooseph, Sutton, Rusch, Halpern, Williamson, Remington, Eisen, Heidelberg, Manning, Li, Jaroszewski, Cieplak, Miller, Li, Mashiyama, Joachimiak, van Belle, Chandonia, Soergel, Zhai, Natarajan, Lee, Raphael, Bafna, Friedman, Brenner, Godzik, Eisenberg, Dixon, Taylor, Strausberg, Frazier, Venter. 2007. The Sorcerer II Global Ocean Sampling expedition: expanding
the universe of protein families. PLoS Biol. **5:**432–466.

Zutic, Svetlicic - 2000 Interfacial processes. The Handbook of Environmental Chemistry, Vol. 5 Part D, Marine Chemistry, Springer-Verlag, Berlin Heidelberg, 149-16

II

Microbial structuring of marine ecosystem

Microbial structuring of marine ecosystems

Farooq Azam and Francesca Malfatti

Abstract | Despite the impressive advances that have been made in assessing the diversity of marine microorganisms, the mechanisms that underlie the participation of microorganisms in marine food webs and biogeochemical cycles are poorly understood. Here, we stress the need to examine the biochemical interactions of microorganisms with ocean systems at the nanometre to millimetre scale — a scale that is relevant to microbial activities. The local impact of microorganisms on biogeochemical cycles must then be scaled up to make useful predictions of how marine ecosystems in the whole ocean might respond to global change. This approach to microbial oceanography is not only helpful, but is in fact indispensable.

Primary production
The original source of organic material in an ecosystem that is due to carbon dioxide fixation by photosynthetic bacteria, plants or algae, or chemosynthetic microorganisms.

Heterotrophic
The acquisition of carbon and metabolic energy by the consumption of living or dead organic matter.

One-half of global primary production occurs in the oceans[1,2], and therefore a fundamental problem for oceanographers is to understand how organisms use this carbon to create spatio-temporal patterns of carbon and energy flux. For example: how much is passed into fish[3]; how much is respired and returned to the atmosphere; and how much descends to support the deep-sea biota or to be sequestered on the seafloor[4]. Interest in the carbon cycle has increased recently owing to global problems, such as climate change, coastal eutrophication and over-fishing[5,6]. Historically, oceanographers believed that most primary production moved through a chain of small and large animals[7–9] and microorganisms were largely ignored[10]. However, several remarkable discoveries[11–13] (reviewed in REFS 14–16) that have been made during the past 30 years have shown that bacteria dominate the abundance, diversity and metabolic activity of the ocean (FIG. 1). A large fraction of primary production becomes dissolved (dissolved organic matter; DOM)[17] by various mechanisms in the food web, and this part of the primary production is almost exclusively accessible to heterotrophic bacteria and archaea (together referred to in this Review as bacteria)[9,18,19]. As a result, the uptake of organic matter by bacteria is a major carbon-flow pathway, and its variability can change the overall patterns of carbon flux[8,20,21]. Further, as bacteria use behavioural and biochemical strategies to acquire organic matter — for example, by the expression of enzymes to solubilize particulate organic matter (POM)[22] — they interact with sources of organic matter and modify the ecosystem and carbon cycle in different ways[23,24]. Our aim throughout this Review is to propose a mechanistic and microspatial framework that promotes a better understanding of how bacteria regulate the biogeochemical state of the oceans.

Ecosystem-level coupling

The effects of bacteria on the carbon flux in the sea have been measured over the past 30 years[25,26]. Although it is impractical to measure the flux of each component of DOM into bacteria, the cumulative carbon flux (bacterial carbon demand; BCD) can be estimated as the sum of the carbon that is assimilated (growth) and respired, which can then be compared with primary production as a measure of the coupling strength (BCD ÷ primary production[27]). This parameter is useful as a global measure of bacterial performance, for example, in concepts that involve the ocean carbon flux or ecosystem-based fisheries[21]. Measurements of coupling strength have been made on many ocean expeditions, in most oceanic locations and in regions that differ in primary production, and this has revealed important geographical and seasonal patterns. The following examples show that the coupling of bacteria with primary production is highly variable and that this variability affects ecosystem functioning.

First, in the eastern Mediterranean bacteria take up most of the primary production, which is consistent with the poor fisheries that are present in this area[28] (although a high BCD might be an effect rather than a cause of poor fisheries). Second, studies carried out on a north–south oceanic transect (53°N in the Atlantic to 65°S in the Southern Ocean)[29] showed latitudinal variation in coupling strength, and, importantly, there were large net-heterotrophic regions. Bacteria took up more DOM than was present as local primary production, which indicates that the spatial or temporal import of organic matter must have occurred. Consequently, these regions have the potential for the net out-gassing of carbon dioxide. More extensive spatial and temporal

Scripps Institution of Oceanography, University of California, San Diego, La Jolla, California 92093, USA.
Correspondence to F. A.
e-mail: fazam@ucsd.edu
doi:10.1038/nrmicro1747

Autotrophic
An organism that synthesizes organic carbon from the fixation of inorganic carbon, for example, by photo- or chemosynthesis.

coverage to account for patchy autotrophic processes might, however, reveal a metabolic imbalance[29–31]. Finally, during the summer, bacteria–DOM coupling in the Antarctic Ocean was found to be weak. Perhaps, the bacterial hydrolysis of polymeric substrates and monomer uptake was slowed owing to low temperature and low substrate concentrations. This could result in the storage and temporal export of slow-to-degrade DOM in productive summers (when primary production is high) to support the energy needs of the Antarctic food web during the winter. During winter, a particle-based food web might incorporate bacterial biomass that is produced through the use of DOM[32]. This example illustrates that even when bacteria–DOM coupling is weak, bacteria can still be important for ecosystem functioning. It has been proposed that there is a low-temperature–low-substrate restriction in the Arctic Ocean[33,34]. Conversely, the excessive external input of organic carbon might have deleterious effects on system functioning. In experimental systems, bacteria outgrew coral-reef communities after the addition of DOM[35] or being placed in contact with decaying macroalgae[36].

These examples illustrate that the ability or inability of a bacterial assemblage to grow on specific types of organic matter, either owing to the constraints of community composition or environmental gene expression, can be important for the functioning of globally significant ecosystems. This underscores the need to understand how bacteria function in their natural environment to influence the flux pathways of fixed carbon. From advances in marine genomics and metagenomics[37–42] it can be inferred that enormous bacterial gene diversity is available for assemblage-level bacterial interactions with the ocean. Environmental genomics and proteomics are also yielding insights into bacterial adaptive strategies to ocean life. The challenge is to determine how these strategies are used by bacteria in natural ecosystems, which will require the exploration of the ocean at the micrometre scale — the scale at which the adaptive strategies of bacteria structure marine ecosystems. Bacteria do more than simply cycle carbon; they interact with the whole ocean ecosystem intimately in a multitude of ways[43].

Microscale interactions

Spatial distribution of microorganisms. Most oceanographic studies assume that bacteria take up homogeneously distributed DOM. This premise relies on the assumption that the DOM that is released from any source diffuses homogenously into the bulk phase before it is taken up by an organism. This view is changing, however, with the recognition of bacterial *in situ* behavioural and physiological responses to DOM-production loci and gradients. The detection of high abundances of decomposer bacteria (10^6 per $ml^{[1]}$) has led to the suggestion that the numbers and activity of primary producers (such as cyanobacteria and algae),

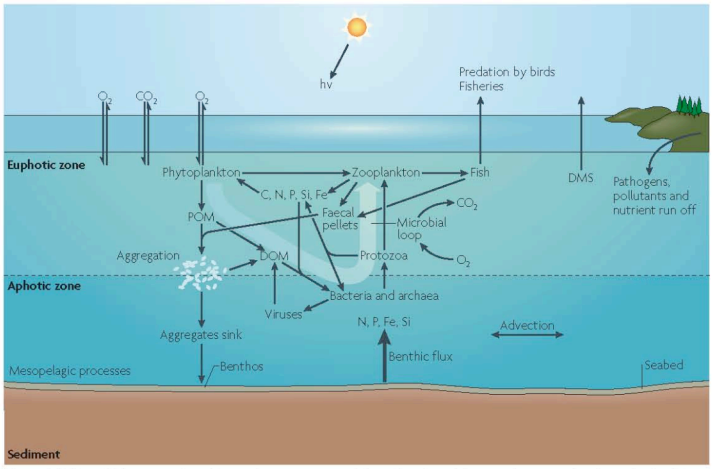

Figure 1 | Microbial structuring of a marine ecosystem. A large fraction of the organic matter that is synthesized by primary producers becomes dissolved organic matter (DOM) and is taken up almost exclusively by bacteria. Most of the DOM is respired to carbon dioxide and a fraction is assimilated and re-introduced into the classical food chain (phytoplankton to zooplankton to fish). The action of bacteria on organic matter plays a major part in carbon cycling through DOM. It therefore influences the air–sea exchange of carbon dioxide, carbon storage through sinking and carbon flux to fisheries. DMS, dimethylsulphide; hv, light; POM, particulate organic matter.

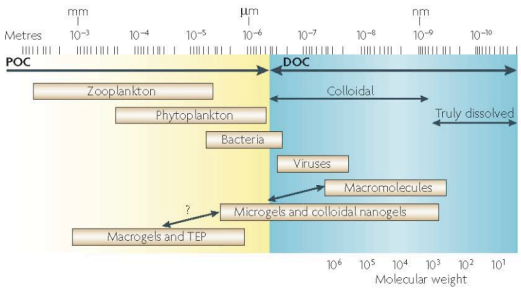

Figure 2 | **The size range of organic matter and microbial interactions in the ocean.** Organic matter has traditionally been divided into dissolved organic matter and particulate organic matter, based on filtration. Here, the full size range of organic matter is shown, from monomers, polymers, colloids and gel particles to traditional particles (divided into particulate organic carbon (POC) and dissolved organic carbon (DOC)). These organic nutrient pools form an intricate three-dimensional architecture of polymers, colloids, gel particles and large aggregates. Living plankton and dead organisms are thought to be embedded in a cobweb-like structure of organic matter that is dynamic over time and space (not shown). The organic matter architecture provides the spatial context within which microorganisms — bacteria, archaea, microalgae, protists and viruses — interact with each other and with the environment. TEP, transparent exopolymer particle. Modified, with permission, from (REF. 72) © (2004) Elsevier Science.

decomposers (such as bacteria) and predators (such as viruses and protists) are similar (Fig. 1). Typically, 1 mm^3 (or µl) of surface seawater — considered in this Review to be the bacterium's microenvironment — contains 10,000 viruses; 1,000 bacteria; 100 *Prochlorococcus* cells; 10 *Synechococcus* cells; 10 eukaryotic algae; and 10 protists, although the numbers are highly variable[16,18,44]. The close proximity (0–1 mm) of individual cells suggests that there is potential for many cell–cell interactions.

We note that all microbial trophic groups are in close proximity, so that the adaptive biology of bacteria occurs in a microspatial context that integrates the interactions between all of the trophic groups. For instance, bacteria might respond behaviourally and metabolically to the DOM that is produced by a range of mechanisms, such as algal exudation and cell lysis[18], predation by viruses, which releases prey DOM[45], and the action of protists, which egest food vacuoles that contain DOM and regenerated N, P and Fe^{2+} (REFS 46,47). Such DOM hot spots might occur in the microenvironment of a bacterium over short timescales, perhaps even minutes, owing to the high abundance of microorganisms.

Motility. Motility and sensing enable bacteria to adapt in environments that contain DOM gradients. Dark-field microscopy has revealed that motility is common in natural assemblages of marine bacteria[48–50], although the fraction of bacteria that are able to swim ranges from 5 to 70%. Motility might enable bacteria to achieve spatial coupling with a DOM source, such as a living or dying alga, or a protist[51,52].

Hydrolytic enzymes and hydrolysis-uptake coupling. Marine bacteria hydrolyse polymers and particles using cell-surface-bound hydrolytic enzymes or ecto-hydrolases (protease, glucosidase, lipase, phosphatase, nuclease and chitinase)[22,53–59]. These enzymes, together with membrane-bound transporters, make the bacterial surface reactive for organic matter transformation and uptake. This is the final step that couples bacteria to primary production in the ocean. The bacterial surface is the dominant biotic surface, and it is proposed that 0.1–1 m^2 of the bacterial surface per m^3 of seawater interacts intimately with DOM[60]. A pelagic bacterium that swims through organic matter leaves a stream of monomers and oligomers behind it. This led J. Stern to refer to bacteria as the "perfect swimming stomachs" (REF. 21).

Bacteria express multiple (multiphasic) transporters that have K_m values that range from nanomolar to millimolar, consistent with adaptation to environments that contain DOM gradients[61–64] (FIG. 2). This raises the question of whether the distinction that is made between oligotrophic and eutrophic bacteria, which is usually based on culturing studies, actually reflects the microspatial adaptations of different strains to nutrient hot spots. Perhaps, bacteria simply move to an appropriate distance from a DOM gradient, so that they can effectively use the carbon resources that are available. The *in situ* behaviour of strains — such as the widely distributed oligotrophic *Candidatus* Pelagibacter ubique (SAR11)[65,66] bacterium or the high-nutrient-loving Roseobacter-clade members — when viewed in such a microspatial context could lead to new predictions about their ecology and distribution[67,68].

A biochemical mechanism that tightly couples the transport and hydrolysis of organic matter would be a useful adaptation in ocean environments, where diffusion rates are high[69] (FIG. 2). The existence of such a coupling mechanism has been difficult to demonstrate experimentally, but genomic, metagenomic and proteomic data might provide hints as to how bacteria obtain sufficient nutrients in an environment such as the ocean.

A bacterium's-eye view of organic matter

In a sense, microbial oceanography has a long history of studying bacteria at the microscale, including studies on the physiology and growth performance of bacteria that are present in seawater, attached to a particle or clustered around algae and detritus. Traditional distinctions between DOM and POM have been based on filtration methods that have used filters with a pore size of 0.45 µm. However, recent research shows that organic matter in seawater is replete with transparent gels that form tangled webs of components in the form of colloids that are approximately 10 nm long (10^8 colloids per ml[70,71]) and mucus sheets and bundles that are up to 100 µm long (1,000 sheets or bundles per ml[72,73]). Colloids, sheets and bundles interact to form macromolecular networks that are 100 µm or more long. The polymeric components of transparent gels are probably derived from microorganisms. Phytoplankton and bacteria produce

Pelagic
Relating to or occurring in the oceanic water column.

Oligotrophic
An aquatic environment that has low levels of nutrients and primary production (for example, high mountain lakes or the open ocean).

Eutrophic
A marine or lake environment with a high nutrient concentration and high levels of primary production.

Phytoplankton
Composed of microscopic plants and photosynthetic cyanobacteria. These are the main primary producers in marine food webs, ranging in size from 1 µm to approximately 100 µm.

cell-surface mucus, which can either be released or, alternatively, solubilized by cell-surface-acting enzymes. Phytoplankton release condensed polysaccharide particles by exocytosis, which form gels in seawater[74]. Most (90–95%) of the DOM is refractory to degradation by bacteria and it has been proposed that some DOM components serve as stable scaffolds of a gel architecture that is inaccessible to bacterial ectohydrolases[75]. Potentially, gels are a nutrient sink and represent a mosaic of nutrient hot spots. This nutrient pool is huge, as approximately 10% of all the DOM (70×10^{15} grams of carbon) that is found in the ocean is present in the form of gels. This represents a carbon pool that is larger than all of the carbon that is present as biomass in the ocean[72]. Depending on their surface properties, gels might adsorb DOM components from seawater, and this could be significant given the large surface area of these gels. Bacteria can attach to gels[76,77] and it is possible that they hydrolyse the nutrients that are present on the gel surface using cell-surface hydrolases[78]. This, in turn, might alter the local architecture of the gel and the nutrient dynamics at the microscale.

The architecture of gels has been detected using stains that target proteoglycan, protein and DNA (FIG. 3). These methods might not be sensitive enough to reveal all of the details of gel architecture, and some, or even most, of the gel might be too diffuse to be detected by imaging technology. Techniques that are useful for macromolecular-level imaging, such as atomic force microscopy[79–81], could also be useful for studying marine gels. In addition, the architecture of organic matter is based on information obtained using methods that can only detect structures in two dimensions, after sample collection on filters. One important, but challenging, goal is to develop methods that can visualize and biochemically characterize the microscale architecture of the organic matter gel matrix in relation to the distribution of bacterial taxa in various physiological states. Confocal laser microscopy might be useful, as gels can be viewed in three dimensions, and this method might be able to more closely pinpoint the physical relationship between bacteria and the organic matter of these gels. Fluorescently labelled lectins, and other probes for biochemical composition, might be useful for determining the composition of gels[82,83]. Microspatial viscosity is probably variable[84] (for example, on the algal surface or near a lysing dinoflagellate) and this might influence bacterial adaptive behaviours[85,86], such as motility, microspatial distribution and *in situ* physiological states[87]. Individual bacteria might experience different microspatial nutrient concentrations at different positions within the organic matter matrix. Also, bacteria could export inhibitory molecules that become bound to the gel matrix, so enabling them to compete with other bacteria by niche modification. Clearly, much remains to be learnt about the structural and chemical dynamics of the microscale architecture of organic matter and its relationship with bacteria.

Research on gel architecture has altered how microbial oceanographers think about the function of bacteria in marine ecosystems. Microspatial architecture provides huge surfaces for bacterial attachment and interactions. Indeed, the enormous genetic diversity of marine bacteria[37–39,88,89] might be explained by the ability of gels to provide niche diversity in seemingly homogeneous ocean waters. For example, many, or all, bacteria that are currently considered to be free-living, for example, SAR11, might in fact be attached to the gel matrix. This would mean that oligotrophs, such as SAR11, do not compete directly for dissolved solutes. Acinas and colleagues[90] suggested that the clusters of microdiversity that they detected in pelagic bacteria might be due to the presence of pelagic microniches. As primary productivity and DOC generally decrease offshore[91,92], the hot spots of DOM production and bacterial activity might be less abundant. A bacterium's-eye view of organic matter offers a more elaborate and dynamic spectrum of choices, rather than the traditional dichotomy that is derived from regarding bacteria as either attached or free living.

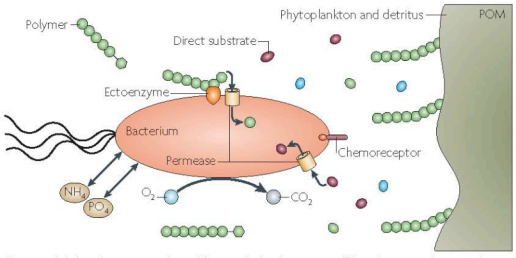

Figure 3 | **Adaptive strategies of bacteria in the ocean.** The adaptions that are shown are relevant to the structuring of marine ecosystems by bacteria at the nanometre–millimetre scale, but they also affect ocean-basin-scale processes, including the cycling of carbon, nitrogen and phosphorus and the biogeochemical behaviour of organic matter (for example, sinking). The strategies that are depicted here include motility, environmental sensing, permeases and cell-surface hydrolases. They enable coupling between bacteria and organic matter. For example, phytoplankton or cell debris, depicted as particulate organic matter (POM) and bacteria. Polymers also require hydrolysis to direct substrates before trans-membrane transport. Note the ability of bacteria to take up, as well as release, NH_4 and PO_4.

In situ *growth rate variability.* A major physiological variable among oceanic bacterial assemblages is the ability to grow over a broad range of growth rates, from nearly zero to more than one doubling per day[12,19,25,93,94]. These growth rates — in combination with population size and biomass — are reflected by the variation in BCD and bacteria–phytoplankton coupling. Marine isolates typically grow fast in enriched culture media (although notably SAR11 cannot grow on rich media[95]). We propose that high growth rates occur periodically in nutrient-rich microzones[96–98], for example, near to, or on, nutrient-rich particles[99,100], plankton surfaces or in the guts of animals. Thus, the slow average-growth rates that are typically observed for pelagic assemblages do not preclude the possibility that a small fraction of the assemblage might be growing rapidly[101–103].

Bacterial growth efficiency (BGE). This is a crucial variable for ecosystem function. The BGE compares the fraction of assimilated carbon that is respired with the fraction that is used to increase bacterial biomass. The BGE for natural assemblages is usually 10–30%, but this can vary widely from 1 to 40%; this means that 60–99% of all assimilated carbon is respired[27,104–106]. The variation in BGE can affect the role of bacteria in carbon cycling, owing to alterations in the partitioning of carbon between carbon dioxide and biomass, which is accessible to animals. BGE varies between oligotrophic and eutrophic ecosystems[107]. A mixed population has a range of BGE's that are dependent on the physiological state of individual bacteria and their spatial and temporal interactions with organic matter[107]. It is important to place BGE in a microspatial context. A goal should be to determine how the environment affects the respiration, growth and phylogenetic identity of individual cells and thereby influences BGE on the microscale.

Bacterial coupling to primary production

Bacterial performance (as measured by growth, respiration and other metabolic activities) is constrained by the fact that bacteria are obligate osmotrophs, whereas primary production mainly produces particulate and polymeric organic matter. As a result, the *in situ* physiological attributes and adaptations of bacteria must be responsive to the production of DOM in the microenvironment of the bacterium. Another adaptive challenge for the bacterium is to position itself optimally in relation to DOM production. For example, is it adapted to growth in DOM-production hot spots or does it exploit the environmental volume-fraction at the tail-end of DOM gradients? Methods that have been developed to determine the growth rate and phylogenetic identity of individual cells within natural assemblages constitute powerful tools to relate *in situ* physiology and taxonomy in the microenvironment[93,94,108–111].

Bacteria, such as SAR11 (REFS 65,66), members of the Roseobacter clade, including the alphaproteobacteria Roseobacter-clade-affiliated cluster[67,68,112], and members of the Bacteroides clades[113,114], might be good models for defining the adaptive strategies that are used by bacteria in relation to DOM-production regimes in microenvironments. Available substrates are maintained at picomolar to nanomolar concentrations in the bulk phase — Hedges and colleagues estimated that "10^{12} diverse organic molecules...[are]...dissolved in every millilitre of seawater…", which are "dynamically shaped and buffered by microbiological action" — and, therefore, DOM production forms DOM gradients against the background of extremely low bulk-phase concentrations.

In proposing how bacteria adapt to use low or high DOM concentrations it is important to recognize that the conversion of POM to DOM involves many different phytoplankton organisms that use varied mechanisms of DOM production. Therefore, numerous adaptive strategies might be used by diverse bacterial taxa.

Phytoplankton are organic matter production loci. The main processes that convert up to half of all the primary production into DOM must occur before substantial amounts are transferred through multiple trophic levels and respired. The most likely mechanisms of DOM formation are direct processes, such as phytoplankton exudation and lysis (by virus attack or nutrient stress), bacterial interactions with live phytoplankton (for example, commensalism or predation) and the bacterial enzymatic degradation of recently dead phytoplankton and protists. The aggregation of phytoplankton and phytoplankton detritus could facilitate bacterial access to DOM. Finally, protists that exhibit boom-and-bust growth cycles could enable bacteria to use protist biomass.

Bacteria–phytoplankton interactions. One way for bacteria to metabolically couple to primary production would be to swim up to phytoplankton and use cell-surface hydrolases to kill them[115]. Bacteria have various adaptations that allow them to attach to dead phytoplankton and cause hydrolysis[116]. If bacteria are randomly distributed, each bacterium would be a few hundred micrometres away from the nearest phytoplankton cell[8] — a distance that most motile marine bacteria could traverse rather quickly (although many bacteria are non-motile and would not use this strategy). Bacteria can cluster around phytoplankton[117] to create considerably higher concentrations than the average for seawater, which is 10^6 bacteria per ml[85]. Tight spatial coupling between marine bacteria (*Pseudoalteromonas haloplanktis* and *Shewanella putrefaciens*) and a motile alga (*Pavlova lutheri*) has been filmed and referred to as the 'pestering' of algae, because the bacteria closely tracked motile phytoplankton[52]. It seems that some phytoplankton–bacteria associations might even be species specific[118–120].

Phytoplankton produce surface mucus, polysaccharides and proteoglycans, which might serve as a protection from bacteria; this is analogous to corals, which convert substantial photosynthate into mucus for defence against microbial invasions[121]. Some phytoplankton also produce inhibitory compounds[122]. Mucus creates a region around the phytoplankton cell that is rich in organic matter, and is known as the phycosphere[117]. The nitrogen- and phosphorus-depleted mucus could adsorb nitrogen- and phosphorous-rich materials, such as polymers and colloids, from seawater, resulting in the development of a rich gel medium. Although much research has been done on bacteria that are attached to phytoplankton it has been technically difficult to study the *in situ* physiology of bacteria (growth, respiration and antibiotic synthesis) in the phycosphere. It is also likely that the community composition of bacteria in the phycosphere will differ from that in the local ocean environment. Significant diurnal alterations in the bacteria–phytoplankton relationship are to be expected, but these need to be addressed in a microspatial context. As the phycosphere is organically rich it has been proposed that it could support the proliferation of human pathogens or other bacteria that are adapted to high-nutrient environments[97].

Although bacteria can cluster near, or attach to, phytoplankton[52,69,123], the biochemistry of the bacteria–phytoplankton interaction is poorly characterized.

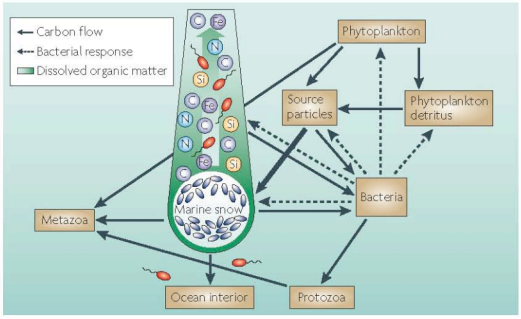

Figure 4 | **Microbial cycling of carbon in marine snow.** The aggregation of organisms and organic matter to form sinking marine snow plays a major part in ocean ecosystems. Marine snow is highly colonized by bacteria, presumably because it is formed from pre-colonized source particles that transport carbon, nitrogen, phosphorus, iron and silicon into the ocean's interior. The high hydrolytic enzyme activities of bacteria convert the aggregate organic matter into non-sinking dissolved organic matter (DOM), forming plumes in the ocean. Free-living bacteria that are attracted to such DOM-rich hot spots respire carbon to carbon dioxide and their biomass production feeds into the pelagic foodweb. Colonizing bacteria might adapt by releasing their progeny into the plume. The intensely colonized marine-snow aggregates create hot spots of life, and the death of bacteria, viruses (decay), protozoa and metazoa — thus having substantial roles in the structuring of the marine ecosystem.

Do bacteria produce either endohydrolases or exohydrolases, or both, and can bacteria couple hydrolysis and the uptake of DOM in the phycosphere? Endohydrolase action could release polymers into the microenvironment that might then be accessible to exohydrolases, which could, in turn, release monomers that bacteria can take up. The released polymers might be detectable as transparent gel particles in seawater[124,125].

Microscale processes in the phycosphere. Because the cell-associated phycosphere has fundamental implications for the adaptive biology of bacteria and phytoplankton, we must address microscale processes within the phycosphere at the mechanistic level. The relationship between clustering bacteria and phytoplankton is probably complex and variable over short timeframes. Clustered bacteria could benefit the phytoplankton cell by enhancing nutrient regeneration in the phycosphere at the expense of dissolved organic nitrogen and phosphorus. The inorganic nutrient hot spot that surrounds the phytoplankton cell could make its microenvironment eutrophic in what might otherwise be oligotrophic water according to bulk seawater analysis. This hot spot of nutrients could also receive protist contributions owing to the intense grazing of bacteria by bacterivorous protozoa, which would release regenerated nitrogen, phosphorus and iron into the microenvironment. However, if seawater becomes depleted in dissolved organic nitrogen and dissolved organic phosphorus then the presence of clustering bacteria might also reduce the release of dissolved inorganic nitrogen and dissolved inorganic phosphorus, thus further limiting primary productivity. Stressed phytoplankton might be unable to defend themselves by the release of mucus or antibiotics[122] and clustering or colonizing bacteria could then kill the phytoplankton for use as a growth substrate. The nutrient-hot-spot premise[9], if supported, would change our concepts and models of the nutrient regulation of primary production. Current models assume there is homogeneity in nutrient distribution. This is another example where further study of a microspatial process promises to yield insights into the regulation of primary production and carbon cycling.

The phycosphere might also be important for the use of dimethylsulphoniopropionate (DMSP) by bacteria. Many marine algae produce this osmolyte and release some of it into the microenvironment. Some marine bacteria, including SAR11 and Roseobacter clades, use DMSP as a source of energy[109,126,127]. Intracellular pools of DMSP are present in algae at approximately 0.2–0.5 M, although bulk seawater concentrations are approximately 10 nM. DMSP and extracts of *Pfiesteria piscicida* function as chemoattractants for *Silicibacter* spp. strain TM1040, an alphaproteobacterium that can grow in close association with the dinoflagellate *P. piscicida*. Chemotaxis might enable *Silicibacter* spp. strain TM1040 to remain close to *P. piscicida*[128]. It would be of interest to know whether community composition and the growth environment in the phycosphere affects the metabolic fate of DMSP[129,130]. This could affect the rate of bacterial hydrolysis of DMSP to dimethyl sulphide (DMS)[131,132]. As DMS can affect climatic processes, understanding the regulation of the conversion of DMSP to DMS at the microscale could lead to more informed global climate models.

The action of cell-surface-associated bacterial protease and glucosidase on diatom surfaces might reduce diatom 'stickiness' and the aggregation potential. This enzymatic 'pruning' of the diatom mucus would require microscale interactions between diatoms and bacteria; a high concentration of bacteria in the phycosphere would probably increase the rate of this process[133]. Diatom aggregation can form large, rapidly sinking aggregates known as marine snow (FIG. 4), which are important for the export of organic matter to the ocean's depths[134] as well as the demise of algal blooms. Understanding the microscale action of bacterial hydrolases on diatom surfaces could help us to predict the timing of bloom termination and the regulation of carbon export in an ecosystem context — this would represent a genome–biogeochemistry connection.

Interaction of bacteria with protists. Protists consume more than half the primary production in many ecosystems[135]. How can we reconcile the large grazing pressure on phytoplankton by protists with an equally high bacterial carbon demand? Perhaps when the BCD and protist grazing are both high, a large fraction of the organic matter that is ingested by protists is released through the lysis of these protists by viruses or other factors[136]. Bacteria can rapidly colonize dead protists and degrade fresh protist detritus. However, it remains to be determined whether heterotrophic bacteria cause significant protist

Chemotaxis
The sensing by bacteria of chemical gradients, and movement up or down a gradient towards or away from a chemical source.

Dimethyl sulphide
(DMS). A sulphur-containing organic chemical compound that is a breakdown product of dimethylsulphoniopropionate (DMSP). It is also produced by the metabolism of methanethiol by marine bacteria that are associated with phytoplankton.

Marine snow
Composed of organic aggregates more than 0.5 mm in diameter. These macroscopic particles are enriched in organic matter and are inhabited by a rich and diverse community of phytoplankton, protozoans and bacteria.

mortality in an 'eat them before they eat you' scenario. In this hypothetical scenario, protists are the processors of primary production, their enzymes convert the POM of prey to DOM and their newly synthesized biomass is consumed by bacteria as predators. Protists are important grazers of small, highly abundant phytoplankton, such as *Synechococcus*, *Prochlococcus* and picoeukaryotes[135]. Therefore, protist processing of primary production might be one mechanism that increases the coupling of bacteria to primary production.

Interactions of bacteria with detritus. Dead phytoplankton cells are a source of organic matter for bacteria, which readily colonize such material to form a detritosphere[133,137] (FIG. 4). Bacterial colonization and enzymatic hydrolysis could convert detritus to DOM. However, not all bacteria attach to dead phytoplankton. In an experimental system, dense clusters of bacteria were recorded swimming around a killed dinoflagellate, and these were modelled to predict bacterial interactions with DOM hot spots[51,123,138]. Depending on the particle sinking rate, the effects of bacteria on dead phytoplankton cells might result in DOM plumes (as discussed later).

Diatoms attract bacteria, and freshly lysed diatoms comprise organic matter hot spots that support the robust growth of bacteria. Because diatoms require silicon for growth, the mechanisms of silicon recycling are important. Unexpectedly, it was found that bacteria that do not require silicon regulate the regeneration of silicon from dead diatoms[116]. Although bacteria use their ectohydrolases to solubilize organic matter, the action of these enzymes also removes the protective proteoglycan silaffins from the silicon frustules[139] and it is the silaffin proteins that normally prevent the dissolution of silicon[116]. This process requires colonization by bacteria, and those bacteria with high cell-specific protease activity cause more rapid dissolution. In view of the importance of diatom production, and the regeneration of silicon, the regulation of the silicon cycle by bacteria could affect the carbon-export flux. Consequently, an understanding of the biochemical basis of this process should be incorporated into biogeochemical models.

This is an example of a bacteria-mediated process at the microscale that results in the regulation of the silicon cycle and coupled silicon–carbon cycles in the global ocean. Bacterial enzymatic action involves a trivial amount of carbon that is contained in the proteoglycan covering and is readily accessible to bacteria. However, the action has a major effect on the biogeochemical behaviour of silicon. This might suggest that bacteria have a more general ability that allows them to de-mineralize living or dead silicoflagellates, radiolarians or calcified phytoplankton, most notably *Emiliania huxleyi*. However, whether bacteria really do de-mineralize these organisms will depend on the relationship between the mineralized structure and organic matter[140].

Marine snow and nutrient hot spots

Aggregation state of the ocean. The aggregation of organic matter is a fundamentally important process in the functioning of marine ecosystems. Aggregation generally increases the sedimentation rate of organic matter[141]; the degree of aggregation influences the residence time of component particles in the upper ocean, where they are acted on by bacteria that respire carbon and regenerate nutrients. Sinking aggregates are a dominant conduit for the export flux of organic matter, the variation of which influences carbon storage. The components of the organic matter continuum tend to aggregate to varying degrees forming a dynamic size spectrum. Bacteria can inhibit, as well as enhance, the aggregation state of the system (by reducing the stickiness with hydrolases or increasing it by mucus production)[78,133]. Aggregates can attract microorganisms, such as bacteria, protists and viruses, as well as gels, colloids and cell debris. Although most aggregates are microscopic, some are large, such as marine snow, which is visible underwater, and has been extensively studied for its ecosystem significance. Next, we discuss a model that illustrates the significance of microscale activities of bacteria in marine snow, and which has implications for ocean-basin and global-scale processes.

Marine snow. Bacteria colonize marine snow in population densities that reach 10^8–10^9 per ml[142]. The expression of several ectohydrolases, such as protease, lipase, chitinase and phosphatase, is high, but glucosidases are not well expressed. This enzyme complement digests some of the DOM in marine snow[78]. However, the colonizing bacteria use only a fraction of the hydrolysate (weak coupling)[78,143] and, therefore, the sinking marine snow leaves an extended plume of DOM behind them that other bacteria can use. One model predicts that approximately half of all the BCD in the ocean is satisfied by bacterial interaction with these plumes[144] (FIG. 4).

Marine-snow plumes help to retain nitrogen, phosphorus and iron within the upper mixed layer of the ocean and this supports primary productivity. In addition, as the glucosidase activity of bacteria in marine snow is low, a disproportionate amount of carbon could sink below the upper mixed layer, thus increasing the carbon:nitrogen and carbon:phosphorus ratios in aggregates and causing carbon storage. Because marine snow is organically enriched, bacterial growth might occur with high growth efficiency[145]. One strategy that might enable such loose organic matter–bacteria coupling to be adaptive is for the attached bacteria to release their progeny into the plume[145,146]. Thus, the microscale interactions of bacteria could influence fundamental biogeochemical processes, such as carbon storage and the regulation of carbon flux, as well as provide a microspatial framework for understanding the behavioural and biochemical strategies of free-living bacteria that might be adapted to using the DOM at high concentrations in the plumes. Such strategies might also be used by bacteria at depth[143] because marine snow can sink to hundreds or even thousands of metres[147]. Further, elucidating the *in situ* expression of ectohydrolytic enzymes should help us to understand the biochemical bases of the interactions of bacteria with organic matter, and link carbon storage and carbon biogeochemistry with gene expression. Whether bacterial action will increase or decrease the

net efficiency of the biological carbon pump cannot currently be predicted, but we think that better models will be possible through such studies on the biochemical bases of bacteria-organic-matter interactions.

How bacteria influence the aggregation and biogeochemical fate of carbon is also relevant to concerns about ocean fertilization and carbon sequestration, in which the goal is to maximize aggregation and export carbon flux. Our discussion in this Review suggests that models that predict the outcome of ocean fertilization should include the roles of bacteria and, specifically, the *in situ* expression of selected ectohydrolases[148].

Many bacteria are non-motile, notably pelagic Bacteroidetes and SAR11 (REF. 65). Bacteroidetes are specialized for colonizing aggregates such as marine snow[113,114,149]. How do non-motile bacteria accumulate to form such large populations on marine snow, which has such a short residence time in the upper ocean? Perhaps, non-motile bacteria, being particle specialists, attach first to the highly abundant small gel particles[113,114], which are in the 10-µm length range and are several orders-of-magnitude more abundant than marine snow (typically 1–10 aggregates per litre in the upper ocean)[72]. Aggregation with larger particles and agglomeration with other materials, such as phytoplankton or detritus, forms marine snow. Therefore, the source particles[150] would contribute diverse bacteria, including non-motile bacteria, that have been selected for by attaching to the particles that eventually aggregate to form marine snow. Future metagenomic surveys should consider these seascapes of organic matter, which potentially contain an immense diversity of bacteria that are attuned to the nature and dynamics of their miniscule worlds.

Conclusion and future prospects

Microbial oceanography is a field that is caught between scales — microbial processes must be understood at the scale of the individual microorganism, but yet we want to understand the cumulative influence of microbial processes on the ocean as a biogeochemical system. We have argued that understanding the biochemical bases of how bacteria interact with the ocean system at the nanometre (molecular) to millimetre scale can provide insights into globally significant biogeochemical processes. Therefore, an understanding of nanoscale biochemistry can be extended hierarchically[151] to the global ocean and the Earth's biogeochemistry. Indeed, some insights are not accessible by large-scale studies alone. We need a robust understanding of microscale biogeochemistry and how it fits with ocean and global biogeochemical studies of all scales. This should result in models of the biochemical bases for the interactions among organisms and the environment.

We need additional methods and instruments that can measure individual bacteria-cell *in situ* growth and respiration rates in natural seawater in three dimensions, without perturbing these assemblages by using filters. It might also be possible to study other basic ecological interactions, such as grazing and phage lysis. Methods and instruments that can be used to study the activities of microorganisms in the context of their ecosystem are on the horizon. They should enable us, for example, to interrogate the chemical and physical characteristics of the environmental architecture in relation to bacterial diversity, distribution and activity. With the current momentum in nanotechnology, nanobiology and advanced imaging we see no reason why microbial ecologists cannot explore the oceans at the nanometre–millimetre scale. Eventually, one goal of microbial oceanographers should be to understand carbon cycling and to visualize microbial interactions that affect the biogeochemical state of the ocean.

Perhaps it is stating the obvious, but we would probably not be concerned for the health of corals or tropical forests if they were invisible. The microscale architecture of the ocean and its relationship with much of the diversity in the sea may well be delicate, and could be sensitive to new patterns of enzyme expression or activity that might arise owing to warming and acidification. It is conceivable that exploration of the ocean at the microscale will yield novel measures of the ocean's biogeochemical state, or ocean health. We stress the need for a concerted research effort in microscale biogeochemistry as a discipline that is integrated with environmental genomic and ecosystem research and climate science.

1. Field, C. B., Behrenfeld, M. J., Randerson, J. T. & Falkowski, P. Primary production of the biosphere: integrating terrestrial and oceanic components. *Science* **281**, 237–240 (1998).
2. Falkowski, P. G., Barber, R. T. & Smetacek, V. Biogeochemical controls and feedbacks on ocean primary production. *Science* **281**, 200–206 (1998).
3. Pauly, D. & Christensen, V. Primary production required to sustain global fisheries. *Nature* **374**, 255–257 (1995).
4. Ocean Biogeochemistry: a Synthesis of the Joint Global Ocean Flux Study (JGOFS) (ed. Fashsam, M. J. R.) (Springer, New York, 2003).
This book describes results from a long-term research program on the role of the ocean carbon cycle in global change.
5. Jackson, J. B. C. *et al.* Historical overfishing and the recent collapse of coastal ecosystems. *Science* **293**, 629–637 (2001).
6. Pauly, D. *et al.* The future for fisheries. *Science* **302**, 1359–1361 (2003).
7. Pomeroy, L. R. Oceans food web, a changing paradigm. *Bioscience* **24**, 499–504 (1974).
An influential paper that proposed that a major fraction of primary production is used by bacteria and other microorganisms.
8. Williams, P. J. L. Microbial contribution to overall marine plankton metabolism: direct measurements of respiration. *Oceanol. Acta* **4**, 359–364 (1981).
9. Azam, F. & Ammerman, J. W. in *Flows of Energy and Materials in Marine Ecosystem* (ed. Fasham, M. J. R.) 345–360 (1984).
10. Steele, J. The Structure of Marine Ecosystems. (Harvard Univ. Press, Massachusetts, 1974).
11. Hobbie, J. E., Daley, R. J. & Jasper, S. Use of nucleopore filters for counting bacteria by fluorescence microscopy. *Appl. Environ. Microbiol.* **33**, 1225–1228 (1977).
12. Fuhrman, J. A. & Azam, F. Bacterioplankton secondary production estimates for coastal waters of British Columbia, Canada, Antarctica, and California, USA. *Appl. Environ. Microbiol.* **39**, 1085–1095 (1980).
13. Hagström, Å., Larsson, U., Horstedt, P. & Normark, S. Frequency of dividing cells: a new approach to the determination of bacterial growth rates in aquatic environments. *Appl. Environ. Microbiol.* **37**, 805–812 (1979).
14. Giovannoni, S. J. & Stingl, U. Molecular diversity and ecology of microbial plankton. *Nature* **437**, 343–348 (2005).
15. DeLong, E. F. & Karl, D. M. Genomic perspectives in microbial oceanography. *Nature* **437**, 336–342 (2005).
An excellent review on the role of microorganisms in marine ecosystems that combined molecular and ecological perspectives.
16. Pomeroy, L. R., Williams, P. J., Azam, F. & Hobbie, E. A. The microbial loop. *Oceanography* **20**, 28–33 (2007).
A concise account of the functioning of the microbial loop in the marine ecosystem.
17. Williams, P. J. I. Incorporation of microheterotrophic processes into the classical paradigm of the planktonic food web. *Kiel. Meeresforsch.* **5**, 1–28 (1981).

18. Azam, F. *et al.* The ecological role of water-column microbes in the sea. *Mar. Ecol. Prog. Ser.* **10**, 257–263 (1983).
19. Ducklow, H. W. & Carlson, C. A. Oceanic bacterial production. *Adv. Microb. Ecol.* **12**, 113–181 (1992).
20. Williams, P. J. I. B. The balance of plankton respiration and photosynthesis in the open oceans. *Nature* **394**, 55–57 (1998).
21. Azam, F. Microbial control of oceanic carbon flux: the plot thickens. *Science* **280**, 694–696 (1998).
22. Hollibaugh, J. T. & Azam, F. Microbial-degradation of dissolved proteins in seawater. *Limnol. Oceanogr.* **28**, 1104–1116 (1983).
23. Ducklow, H. W. The bacterial component of the oceanic euphotic zone. *FEMS Microbiol. Ecol.* **30**, 1–10 (1999).
24. Karl, D. M. Nutrient dynamics in the deep blue sea. *Trends Microbiol.* **10**, 410–418 (2002).
25. Ducklow, H. W. Production and fate of bacteria in the oceans. *Bioscience* **33**, 494–501 (1983).
26. Ducklow, H. W. Modeling the microbial food-web. *Microb. Ecol.* **28**, 303–319 (1994).
27. Cole, J. J., Findlay, S. & Pace, M. L. Bacterial production in fresh and saltwater ecosystems — a cross-system overview. *Mar. Ecol. Prog. Ser.* **43**, 1–10 (1988).
28. Turley, C. M. *et al.* Relationship between primary producers and bacteria in an oligotrophic sea — the Mediterranean and biogeochemical implications. *Mar. Ecol. Prog. Ser.* **193**, 11–18 (2000).
29. Hoppe, H. G., Gocke, K., Koppe, R. & Begler, C. Bacterial growth and primary production along a north–south transect in the Atlantic Ocean. *Nature* **416**, 168–171 (2002).
30. Williams, P. J. I. B. & Bower, D. G. Regional carbon imbalances in the oceans. *Science* **284**, 1735 (1999).
31. Karl, D. M., Laws, E. A., Morris, P., Williams, P. J. I. & Emerson, S. Global carbon cycle (communication arising): metabolic balance of the open sea. *Nature* **426**, 32 (2003).
32. Azam, F., Smith, D. C. & Hollibaugh, J. T. The role of the microbial loop in Antarctic pelagic ecosystems. *Polar Res.* **10**, 239–243 (1991).
33. Pomeroy, L. R., Wiebe, W. J., Deibel, D., Thompson, R. J. & Rowe, G. T. Bacterial responses to temperature and substrate concentration during the Newfoundland spring bloom. *Mar. Ecol. Prog. Ser.* **75**, 143–159 (1991).
34. Pomeroy, L. R. & Wiebe, W. J. Temperature and substrates as interactive limiting factors for marine heterotrophic bacteria. *Aquat. Microb. Ecol.* **23**, 187–204 (2001).
35. Kline, D., Kuntz, N., Brietbart, M., Knowlton, N. & Rohwer, F. The unexpected and critical role of elevated organic carbon in coral mortality. *Mar. Ecol. Prog. Ser.* **314**, 119–125 (2006).
36. Smith, J. E. *et al.* Effects of algae on coral: algal-mediated, microbe-induced coral mortality. *Ecol. Lett.* **9**, 835–845 (2006).
37. Venter, J. C. Environmental genome shotgun sequencing of the Sargasso Sea. *Science* **304**, 66–74 (2004).
38. DeLong, E. F. *et al.* Community genomics among stratified microbial assemblages in the ocean's interior. *Science* **311**, 496–503 (2006).
39. Yooseph, S. *et al.* The Sorcerer II Global Ocean Sampling Expedition: expanding the universe of protein families. *PLoS Biol.* **5**, e16 (2007).
40. Rusch, D. B. *et al.* The Sorcerer II Global Ocean Sampling Expedition: northwest Atlantic through eastern Tropical Pacific. *PLoS Biol.* **5**, e77 (2007).
41. Béjà, O. *et al.* Bacterial rhodopsin: evidence for a new type of phototrophy in the sea. *Science* **289**, 1902–1906 (2000).
42. de la Torre, J. R. *et al.* Proteorhodopsin genes are distributed among divergent marine bacterial taxa. *Proc. Natl Acad. Sci. USA* **100**, 12830–12835 (2003).
43. Azam, F. & Worden, A. Z. Microbes, molecules, and marine ecosystems. *Science* **303**, 1622–1624 (2004).
44. Gray, J. S. *et al.* in *Flows of Energy and Materials in Marine Ecosystems* (ed. Fasham, M. R. J.) 706–723 (Plenum, New York, 1984).
45. Riemann, L. & Middelboe, M. Viral lysis of marine bacterioplankton: implications for organic matter cycling and bacterial clonal composition. *Ophelia* **56**, 57–68 (2002).
46. Barbeau, K., Moffett, J. W., Caron, D. A., Croot, P. L. & Erdner, D. L. Role of protozoan grazing in relieving iron limitation of phytoplankton. *Nature* **380**, 61–64 (1996).
47. Barbeau, K., Kujawinski, E. B. & Moffett, J. W. Remineralization and recycling of iron, thorium and organic carbon by heterotrophic marine protists in culture. *Aquat. Microb. Ecol.* **24**, 69–81 (2001).
48. Grossart, H. P., Riemann, L. & Azam, F. Bacterial motility in the sea and its ecological implications. *Aquat. Microb. Ecol.* **25**, 247–258 (2001).
49. Mitchell, J. G., Pearson, L., Dillon, S. & Kantalis, K. Natural assemblages of marine-bacteria exhibiting high-speed motility and large accelerations. *Appl. Environ. Microbiol.* **61**, 4436–4440 (1995).
50. Mitchell, J. G. *et al.* Long lag times and high velocities in the motility of natural assemblages of marine-bacteria. *Appl. Environ. Microbiol.* **61**, 877–882 (1995).
51. Blackburn, N., Fenchel, T. & Mitchell, J. Microscale nutrient patches in planktonic habitats shown by chemotactic bacteria. *Science* **282**, 2254–2256 (1998).
An experimental demonstration of the response of marine bacteria to organic matter hot spots and a simulation by numerical modelling.
52. Barbara, G. M. & Mitchell, J. G. Bacterial tracking of motile algae. *FEMS Microbiol. Ecol.* **44**, 79–87 (2003).
53. Martinez, J., Smith, D. C., Steward, G. F. & Azam, F. Variability in ectohydrolytic enzyme activities of pelagic marine bacteria and its significance for substrate processing in the sea. *Aquat. Microb. Ecol.* **10**, 223–230 (1996).
54. Arrieta, J. M. & Herndl, G. J. Assessing the diversity of marine bacterial β-glucosidases by capillary electrophoresis zymography. *Appl. Environ. Microbiol.* **67**, 4896–4900 (2001).
55. Kirchman, D. L. & White, J. Hydrolysis and mineralization of chitin in the Delaware Estuary. *Aquat. Microb. Ecol.* **18**, 187–196 (1999).
56. Nagata, T., Meon, B. & Kirchman, D. L. Microbial degradation of peptidoglycan in seawater. *Limnol. Oceanogr.* **48**, 745–754 (2003).
57. Arnosti, C., Durkin, A. S. & Jeffrey, W. H. Patterns of extracellular enzyme activities among pelagic marine microbial communities: implication for cycling of dissolved organic carbon. *Aquat. Microb. Ecol.* **38**, 135–145 (2005).
58. Obayashi, Y. & Suzuki, S. Proteolytic enzymes in coastal surface seawater: significant activity of endopeptidases and exopeptidases. *Limnol. Oceangr.* **50**, 722–726 (2005).
59. Cottrell, M. T., Yu, L. Y. & Kirchman, D. L. Sequence and expression analyses of *Cytophaga*-like hydrolases in a western Arctic metagenomic library and the Sargasso Sea. *Appl. Environ. Microbiol.* **71**, 8506–8513 (2005).
60. Williams, P. J. in *Microbial Production and the Decomposition of Organic Material* Ch. 3 (eds. Kaiser, M., Attrill, M., Jennings, S., Thomas, D. N. & Williams, P. J. le B) (Oxford Univ. Press, 2005).
61. Azam, F. & Hodson, R. E. Multiphasic kinetics for D-glucose uptake by assemblages of natural marine-bacteria. *Mar. Ecol. Prog. Ser.* **6**, 213–222 (1981).
62. Nissen, H., Nissen, P. & Azam, F. Multiphasic uptake of D-glucose by an oligotrophic marine bacterium. *Mar. Ecol. Prog. Ser.* **16**, 155–160 (1984).
63. Riemann, L. & Azam, F. Widespread *N*-acetyl-D-glucosamine uptake among pelagic marine bacteria and its ecological implications. *Appl. Environ. Microbiol.* **68**, 5554–5562 (2002).
64. Alonso, C. & Pernthaler, J. Concentration-dependent patterns of leucine incorporation by coastal picoplankton. *Appl. Environ. Microbiol.* **72**, 2141–2147 (2006).
65. Giovannoni, S. J. *et al.* Genome streamlining in a cosmopolitan oceanic bacterium. *Science* **309**, 1242–1245 (2005).
66. Morris, R. M. *et al.* SAR11 clade dominates ocean surface bacterioplankton communities. *Nature* **420**, 806–810 (2002).
67. Moran, M. A. Genome sequence of *Silicibacter pomeroyi* reveals adaptations to the marine environment. *Nature* **432**, 910–913 (2004).
68. Moran, M. A. *et al.* Ecological genomics of marine Roseobacters. *Appl. Environ. Microbiol.* **73**, 4559–4569 (2007).
69. Blackburn, N., Azam, F. & Hagstrom, A. Spatially explicit simulations of a microbial food web. *Limnol. Oceanogr.* **42**, 613–622 (1997).
70. Koike, I., Hara, S. I., Terauchi, K. & Kogure, K. Role of sub-micrometre particles in the ocean. *Nature* **345**, 242–244 (1990).
A fundamental discovery that showed the existence of highly abundant sub-micrometre organic particles in the ocean.
71. Wells, M. L. & Goldberg, E. Occurrence of small colloids in seawater. *Nature* **353**, 342–344 (1992).
72. Verdugo, P. *et al.* The oceanic gel phase: a bridge in the DOM–POM continuum. *Mar. Chem.* **92**, 67–85 (2004).
An excellent synthesis that showed that organic matter in the sea consists of a gel phase that forms a size continuum. This framework is crucial for understanding the ecology of bacteria and their biogeochemical activities.
73. Chin, W. C., Orellana, M. V. & Verdugo, P. Spontaneous assembly of marine dissolved organic matter into polymer gels. *Nature* **391**, 568–572 (1988).
74. Chin, W. C., Orellana, M. V., Quesada, I. & Verdugo, P. Secretion in unicellular marine phytoplankton: demonstration of regulated exocytosis in *Phaeocystis globosa*. *Plant Cell Physiol.* **45**, 535–542 (2004).
This paper describes how phytoplankton might contribute to the gel phase of seawater by exocytosis.
75. Ogawa, H., Amagai, Y., Koike, I., Kaiser, K. & Benner, R. Production of refractory dissolved organic matter by bacteria. *Science* **292**, 917–920 (2001).
76. Long, R. A. & Azam, F. Abundant protein-containing particles in the sea. *Aquat. Microb. Ecol.* **10**, 213–221 (1996).
77. Alldredge, A. L., Passow, U. & Haddock, S. H. D. The characteristics and transparent exopolymer particle (TEP) content of marine snow formed from thecate dinoflagellates. *J. Plankton Res.* **20**, 393–406 (1998).
78. Smith, D. C., Simon, M., Alldredge, A. L. & Azam, F. Intense hydrolytic enzyme activity on marine aggregates and implications for rapid particle dissolution. *Nature* **359**, 139–142 (1992).
79. Santschi, P. H. *et al.* Fibrillar polysaccharides in marine macromolecular organic matter, as imaged by atomic force microscopy and transmission electron microscopy. *Limnol. Oceanogr.* **43**, 896–908 (1998).
80. Dupres, V. *et al.* Nanoscale mapping and functional analysis of individual adhesins on living bacteria. *Nature Methods* **2**, 515–520 (2005).
81. Dufrêne, Y. F. Nanoscale exploration of microbial surfaces using the atomic force microscope. *Future Microbiol.* **1**, 387–396 (2006).
82. Neu, T. R., Walczysko, P. & Lawrence, J. R. Two-photon imaging for studying the microbial ecology of biofilm systems. *Microb. Environ.* **19**, 1–6 (2004).
83. Decho, A. W. & Kawaguchi, T. Confocal imaging of *in situ* natural microbial communities and their extracellular polymeric secretions (EPS) using nanoplast resin. *BioTechniques* **27**, 1246–1251 (1999).
84. Belas, R., Simon, M. & Silverman, M. Regulation of lateral flagella gene transcription in *Vibrio parahaemolyticus*. *J. Bacteriol.* **167**, 210–218 (1986).
85. Bowen, J. D., Stolzenbach, K. D. & Chisholm, S. W. Simulating bacterial clustering around phytoplankton cells in a turbulent ocean. *Limnol. Oceangr.* **38**, 56–51 (1993).
86. Fenchel, T. & Blackburn, N. Motile chemosensory behaviour of phagotrophic protists: mechanisms for and efficiency in congregating at food patches. *Protist* **150**, 325–336 (1999).
87. Seymour, J. R., Mitchell, J. G. & Seuront, L. Microscale heterogeneity in the activity of coastal bacterioplankton communities. *Aquat. Microb. Ecol.* **35**, 1–16 (2004).
88. Rocap, G., Distel, D. L., Waterbury, J. B. & Chisholm, S. W. Resolution of *Prochlorococcus* and *Synechococcus* ecotypes by using 16s–23s ribosomal DNA internal transcribed spacer sequences. *Appl. Environ. Microbiol.* **68**, 1180–1191 (2002).
89. Johnson, Z. I. *et al.* Niche partitioning among *Prochlorococcus* ecotypes along ocean-scale environmental gradients. *Science* **311**, 1737–1740 (2006).
90. Acinas, S. G. Fine-scale phylogenetic architecture of a complex bacterial community. *Nature* **430**, 551–554 (2004).
This study shows the existence of microscale phylogenetic clusters among marine bacteria assemblages, which has significance for gene diversity and the interaction with ocean systems.
91. Kolber, Z. S., Van Dover, C. L., Niederman, R. A. & Falkowski, P. G. Bacterial photosynthesis in surface waters of the open ocean. *Nature* **407**, 177–179 (2000).
92. Aluwihare, L. I., Repeta, D. J. & Chen, R. F. A major biopolymeric component to dissolved organic carbon in surface sea water. *Nature* **387**, 166–169 (1997).

93. Teira, E., Reinthaler, T., Pernthaler, A., Pernthaler, J. & Herndl, G. J. Combining catalyzed reporter deposition-fluorescence *in situ* hybridization and microautoradiography to detect substrate utilization by bacteria and archaea in the deep ocean. *Appl. Environ. Microbiol.* **70**, 4411–4414 (2004).
94. Cottrell, M. T. & Kirchman, D. L. Single-cell analysis of bacterial growth, cell size, and community structure in the Delaware estuary. *Aquat. Microb. Ecol.* **34**, 139–149 (2004).
Presents a method for the simultaneous phylogenetical and physiological interrogation of individual cells in natural marine assemblages.
95. Rappe, M. S., Connon, S. A., Vergin, K. L. & Giovannoni, S. J. Cultivation of the ubiquitous SAR11 marine bacterioplankton clade. *Nature* **418**, 630–633 (2002).
96. Mourino-Perez, R. R., Worden, A. Z. & Azam, F. Growth of *Vibrio cholerae* O1 in red tide waters off California. *Appl. Environ. Microbiol.* **69**, 6923–6931 (2003).
97. Worden, A. Z. *et al.* Trophic regulation of *Vibrio cholerae* in coastal marine waters. *Environ. Microbiol.* **8**, 21–29 (2006).
98. Hamasaki, K., Long, R. A. & Azam, F. Individual cell growth rates of marine bacteria, measured by bromodeoxyuridine incorporation. *Aquat. Microb. Ecol.* **35**, 217–227 (2004).
99. Fandino, L. B., Riemann, L., Steward, G. F., Long, R. A. & Azam, F. Variations in bacterial community structure during a dinoflagellate bloom analyzed by DGGE and 16s rDNA sequencing. *Aquat. Microb. Ecol.* **23**, 119–130 (2001).
100. Riemann, L., Steward, G. F. & Azam, F. Dynamics of bacterial community composition and activity during a mesocosm diatom bloom. *Appl. Environ. Microbiol.* **66**, 578–587 (2000).
101. Rodriguez, G. G., Phipps, D., Ishiguro, K. & Ridgway, H. F. Use of a fluorescent redox probe for direct visualization of actively respiring bacteria. *Appl. Environ. Microbiol.* **58**, 1801–1808 (1992).
102. Lebaron, P., Servais, P., Agogue, H., Courties, C. & Joux, F. Does the high nucleic acid content of individual bacterial cells allow us to discriminate between active cells and inactive cells in aquatic systems? *Appl. Environ. Microbiol.* **67**, 1775–1782 (2001).
103. Gasol, J. M., Zweifel, U. L., Peters, F., Fuhrman, J. A. & Hagstrom, A. Significance of size and nucleic acid content heterogeneity as measured by flow cytometry in natural planktonic bacteria. *Appl. Environ. Microbiol.* **65**, 4475–4483 (1999).
104. Reinthaler, T. & Herndl, G. J. Seasonal dynamics of bacterial growth efficiencies in relation to phytoplankton in the southern North Sea. *Aquat. Microb. Ecol.* **39**, 7–16 (2005).
105. Reinthaler, T., Winter, C. & Herndl, G. J. Relationship between bacterioplankton richness, respiration, and production in the southern North Sea. *Appl. Environ. Microbiol.* **71**, 2260–2266 (2005).
106. Alonso-Saez, L. *et al.* Large-scale variability in surface bacterial carbon demand and growth efficiency in the subtropical northeast Atlantic Ocean. *Limnol. Oceanogr.* **52**, 533–546 (2007).
107. Del Giorgio, P. A. & Cole, J. J. Bacterial growth efficiency in natural aquatic systems. *Ann. Rev. Ecol. Syst.* **29**, 503–541 (1998).
108. Ouverney, C. C. & Fuhrman, J. A. Combined microautoradiography —16s rRNA probe technique for determination of radioisotope uptake by specific microbial cell types *in situ*. *Appl. Environ. Microbiol.* **65**, 1746–1752 (1999).
109. Malmstrom, R. R., Cottrell, M. T., Elifantz, H. & Kirchman, D. L. Biomass production and assimilation of dissolved organic matter by SAR11 bacteria in the Northwest Atlantic Ocean. *Appl. Environ. Microbiol.* **71**, 2979–2986 (2005).
110. Cottrell, M. T. & Kirchman, D. L. Natural assemblages of marine proteobacteria and members of the *Cytophaga–Flavobacter* cluster consuming low- and high-molecular-weight dissolved organic matter. *Appl. Environ. Microbiol.* **66**, 1692–1697 (2000).
111. Alonso, C. & Pernthaler, J. Incorporation of glucose under anoxic conditions by Bacterioplankton from coastal North Sea surface waters. *Appl. Environ. Microbiol.* **71**, 1709–1716 (2005).
112. Selje, N., Simon, M. & Brinkhoff, T. A newly discovered Roseobacter cluster in temperate and polar oceans. *Nature* **427**, 445–448 (2004).
113. Kirchman, D. L. The ecology of *Cytophaga–Flavobacteria* in aquatic environments. *FEMS Microbiol. Ecol.* **39**, 91–100 (2002).
114. Alonso, C., Warnecke, F., Amann, R. & Pernthaler, J. High local and global diversity of *Flavobacteria* in marine plankton. *Environ. Microbiol.* **9**, 1253–1266 (2007).
115. Mayali, X. & Azam, F. Algicidal bacteria in the sea and their impact on algal blooms. *J. Eukaryot. Microbiol.* **51**, 139–144 (2004).
116. Bidle, K. D. & Azam, F. Accelerated dissolution of diatom silica by marine bacterial assemblages. *Nature* **397**, 508–512 (1999).
Reports the surprising finding that marine assemblages that do not require silicon mediate and regulate the dissolution of diatom frustules, by proteolytically removing the proteoglycan that can protect the frustule from dissolving. This has implications for carbon and silicon cycles in the ocean.
117. Bell, W. H., Lang, J. M. & Mitchell, R. Selective stimulation of marine bacteria by algal extracellular products. *Limnol. Oceanogr.* **19**, 833–839 (1974).
118. Rooney-Varga, J. N. *et al.* Links between phytoplankton and bacterial community dynamics in a coastal marine environment. *Microb. Ecol.* **49**, 163–175 (2005).
119. Grossart, H. P., Levold, F., Allgaier, M., Simon, M. & Brinkhoff, T. Marine diatom species harbour distinct bacterial communities. *Environ. Microbiol.* **7**, 860–873 (2005).
120. Sapp, M. *et al.* Species-specific bacterial communities in the phycosphere of microalgae? *Microb. Ecol.* **53**, 683–699 (2007).
121. Wild, C. *et al.* Coral mucus functions as an energy carrier and particle trap in the reef ecosystem. *Nature* **428**, 66–70 (2004).
122. Trick, C. G., Harrison, P. & Anderson, R. J. Extracellular secondary metabolite production by the marine dinoflagellate *Prorocentrum minimum* in culture. *Can. J. Fish. Aquat. Sci.* **38**, 864–867 (1981).
123. Mitchell, J. G., Pearson, L. & Dillon, S. Clustering of marine bacteria in seawater enrichments. *Appl. Environ. Microbiol.* **62**, 3716–3721 (1996).
124. Smith, D. C., Steward, G. F., Long, R. A. & Azam, F. Bacterial mediation of carbon fluxes during a diatom bloom in a mesocosm. *Deep-Sea Res. II* **42**, 75–97 (1995).
125. Alldredge, A. L., Passow, U. & Logan, B. E. The abundance and significance of a class of large, transparent organic particles in the Ocean. *Deep-Sea Res. I* **40**, 1131–1140 (1993).
Reports the finding of abundant mucopolysaccharide particles from 2 to 200 µm in length. These particles provide large surface areas for bacterial interactions and activities.
126. Malmstrom, R. R., Kiene, R. P. & Kirchman, D. L. Identification and enumeration of bacteria assimilating dimethylsulfoniopropionate (DMSP) in the North Atlantic and Gulf of Mexico. *Limnol. Oceanogr.* **49**, 597–606 (2004).
127. Gonzalez, J. M. *et al. Silicibacter pomeroyi* sp nov and *Roseovarius nubinhibens* sp nov., dimethylsulfoniopropionate-demethylating bacteria from marine environments. *Int. J. Syst. Evol. Microbiol.* **53**, 1261–1269 (2003).
128. Miller, T. R., Hnilicka, K., Dziedzic, A., Desplats, P. & Belas, R. Chemotaxis of *Silicibacter* sp. strain TM1040 toward dinoflagellate products. *Appl. Environ. Microbiol.* **70**, 4692–4701 (2004).
129. Yoch, D. C., Ansede, J. H. & Rabinowitz, K. S. Evidence for intracellular and extracellular dimethylsulfoniopropionate (DMSP) lyase and DMSP uptake sites in two species of marine bacteria. *Appl. Environ. Microbiol.* **63**, 3182–3188 (1997).
130. Howard, E. C. *et al.* Bacterial taxa that limit sulfur flux from the ocean. *Science* **314**, 649–652 (2006).
131. Moran, M. A., González, J. M. & Kiene, R. P. Linking a bacterial taxon to organic sulfur cycling in the sea: studies of the marine Roseobacter group. *Geomicrobiol. J.* **20**, 375–388 (2003).
132. Lovelock, J. E., Maggs, R. J. & Rasmussen, R. A. Atmospheric dimethyl sulphide and the natural sulphur cycle. *Nature* **237**, 452–453 (1972).
133. Azam, F. & Smith, D. C. in *Particle Analysis in Oceanography* (ed. Demers, S.) 213–235 (Springer-Verlag, Berlin, 1991).
134. Richardson, T. L. & Jackson, G. A. Small phytoplankton and carbon export from the surface ocean. *Science* **315**, 838–840 (2007).
135. Landry, M. R. & Calbet, A. Microzooplankton production in the oceans. *ICES J. Mar. Sci.* **61**, 501–507 (2004).
136. Hagstrom, A., Azam, F., Andersson, A., Wikner, J. & Rassoulzadegan, F. Microbial loop in an oligotrophic pelagic marine ecosystem — possible roles of cyanobacteria and nanoflagellates in the organic fluxes. *Mar. Ecol. Prog. Ser.* **49**, 171–178 (1988).
137. Biddanda, B. A. & Pomeroy, L. R. Microbial aggregation and degradation of phytoplankton-derived detritus in seawater.1. Microbial succession. *Mar. Ecol. Prog. Ser.* **42**, 79–88 (1988).
138. Mueller, R. S. *et al. Vibrio cholerae* strains possess multiple strategies for abiotic and biotic surface colonization. *J. Bacteriol.* **189**, 5348–5360 (2007).
139. Kroger, N., Lorenz, S., Brunner, E. & Sumper, M. Self-assembly of highly phosphorylated silaffins and their function in biosilica morphogenesis. *Science* **298**, 584–586 (2002).
140. Hedges, J. I. *et al.* Evidence for non-selective preservation of organic matter in sinking marine particles. *Nature* **409**, 801–804 (2001).
141. Turley, C. M. & Stutt, E. D. Depth-related cell-specific bacterial leucine incorporation rates on particles and its biogeochemical significance in the Northwest Mediterranean. *Limnol. Oceanogr.* **45**, 419–425 (2000).
142. Alldredge, A. L., Cole, J. J. & Caron, D. A. Production of heterotrophic bacteria inhabiting macroscopic organic aggregates (marine snow) from surface waters. *Limnol. Oceanogr.* **31**, 68–78 (1986).
143. Cho, B. C. & Azam, F. Major role of bacteria in biogeochemical fluxes in the ocean's interior. *Nature* **332**, 441–443 (1988).
144. Kiorboe, T. & Jackson, G. A. Marine snow, organic solute plumes, and optimal chemosensory behavior of bacteria. *Limnol. Oceanogr.* **46**, 1309–1318 (2001).
This paper presents a model of marine snow colonized by bacteria that solubilize organic matter, and shows that an extended plume of DOM persists behind the sinking marine snow, which attracts bacteria from surrounding seawater. It predicts that half of the organic matter that is used in the sea by bacteria is from these microenvironments.
145. Azam, F. & Long, R. A. Oceanography — sea snow microcosms. *Nature* **414**, 495–498 (2001).
146. Helmstetter, C. E. & Cummings, D. J. An improved method for the selection of bacterial cells at division. *Biochim. Biophys. Acta* **82**, 608–610 (1964).
147. Lochte, K. & Turley, C. Bacteria and cyanobacteria associated with phytodetritus in the deep-sea. *Nature* **333**, 67–69 (1988).
148. Oliver, J. L., Barber, R. T., Smith, W. O. & Ducklow, H. W. The heterotrophic bacterial response during the Southern Ocean iron experiment (SOFeX). *Limnol. Oceanogr.* **49**, 2129–2140 (2004).
149. Bauer, M. *et al.* Whole genome analysis of the marine *Bacteroidetes 'Gramella forsetii'* reveals adaptations to degradation of polymeric organic matter. *Environ. Microbiol.* **8**, 2201–2213 (2006).
This paper presents whole-genome analyses of a marine *Bacteroidetes* spp. and makes a prediction about its adaptive biology that is important for the solubilization and degradation of particulate organic matter in the ocean.
150. Azam, F., Smith, D. C., Steward, G. F. & Hagstrom, Å. Bacteria-organic matter coupling and its significance for oceanic carbon cycling. *Microb. Ecol.* **28**, 167–179 (1994).
151. Allen, T. Scale in microscopic algal ecology: a neglected dimension. *Phycologia* **16**, 253–257 (1977).

Acknowledgements
We thank T. Hollibaugh, G. Steward, D. Smith and J. Fuhrman for insightful comments on the manuscript. This work was supported by the Gordon and Betty Moore Foundation and grants to F.A. from the National Science Foundation.

Competing interests statement
The authors declare no competing financial interests.

DATABASES
Entrez Genome Project: http://www.ncbi.nlm.nih.gov/entrez/query.fcgi?db=genomeprj
Candidatus Pelagibacter ubique | *Emiliania huxleyi* | *Pavlova lutheri* | *Pseudoalteromonas haloplanktis* | *Shewanella putrefaciens* | TM1040

ALL LINKS ARE ACTIVE IN THE ONLINE PDF

ERRATUM

Microbial structuring of marine ecosystems

Farooq Azam and Francesca Malfatti

Nature Reviews Microbiology **5**, 782–791 (2007), doi: 10.1038/nrmicro1747

In the above article, an arrow was missing from figure 1. The correct figure is shown below. In the same article, the legend to figure 4 should have indicated that the figure was first published in reference 145. We wish to apologize to the author, and to readers, for any confusion caused.

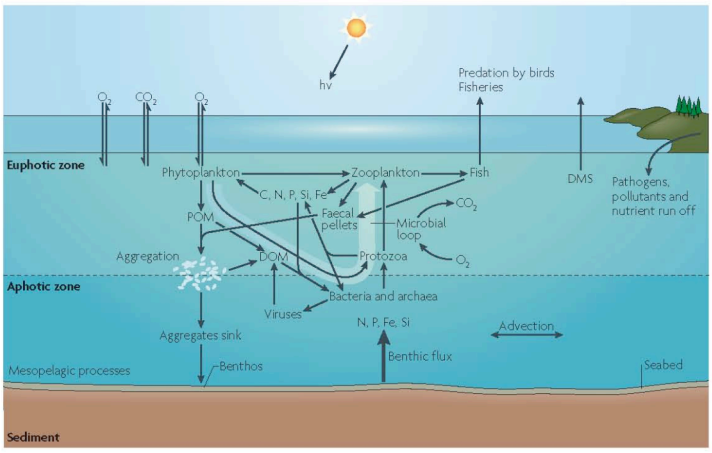

CORRIGENDUM

Microbial structuring of marine ecosystems

Farooq Azam and Francesca Malfatti

Nature Reviews Microbiology **5**, 782–791 (2007), doi: 10.1038/nrmicro1747

In the above article, the following passage of text on page 783 might have been misleading: 'The detection of high abundances of decomposer bacteria (10^6 per $ml^{[1]}$) has led to the suggestion that the numbers and activity of primary producers (such as cyanobacteria and algae), decomposers (such as bacteria) and predators (such as viruses and protists) are similar (Fig. 1).' It should have read: 'The detection of high abundances of decomposer bacteria (10^6 per $ml^{[1]}$) has led to the suggestion that every microlitre of seawater contains all the components of the microbial loop: primary producers (such as cyanobacteria and algae), decomposers (such as bacteria) and predators (such as viruses and protists) (Fig. 1).' The authors apologize to the readers for any confusion caused.

The text in Chapter II, in full, is a reprint of the material, as it appears in 'Nature Review of Microbiology' 5 (10): 782-791: Azam, F., Malfatti, F. (2007). Microbial structuring of marine ecosystems.

III

Major role of microbes in carbon fluxes during austral winter in the southern Drake Passage

Major role of microbes in carbon fluxes during austral winter in the southern Drake Passage

M. Manganelli[1,4*], F. Malfatti[2,4*], T.J. Samo[2], B.G. Mitchell[3], H. Wang[3] & F. Azam[2]

[1]Istituto Superiore per la Prevenzione e la Sicurezza del Lavoro (ISPESL) - DIPIA, via Fontana Candida 1, 00040 Monteporzio Catone (RM), Italy. [2]Marine Biology Research Division, 0202, Scripps Institution of Oceanography, University of California San Diego, La Jolla, California 92093, USA. [3]Integrative Oceanography Division, 0218, Scripps Institution of Oceanography, University of California San Diego, La Jolla, California 92093, USA

[4]These authors contributed equally to this work.

Abstract: Carbon cycling in Southern Ocean is a major issue in climate change, and currently little is known about biogeochemical dynamics during the dark winter. Here we show that in winter, when the primary production is greatly reduced, *Bacteria* and *Archaea* become the major producers of biogenic particles, at the expense of dissolved organic carbon drawdown. Heterotrophic production and chemoautotrophic CO_2 fixation rates were substantial and bacterial populations were controlled by protists and viruses. A dynamic food web is also consistent with temporal and spatial variations in archaeal and bacterial communities that might exploit various niches. Thus, the Southern Ocean microbial loop may substantially maintain a wintertime food web and system respiration at the expense of DOC as well as regenerate nutrients and iron. Our

findings have important implications for Southern Ocean ecosystem functioning and carbon cycle and its manipulation by iron enrichment to achieve net sequestration of atmospheric CO2.

Introduction. The Southern Ocean plays a crucial role in the global carbon cycle, exerting a major control on atmospheric CO_2 concentration, hence the need to understand the role of biota in the regulation of carbon fixation and cycling. It is a large and heterogeneous biogeochemical system. The coastal and ice edge waters experience intense spring and summer blooms-- mainly diatoms and *Phaeocystis*-- that support a food web via zooplankton and krill to penguins and whales. In contrast, the open ocean is the largest high-nutrients low-chlorophyll (HNLC) area, characterized by low primary productivity (PP), mainly iron-limited, as demonstrated by several iron enrichment experiments[1]. Iron fertilization to stimulate net phytoplankton growth has been proposed as one method for mitigating rising atmospheric CO_2[(ref. 2)]. Yet, the fate of the carbon accumulating in the productive areas during summertime or in artificially fertilized areas is critical to how biological forces make the Southern Ocean a source or a sink for carbon. There is much interest in whether the southern ocean food web is dominated by microbial loop processes-- as in tropical and temperate oligotrophic ocean[3,4]. Previous studies showed weak bacteria-PP coupling and ascribed this to temperature restriction of dissolved organic matter (DOM) utilization[5], limited DOM availability[6] or strong grazing

pressure[6,7]. However, others found that bacteria use substantial PP[8,9, 10,11, 12]. The differences may reflect the heterogeneity of Southern Ocean.

Results and Discussion. We studied an area that had strong gradients of chlorophyll-*a* (*Chl a*) (0.05 to 0.74 μg *Chl a* l^{-1}) from oligotrophic ACC waters to east of Shackleton Transverse Ridge (STR) (Fig. 1a, b). The ACC current is steered south by STR and mixes with the iron rich Shelf water, stimulating high PP downstream[13]. During a summer (2004) and a winter (2006) cruise in Southern Drake Passage (Fig. 1a) we studied microbial communities and processes during sharply contrasting productivity regimes. Our goal was to address the significance of the microbial loop in carbon fluxes and food web dynamics particularly in winter.

In summer (2004) we sampled only the epipelagic layer (~67m). Bacterial abundance ($1.9 \times 10^8 \pm 0.9 \times 10^8$ l^{-1} s.d.), bacterial carbon production (BCP) (0.63 ± 0.57 μg C $l^{-1}d^{-1}$ s.d.) and growth rates (μ) (0.16 ± 0.14 d^{-1} s.d.) (Fig. 2) were in the low end of the range for other oligotrophic regions. They were positively correlated with *Chl a* (Spearman R, $p<0.05$, BCP vs *Chl* a R=0.49, μ vs *Chl* a R=0.46, n=21). Carbon flux into bacteria as fraction of co-local PP is a measure of the strength of bacteria-organic matter (OM) coupling. In summer, BCP was equivalent to ~30% of PP in low chlorophyll ACC waters and ~ 13% in high PP mixed water. Assuming bacterial growth efficiency (BGE) of 20-36%[14,15] the bacterial carbon demand (BCD) over the whole area would be 40-72% of PP. Thus, bacteria-OM coupling was robust and comparable to other oligotrophic and

mesotrophic waters. (Yet, it would spare ~1/2 of PP, some of which could accumulate and support the wintertime food web.)

In winter (2006) we occupied 38 stations and sampled depths from surface to 300-750 m (Fig. 1a). In the epipelagic layer, as expected, *Chl a* and PP were much lower than in summer (Fig. 1b and Table 1) yet, bacterial abundance was similar to summer and these populations were active in terms of μ and BCP (Fig. 2). Although our summer sampling was limited, the winter and summer ranges for both μ and BCP were comparable. Indeed, the winter bacterial abundance, BCP and μ in our study area were comparable to those reported for low latitude oligotrophic systems such as the central North Pacific gyre and Sargasso Sea. Bacteria were also abundant and active in the mesopelagic layer, and could mediate significant carbon flux. The mesopelagic bacteria abundances were within a factor of 2 and mesopelagic BCP and μ were comparable to their ranges in the epipelagic layer (Fig. 2). Notably, the high BCP at depth was due to higher μ (0.70 d^{-1} at 400 m; Fig. 2). Thus, wintertime bacterial populations throughout the epipelagic and mesopelagic layers were abundant, growing and displayed substantial carbon demand. Further, since PP was greatly reduced in winter the epipelagic PP was ~3 fold *lower* than BCP and an order of magnitude *lower* than BCD (estimating epipelagic BCD at BGE ~39%[15]). PP could therefore have supported only ~10% of BCD and majority of BCD must have been met by sources other than the contemporaneous PP.

We compared summer and winter data on an areal basis to assess possible sources of carbon to support bacteria in winter (Table 1). SeaWiFS composite images of summer

2006 (Jan-Mar) for our study area showed a *Chl a* pattern similar to 2004; so we assume that summer 2004 values can be applied to summer 2006. Mesopelagic BCD would usually be met by sinking POC (or DOC mixing from surface[16]). In our area sinking particles from contemporaneous PP in winter could have supported only ~3% of mesopelagic BCD even if, improbably, all PP sank into the mesopelagial. Since sinking POC could not have supported winter mesopelagic BCD, DOC is a likely source. DOC accumulated in the upper 200 m in the productive summer (Fig. 3a), presumably as slow-to-degrade components of phytoplankton production which evadee attack by the summer bacterial communities. In winter DOC was very low (36.5 $\pm$ 2.8 μM s.d.; Fig. 3a), in the low range of persistent background[17]. The summer-to-winter DOC decline (37.4 g C m^{-2} in the epipelagic zone and 82.8 g C m^{-2} in the mesopelagic zone; Table 1) would suffice to support the observed BCD. In terms of carrying capacity the DOC drawdown could have supported the epipelagic BCD for ~570 d and mesopelagic BCD for ~365 d. At a lower BGE (20%[14]) it would have supported BCD for ~297 d (epipelagic) and ~196 d (mesopelagic). Integrating over the entire water column, the DOC drawdown would be 120.0 g C m^{-2}, enough to support BCD for ~220 - 410 d, depending on the BGE. The excess DOC drawdown may indicate a lower BGE since energy requirement to utilize semi-refractory DOM in winter may be higher. Alternatively, the excess DOC may have had other fate (s), such as POC → DOC transformation and currently unrecognized biotic sinks.

Interestingly, the winter POC pool, although not sustainable by the meager surface PP, was persistent and vertically homogeneous (Fig. 3b). It may be comprised of

refractory non-sinking organic matter. Alternatively, it may be produced dynamically from DOC by polymer cross-linking (above) and provide organic rich microenvironments for bacterial growth in winter. This would be consistent with significant bacterial growth rates and carbon cycling during winter.

In winter bacteria produced biomass at 110 mg C m^{-2} d^{-1} (Table 1), a source of protein rich biomass potentially available to all particle-feeding organisms (depending on the state of bacterial aggregation). Our data on protist and virus abundances from a limited number of stations support the hypothesis of a dynamic bacterial community channeling DOM-carbon to protists and on to larger animals[18]. A strong predation pressure is consistent with the observed low variability in bacterial biomass despite substantial growth. Protist abundance was $3.2 \times 10^5 \pm 0.9 \times 10^5$ cell l^{-1} s.d. (in the range reported for summer in Southern Ocean[19]). Assuming ingestion rate of 0.1-7.8 bacteria $HNF^{-1}h^{-1}$[19] protists would consume 1% to >200% of our winter BCP. Bacteria/protists ratio of ~400 is within the range of other Antarctic surface waters where significant grazing rates have been measured[19,20]. Viruses were also likely a significant source of bacterial mortality since they persisted at substantial populations ($1.4 \times 10^9 \pm 0.4 \times 10^9$ l^{-1} s.d.) comparable to a summer study in the Drake Passage[21]. Virus/bacteria ratio was 6 – 22 (abundance/abundance), found typically in marine waters, including a summer study in Southern ocean that showed significant virus induced bacteria mortality[22]. Thus, BCP could have supported carbon flux to protists and possibly on to larger animals; and an active viral loop that might enhance system respiration[22, 23].

We considered that in addition to heterotrophic BCP there might also be chemoautotrophic production[24], probably due to *Archaea*[24,25]. Dark $^{14}CO_2$ assimilation in winter 2006 showed significant but highly variable carbon fixation (Supplementary Fig. 1), 0.1-40 ng C $l^{-1}d^{-1}$ corresponding to 7.4 $\pm$ 13.8 % s.d. of the total prokaryotic carbon production. For the near surface experiments we cannot exclude a potential contribution of dark CO_2 fixation by phytoplankton; however this is probably insignificant, since the incubations lasted from 55 to 100h and further we did not find a significant correlation between DIC uptake and *Chl a (not shown)*. While our measurements were limited it would be important to determine whether chemoautotrophic production in winter is a significant factor in the Southern Ocean carbon cycle in a broader geographical context.

Bacterial community shifts might be expected between summer and winter productivity regimes[26, 27]. We addressed this by denaturing gradient gel electrophoresis (DGGE) and 16S rRNA sequence analysis for both *Bacteria* and *Archaea*. *Bacteria* communities were different in summer and winter (Supplementary Table 1; Supplementary Fig. 2). In summer, in the epipelagic layer, we detected only seven *Bacteria* phylotypes (and six *Eukarya* plastids)— three *α-Proteobacteria*, three CFB and one *γ-Proteobacteria*. All had 99-100% sequence homology to known uncultured *Bacteria*. Winter epipelagic samples had much greater community richness—24 phylotypes—possibly reflecting molecular complexity of available substrates. All winter phylotypes had 98-100% sequence similarity to uncultured *Bacteria* from environmental clone libraries, the majority (17/24) of them from Antarctic or Arctic waters. (We were successful in culturing one of the phylotypes). However, the seasonal variation was great.

Only one phylotype, a *γ-Proteobacteria* (displaying100 % sequence similarity to an uncultured Arctic bacteria) was present both in summer and winter epipelagic samples.

In winter we also analyzed mesopelagic samples. Most (23/27) *Bacteria* phylotypes were common with the winter epipelagic phylotypes and only 4 were unique to the mesopelagic communities (and these displayed 100% sequence similarity with uncultured environmental bacteria). The clear and major shift in *Bacteria* community composition and richness between summer and winter was likely in response to changes in productivity regime and the nature and concentration of organic matter[28] (and possibly other environmental factors as well).

We might expect *Archaea*, which exploit different niches[26,27], to respond differently than *Bacteria*. In winter, in the epipelagic layer, we detected 12 archaea phylotypes compared with 6 in summer (Supplementary Fig. 3). As was the case for *Bacteria,* archaea community richness was also greater in winter than in summer. However, unlike *Bacteria,* all 6 summer archaea phylotypes were also present in winter (Supplementary Table 1). Five of 6 were *Euryarchaeota* and one was *Crenarchaeota*, and all 6 showed 97-98% sequence similarity to uncultured Arctic or Antarctic *Archaea*. Six *Archaea* unique to winter were all *Euryarchaeota* and showed 97- 99% sequence similarity to uncultured Arctic and Antarctic *Archaea*.

Of the 12 epipelagic *Archaea* in winter 9 were present also in the mesopelagic zones, where we also found 2 phylotypes unique to the mesopelagic zone (98% sequence similarity to uncultured Arctic *Archaea*).

Both *Crenarchaeota* and *Euryarchaeota* have been shown to incorporate DIC[23] and this is consistent with our finding of DIC incorporation. The *Crenarchaeota* (EF640727) DGGE band was very intense in Shelf samples where DIC uptake was the highest. It would be interesting to determine if this *Crenarchaeota* is a significant autotrophic producer. Our results support the hypothesis that bacterial phylotypes are more affected by environmental variable associated with summer to winter transition than *Archaea*[27].

Conclusion. This study has shown that active and dynamic *Bacteria* and *Archaea* communities in Southern Ocean play a significant role in Antarctic food web and biogeochemical dynamics through the austral winter. They maintain substantial rates of secondary productivity during protracted periods of diminished primary productivity. They reset the system by organic matter decomposition and nutrient regeneration—setting the stage for the next summer. Our results have important implications for models of the functioning of Antarctic Ocean ecosystem and carbon cycle. The persistence of high microbial loop activity causing strong wintertime system net heterotrophy is highly relevant to considerations of the efficacy of Southern Ocean iron enrichment to control the level of atmospheric CO_2.

Acknowledgments: We thank the captain, crews, and RPSC support staff aboard the R/Vs Laurence M. Gould (2004) and Nathaniel B. Palmer (2006) for help working in

the Drake Passage. This research was supported by US NSF Office of Polar Program and other NSF grants to F.A. M.M. was mainly funded by ISPESL (Istituto Superiore per la Prevenzione e la Sicurezza del Lavoro, Italy).

Literature cited

1. PW. Boyd, et al., Science 315, 612-617 (2007).

2. K.O. Buesseler, *et al*., *Science* **319**, 162 (2008).

3. J. Cole, S. Findlay, M.L. Pace, *Mar Ecol Progr Ser* **43**, 1-10 (1988)

4. B.C. Cho, F. Azam, *Mar Ecol Progr Ser* **63**, 253-259 (1990)

5. L.R. Pomeroy, W.J. Wiebe, *Aquat Microb Ecol* **23**, 187-204 (2001).

6. D.F. Bird, D.M. Karl, *Aquat Microb Ecol* **19**, 13-27 (1999).

7. C.M. Duarte, *et al*., *Limnol. Oceanogr*. **50**, 1844-1854 (2005).

8. X.A.G. Moran, J.M. Gasol, C. Pedros-Alio, M. Estrada, *Mar Ecol Progr Ser* **222**, 25-39 (2001).

9. I. Obernosterer, *et al*., *Deep Sea Res. II* **55**, 777-789 (2008).

10. G.F. Cota, S.T. Kottmeier, D.H. Robinson, W.O. Smith Jr., C.W. Sullivan, *Deep Sea Res*. **37**, 1145-1167 (1990).

11. S.T. Kottmeier, C.W. Sullivan, *Mar Ecol Progr Ser* **36**, 287-298 (1987).

12. R.B. Hanson, D. Shafer, T. Ryan, D.H. Pope, H.K. Lowery, *Appl. Environ. Microbiol*. **45**, 1622-1632 (1983).

13. B.M. Hopkinson, *et al*., *Limnol. Oceanogr*. **52**, 2540-2554 (2007).

14. C.A. Carlson, N.R. Bates, H.W. Ducklow, D.A. Hansell, *Aquat Microb Ecol* **19**, 229-244 (1999).

15. R.B. Rivkin, L. Legendre, *Science* **291**, 2398-2400 (2001).

16. C.A. Carlson, H.W. Ducklow, A.F. Michaels, *Nat* **371**, 405-408 (1994).

17. C.J. Wiebinga, H.J.W. de Baar, *Mar. Chem*. **61** 185-201 (1998).

18. F. Azam, D.C. Smith, J.T. Hollibaugh, *Pol Res* **10**, 239-243 (1991).

19. D. Vaqué, N. Guixa-Boixereu, J.M. Gasol, C. Pedros-Alio, *Deep Sea Res. II* **49**, 847-867 (2002).

20. U. Christaki, *et al*. *Deep Sea Res. II* **55**, 706-719 (2008).

21. D.C. Smith, G.F. Steward, *Antarctic Journal of the United States* **27,** 125. Academic Search Complete. EBSCO. [UCSD Library], [La Jolla], [CA]. http://search.ebscohost.com/login.aspx?direct=true&db=a9h&AN=9604166608&site=ehost-live>.

22. O. Bonilla-Findji, *et al*. *Deep Sea Res. II* **55**, 790-800 (2008).

23. J.A. Fuhrman, *Nature*, **399**, 541–548 (1999).

24. S.G. Horrigan, *Limnol. Oceanogr.* **26**, 378-382 (1981).

25. G.J. Herndl, *et al*. *Appl. Environ. Microbiol*. **71**, 2303-2309 (2005).

26. A.E. Murray, *et al. Appl. Environ. Microbiol*. **64**, 2585-2595 (1998).

27. M.J. Church, *et al*. *Limnol. Oceanogr.* **48**, 1893-1902 (2003)

28. C.A. Carlson, *et al*. *Limnol. Oceanogr.* **49**, 1073-1083 (2004)

29. S. Lee, J.A. Fuhrman, *Appl. Environ. Microbiol*. **53**, 1298-1303 (1987).

30. M.D. Doval, X.A. Alvarez-Salgado, C.G. Castro, F.F. Pérez, *Deep Sea Res. II* **49**, 663-674 (2002).

Supporting Online Material.

*To whom correspondence should be addressed. E-mail: maura.manganelli@ispesl.it; fmalfatt@ucsd.edu

Table 3.1 Areal data from summer 2004 and winter 2006 cruises. All parameters for the summer cruise have been integrated over the entire euphotic layer (1% incident PAR at surface; it was similar to the mixed layer depth or deeper). The winter PP has been integrated over the euphotic layer while other parameters have been integrated over the mixed layer depth (epipelagic) and from there down to 750 m (mesopelagic) layers. Averages and standard deviation in parenthesis.

PP=primary production; BCP=bacterial carbon production; Summer excess DOC=summer dissolved organic carbon values minus winter background value (36.5 $\pm$ 2.8 μM C s.d.); BCD=bacterial carbon demand (BCP/bacterial growth efficiency); N.D.=not determined.

* BCD calculated using a bacterial growth efficiency derived by the curve in ref. [14] (~36% in summer and 39% in winter)

** BCD calculated using bacterial growth efficiency of 20%[13]

§ no s.d. reported because the value is derived from a single depth profile

° DOC data for winter are not reported, since they are considered as persistent background values, and have been used to determine summer excess DOC.

		Number of stations	Depth of integration (m)	PP (mg C m^{-2} d^{-1})	BCP (mg C m^{-2} d^{-1})	Summer excess DOC (g C m^{-2})	BCD* (mg C m^{-2} d^{-1})	BCD** (mg C m^{-2} d^{-1})
Summer	Epipelagic	10	65 (17)	354.8 (197.1)	51.9 (30.7)	37.4 (18.8)	143.1 (87.0)	255.0 (153.2)
	Mesopelagic	1	685 §	-	N.D.	82.8 §	N.D.	N.D.
Winter	Epipelagic	38	156 (75)	7.6 (5.4)	25.2 (21.3)	°	65.2 (55-0)	126.1 (106.5)
	Mesopelagic	38	600 (64)	-	84.5 (90.5)	°	227.2 (249.0)	422.3 (452.3)

Table 3.1

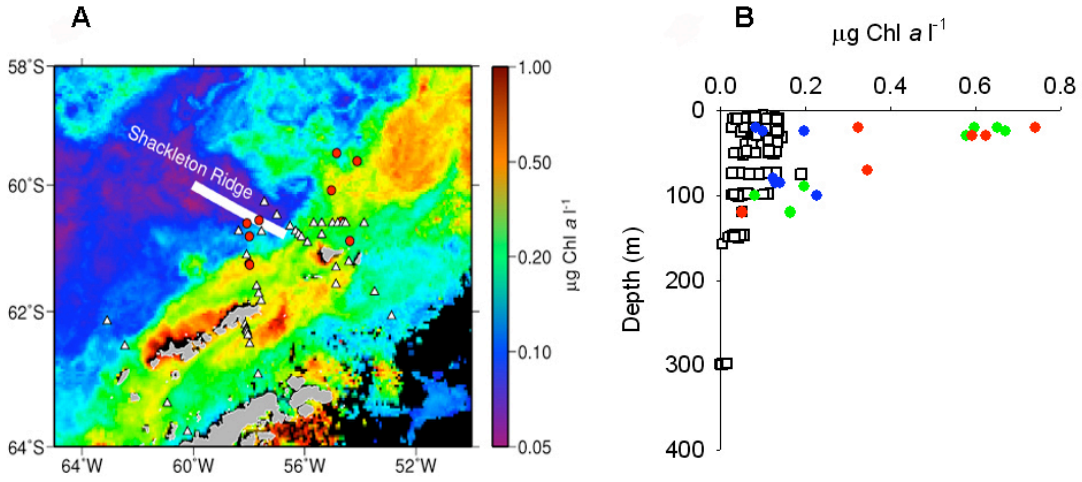

Figure 3.1. (A) MODIS-Aqua composite image of the chlorophyll-*a* gradient during 2004 summer. Red dots: summer 2004 sampling stations; white triangles: winter 2006 sampling stations. **(B)** Depth profile of chlorophyll-*a* (*Chl a*) from summer 2004 cruise (blue circles=ACC water; green circles=mixed water; red circles=shelf water) and winter 2006 cruise (empty squares).

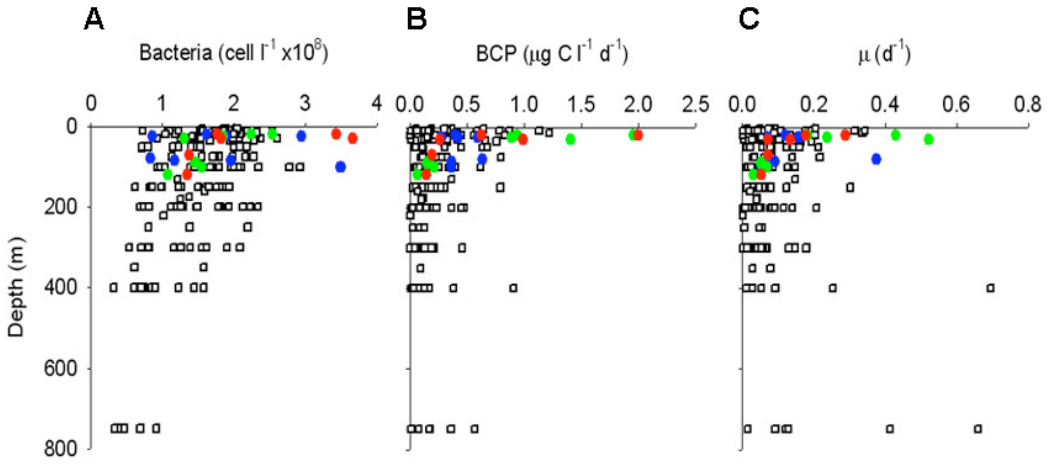

Figure 3.2. Depth profile of bacterial parameters in summer 2004 and winter 2006.

(A) Bacterial abundance; **(B)** BCP=bacterial carbon production; BCP calculated from ^{3}H-Leucine incorporation, employing a conversion factor of 3.1 kg C per mol of Leu; **(C)** µ=bacterial growth rate. Cell-specific growth rate calculations assumed 20 fg C per cell[29]. Winter data are from 32 stations from 5 to 400 m; at 6 stations samples were also taken from 750 m. Summer: blue circles=ACC water; red circles=shelf water; green circles=mixed water; empty square= Winter.

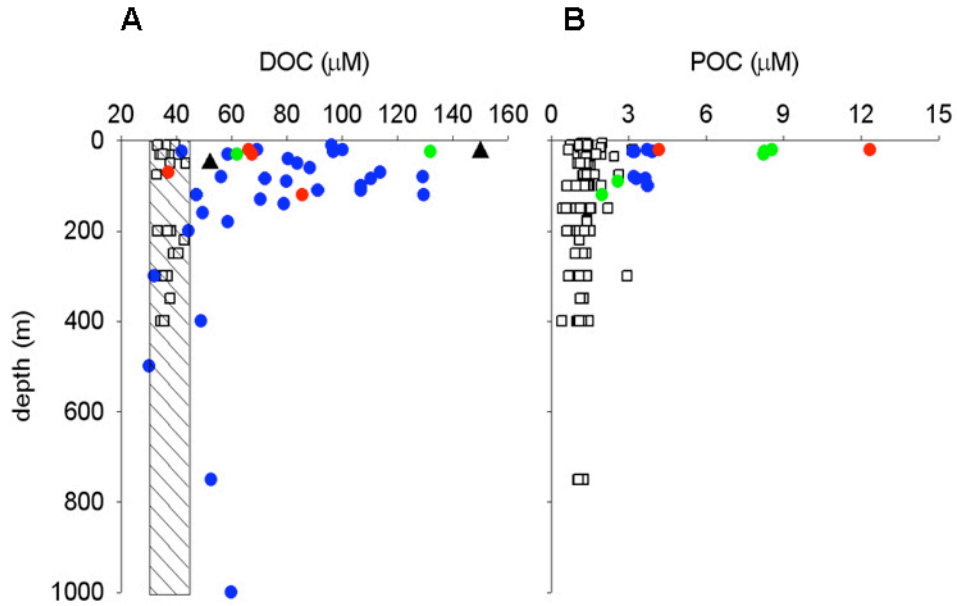

Figure 3.3. Depth distribution of organic matter pools during summer and winter cruises. **(A)** DOC=Dissolved organic carbon. The data presented are measurements of total organic carbon, but since POC represents a negligible contribution to total organic carbon (POC represented only between 7% and 2% of the total pool) we can consider the analysis as DOC values**.** The shaded area covers the range of winter concentration. For a comparison, a range of variations of DOC from the FRUELA cruise study area in summer (Gerlache Strait, Bransfield Strait and Bellinghausen Strait)[30] has been reported (black triangles). **(B)** POC=Particulate organic carbon. Summer 2004: blue circles=ACC water; red circles=shelf water; green circles=mixed water. empty square: winter 2006.

Supporting On Line Material for

Major role of microbes in carbon fluxes during austral winter in the southern Drake Passage

M. Manganelli[1,4*], F. Malfatti[2,4*], T.J. Samo[2], B.G. Mitchell[3], H. Wang[3] & F. Azam[2]

[1]Istituto Superiore per la Prevenzione e la Sicurezza del Lavoro (ISPESL) - DIPIA, via Fontana Candida 1, 00040 Monteporzio Catone (RM), Italy. [2]Marine Biology Research Division, 0202, Scripps Institution of Oceanography, University of California San Diego, La Jolla, California 92093, USA. [3]Integrative Oceanography Division, 0218, Scripps Institution of Oceanography, University of California San Diego, La Jolla, California 92093, USA

[4]These authors contributed equally to this work.

*To whom correspondence should be addressed. E-mail:

maura.manganelli@ispesl.it; fmalfatt@ucsd.edu

This file contains:

Materials and Methods

Chlorophyll-*a* was determined by high performance liquid chromatography HPLC (S1). Net primary production was estimated by a modification of the VGPM (Vertically Generalized Productivity Model) (S2). The model was parameterized for the Antarctic temperature range considering a large dataset of ^{14}C PP measurements, including ~ 30 stations for each of our cruises.

Bacteria, viruses and protists were counted by epifluorescence microscopy. For bacteria and protists, samples were DAPI stained and filtered onto a 0.2 μm polycarbonate black filter (Nuclepore). For viruses, samples were fixed with 0.5% paraformaldehyde, and stored at -80°C until analysis. 1 to 3 ml of samples were filtered onto 0.02 μm Anodisc filter and stained with SybrGreen (S3).

Heterotrophic production was measured by ^{3}H-leucine method (S4) in 4 hours dark incubations, at *in situ* temperature. Chemotrophic production was measured by $DI^{14}C$ incorporation (10 to 50 μCi of sodium^{14}C-carbonate final concentration) in 55-100 hours dark incubations (S5) at *in situ* temperature.

Shifts in bacterial community composition were analyzed by polymerase chain reaction (PCR) amplification of a portion of the bacterial 16S rRNA gene, followed by DGGE and sequencing. Bacterial community DNA was extracted

from 500 ml of seawater filtered onto 0.2 μm SUPOR-200 polyhetersulfone filters (S6). Bacterial 16S rRNA genes amplification and DGGE were performed as in ref. S7. Archaeal 16S rRNA gene fragments ~ 190 bp long for DGGE analysis were generated by nested PCR. The first PCR was performed using specific 21f and 958r primers and PCR conditions (S8). The resulting PCR products were used as templates for the second PCR, which was performed with an *Archaea*-specific 344f, and a universal 517r (S9), at the same reaction conditions used for *Bacteria*. The denaturant gradients in DGGE was of 30-60% for *Bacteria* and 20-55% for *Archaea* top to bottom (where 100% is defined as 7 M urea and 40% vol/vol formamide). Eluted gene fragments from selected bands were cloned using the TOPO-TA cloning kit (Invitrogen) and sequenced by Agencourt.The sequences submitted to GenBank are available under accession numbers listed in Supplementary Table 1.

POC was measured with a CHN elemental analyzer as in Ref (10). TOC samples were acidified (pH 2) with ultrapure HCl and stored in precombusted glass vials at 4°C until analysis with a Shimadzu TOC 5000A.

Statistical differences were tested with non parametric tests, with the software Statistica 6.0 (Statsoft); Kolmogorov-Smirnov test was applied to test differences between means and Spearman R to correlate two variables.

S1. L. Van Heukelem, C.S. Thomas, *J. Chromatogr. A*, **910**, 31-49 (2001).

S2. M.J. Behrenfeld, P.G. Falkowski, *Limnol. Oceanogr*. **42**, 1-20 (1997).

S3. A. Patel, *et al*. *Nature Protocols* **2**, 269 - 276 (2007).

S4. D.C. Smith, F. Azam, *Mar. Microb. Food Webs* **6**, 107-114 (1992).

S5. G.J. Herndl, *et al*. *Appl. Environ. Microbiol*. **71**, 2303-2309 (2005).

S6. K.H. Boström, K. Simu, Å. Hagström, L. Riemann, *Limnol. Oceanogr.: Methods* **2**, 365-373 (2004).

S7. L. Riemann, *et al*. *Deep Sea Res. II*, **46**, 1791-1811 (1999).

S8. DeLong, E.F. *PNAS* **89**, 5685-5689 (1992).

S9. N. Bano, S. Ruffin, B. Ransom, J.T. Hollibaugh, *Appl. Environm. Microbiol.* **70**, 781-789 (2004).

S10. B.M. Hopkinson, et al., Limnol. Oceanogr. 52, 2540-2554 (2007).

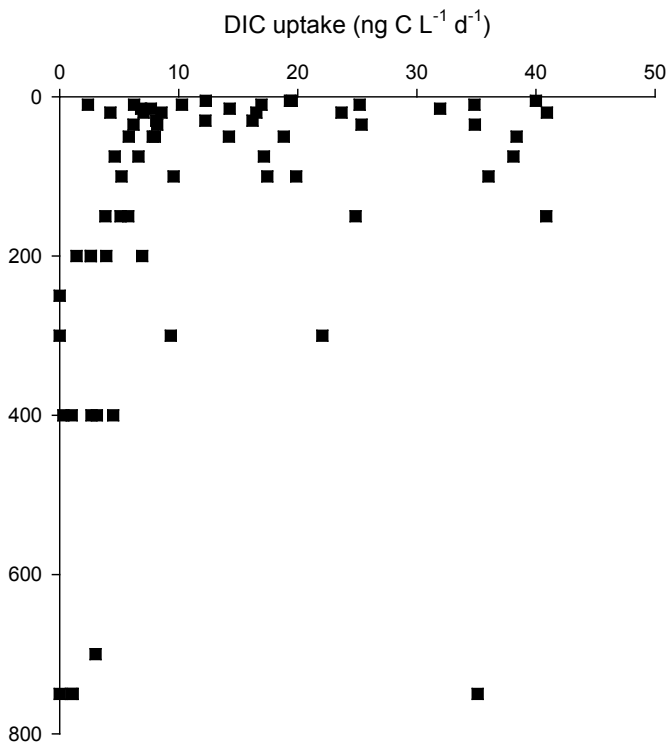

Figure 3.4-S1 Depth profile of chemotrophic carbon production in winter 2006. DIC=dissolved inorganic carbon

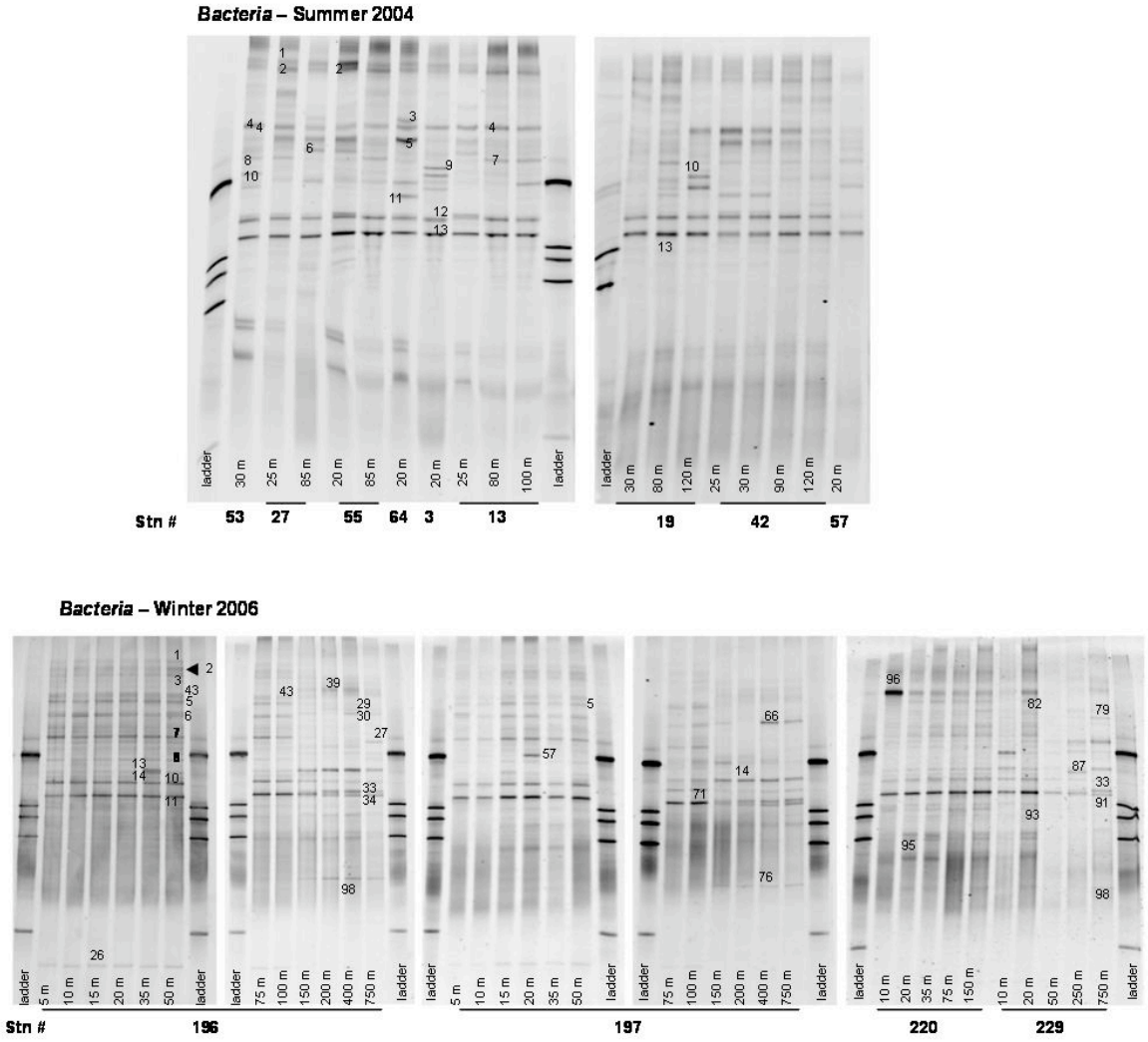

Figure 3.5-S2 DGGE fingerprint of *Bacteria* amplicons from Summer 2004 and Winter 2006 samples. The numbered bands have been excised for sequencing.

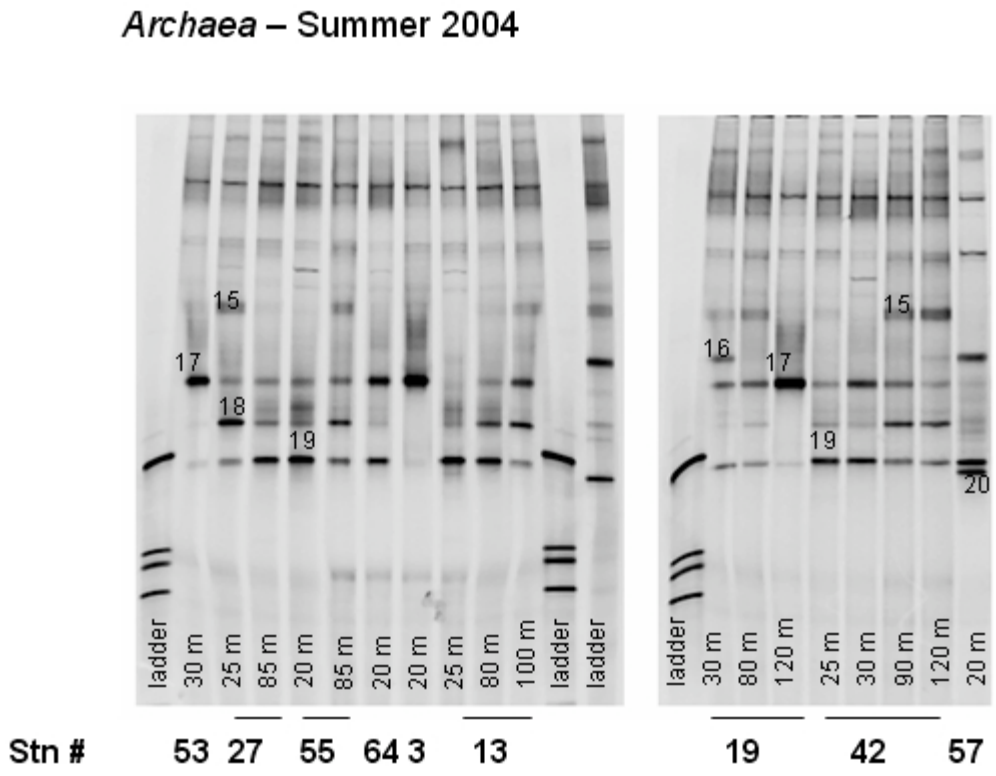

Figure 3.6-S3 DGGE fingerprint of *Archaea* amplicons from Summer 2004 and Winter 2006 samples. The numbered bands have been excised for sequencing.

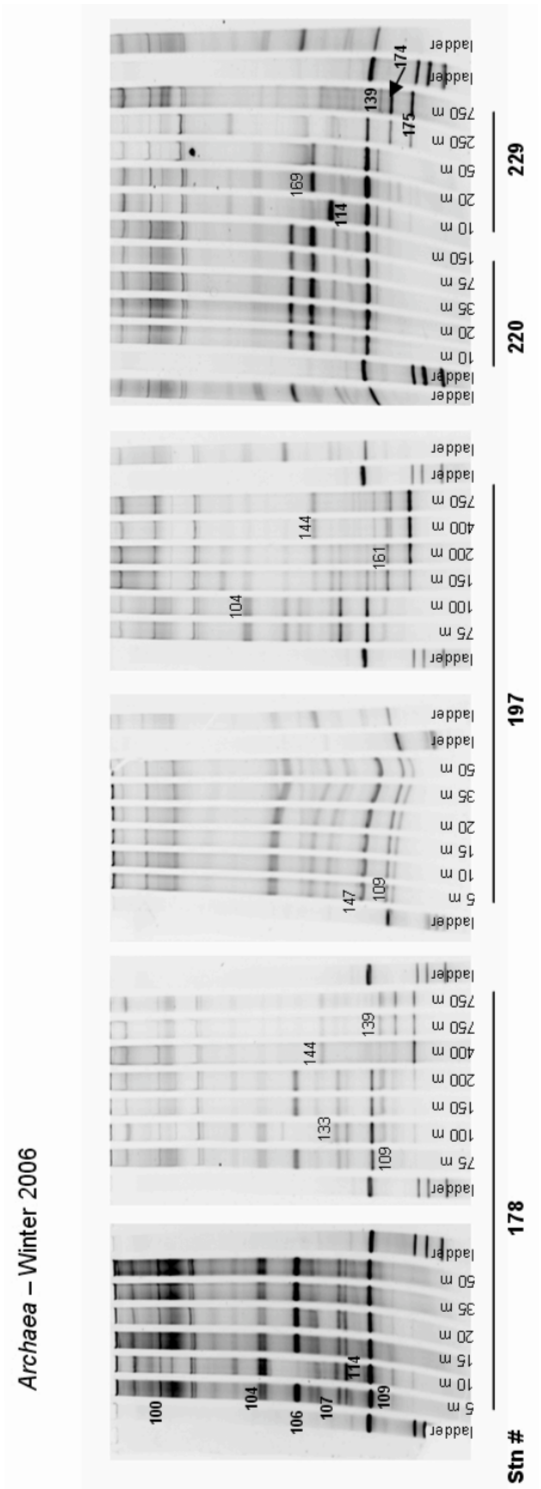

Figure 3.6-S3 continued

Table 3.2-S1 List of GenBank accession number and closest relatives to 16S rDNA sequences obtained from Summer 2004 and Winter 2006 DGGE.

*phylotypes found in both seasons

Clone ID	Accession number	Band number	Percentage identity	Closest relative	Phylogenetic group
			Bacteria		
Summer 2004					
DPEU01	EF127653	1	100%	Uncultured Cytophagales bacterium Arctic97A-14	Bacteroidetes
DPEU02	EF127654*	2	100%	Uncultured γ proteobacterium	γ Proteobacteria
DPEU04	EF127656	3	97%	Uncultured phototrophic eukaryote, chloroplast	Eukarya
DPEU05	EF127657	4	99%	Uncultured eukaryote clone S2-72, chloroplast	Eukarya
DPEU07	EF127659	5	99%	Uncultured phototrophic eukaryote clone MPWIC_C08	Eukarya
DPEU08	EF127660	6	99%	Uncultured bacterium clone LV_38	Bacteroidetes
DPEU09	EF127661	7	99%	Uncultured marine bacterium	Bacteroidetes
DPEU10	EF127662	8	98%	Uncultured marine eukaryote	Eukarya
DPEU11	EF127663	9	100%	Uncultured phototrophic eukaryote, chloroplast	Eukarya
DPEU12	EF127664	10	100%	Uncultured bacterium	Eukarya
DPEU14	EF127666	11	99%	Uncultured Roseobacter sp.	α Proteobacteria
DPEU15	EF127667	12	99%	Uncultured Rhodobacteraceae bacterium	α Proteobacteria
DPEU16	EF127668	13	100%	Uncultured α proteobacterium	α Proteobacteria

Table 3.2-S1 continued

Clone ID	Accession number	Band number	Percentage identity	Closest relative	Phylogenetic group
			Bacteria		
Winter 2006					
DPEUW01	EF648172*	1	100%	Uncultured proteobacterium DPEU02	γ Proteobacteria
DPEUW02	EF648173	2	99%	Uncultured Bacteroidetes bacterium DPCF20	Bacteroidetes
DPEUW03	EF648174	3	99%	Uncultured marine bacterium clone KG_C11_100m18	γ Proteobacteria
DPEUW04	EF648175	5	100%	Uncultured prasinophyte clone OM5	Eukarya
DPEUW05	EF648176	6	100%	Uncultured marine bacterium clone KG_A3_120m16	γ Proteobacteria
DPEUW06	EF648177	7	100%	Uncultured marine bacterium clone AntCL2E12	Bacteroidetes
DPEUW07	EF648178	8	100%	Uncultured prasinophyte clone LS-E12 chloroplast	Eukarya
DPEUW08	EF648179	10	100%	Uncultured bacterium clone SG_116	α Proteobacteria
DPEUW09	EF648180	11	100%	Uncultured gamma proteobacterium clone SBI04_1	γ Proteobacteria
DPEUW10	EF648181	13	100%	bacterium Antarctica-16	γ Proteobacteria
DPEUW11	EF648182	14	100-99%	Uncultured delta proteobacterium Arctic95C-5	δ Proteobacteria
DPEUW12	EF648183	26	100%	Uncultured marine bacterium Ant4E12	Actinobacteria
DPEUW13	EF648184	27	100%	Psychrobacter sp. wp30 isolate wp30	γ Proteobacteria
DPEUW14	EF648185	29	99%	Uncultured bacterium clone Arctic6-G12	γ Proteobacteria
DPEUW15	EF648186	30	99%	Uncultured gamma proteobacterium Arctic96BD-19	γ Proteobacteria
DPEUW16	EF648187	33	100%	Uncultured bacterium clone PB_53	α Proteobacteria
DPEUW17	EF648188	34	100%	Uncultured bacterium clone EI_91	α Proteobacteria
DPEUW18	EF648189	39	100%	Uncultured alpha proteobacterium CTD44B	α Proteobacteria

Table 3.2-S1 continued

Clone ID	Accession number	Band number	Percentage identity	Closest relative	Phylogenetic group
			Bacteria		
Winter 2006					
DPEUW19	EF648190	43	98%-100%	Uncultured marine bacterium clone ANT10A4	γ Proteobacteria
DPEUW20	EF648191	57	100%	Uncultured beta proteobacterium MoDE-9	β Proteobacteria
DPEUW21	EF648192	66	100%	Uncultured Alcanivorax sp.	γ Proteobacteria
DPEUW22	EF648193	71	100%	Uncultured marine bacterium clone KG_A3_120m134	γ Proteobacteria
DPEUW23	EF648194	76	100%	Uncultured bacterium clone CTD005-4B-02	α Proteobacteria
DPEUW24	EF648195	79	99%	Uncultured bacterium clone CTD005-74B-02	Bacteroidetes
DPEUW25	EF648196	82	100%	Uncultured marine bacterium clone AntCL1D8	γ Proteobacteria
DPEUW26	EF648197	87	100%	Uncultured Pseudoalteromonas sp. clone JL-BS-K75	γ Proteobacteria
DPEUW27	EF648198	91	100%	Uncultured alpha proteobacterium clone T41_120	α Proteobacteria
DPEUW28	EF648199	93	98%	Aequorivita lipolytica Y10-2T	Bacteroidetes
DPEUW29	EF648200	95	100%	Uncultured gamma proteobacterium clone SBI04_175	γ Proteobacteria
DPEUW30	EF648201	96	98%	Uncultured phototrophic eukaryote DL27-11	Eukarya
DPEUW31	EF648202	98	100%	Uncultured clone CTD005-31B-02	Actinobacteria

Table 3.2-S1 continued

Clone ID	Accession number	Band number	Percentage identity	Closest relative	Phylogenetic group
				Archaea	
Summer 2004					
DPAR02	EF640719*	15	98%	Uncultured archaeon clone iBSZ2f.80	Euryarchaeota
DPAR03	EF640720*	16	97%	Uncultured crenarchaeote clone FB04aw.90	Crenarchaeota
DPAR04	EF640721*	17	98%	Uncultured euryarchaeote clone M05a039.03	Euryarchaeota
DPAR05	EF640722*	18	97%	Uncultured marine group III euryarchaeote clone HF770_038E01	Euryarchaeota
DPAR06	EF640723*	19	97%	Uncultured euryarchaeote clone FB04ai.76	Euryarchaeota
DPAR07	EF640724*	20	98%	Uncultured euryarchaeote 97D-131-22A	Euryarchaeota
Winter 2006					
DPARW01	EF640725	100	97%	Uncultured euryarchaeote clone FB04aw.35	Euryarchaeota
DPARW02	EF640726*	104	100%	Uncultured marine archaeon clone DPAR02	Euryarchaeota
DPARW03	EF640727*	106	100%	Uncultured marine archaeon clone DPAR03	Crenarchaeota
DPARW04	EF640728	107	98%	Uncultured euryarchaeote AM-20A_123	Euryarchaeota
DPARW05	EF640729*	109	100%	Uncultured marine archaeon clone DPAR06	Euryarchaeota
DPARW06	EF640730*	114	100%	Uncultured marine archaeon clone DPAR05	Euryarchaeota
DPARW07	EF640731	133	99%	Uncultured archaeon clone CTD005-2A	Euryarchaeota
DPARW08	EF640732*	139	100%	Uncultured marine archaeon clone DPAR07	Euryarchaeota
DPARW09	EF640733	144	97%	Uncultured euryarchaeote 97E-131-20	Euryarchaeota
DPARW10	EF640734	147	99%	Uncultured euryarchaeote 97D-235-10	Euryarchaeota
DPARW11	EF640735	161	97%	Uncultured marine euryarchaeote DH148-W1	Euryarchaeota
DPARW12	EF640736*	169	100%	Uncultured marine archaeon clone DPAR04	Euryarchaeota
DPARW13	EF640737	174	98%	Uncultured euryarchaeote 95B-131-15H	Euryarchaeota
DPARW14	EF640738	175	98%	Uncultured euryarchaeote 97E-131-15	Euryarchaeota

Chapter III has been submitted to Plos One as: M. Manganelli, F. Malfatti, T.J. Samo, B.G. Mitchell, H. Wang and F. Azam - Major role of microbes in carbon fluxes during austral winter in the southern Drake Passage.

IV

High-resolution imaging of pelagic bacteria by Atomic Force Microscopy and implications for carbon cycling

High-resolution imaging of pelagic bacteria by Atomic Force Microscopy and implications for carbon cycling

Francesca Malfatti[1*], Ty J. Samo[1] and Farooq Azam[1]

[1]*Marine Biology Research Division, 0202, Scripps Institution of Oceanography, University of California San Diego, La Jolla, California 92093, USA.*

** Corresponding author: fmalfatt@ucsd.edu*

ABSTRACT: Marine bacteria are important players in the ocean's carbon cycle. In microbial oceanography cell volume, size-frequency distribution and carbon content of pelagic bacteria and archaea ("bacteria") are critical parameters in ecophysiology and functions of bacteria in the food web and carbon cycle. We used Atomic Force Microscopy (AFM) to create high-resolution images of pelagic bacteria and Synechococcus cells. This allowed us to measure cell height, Z, and to compute the volume of live and formalin fixed bacteria. Exhaustive AFM imaging was combined with imaging by epifluorescence microscopy (EFM) using current protocols as well as two new epifluorescence protocols developed in this study based on a protein and a lipid stain. This study provides a reliable basis for bacteria volume determination as well as shows that previous EFM-based measurements DAPI may have significantly (~50%) underestimated bacterial volume and bacterial carbon pool in the ocean. Our results show that fixation and drying flatten the cells to greatly reduce Z, and a 3-D ellipse better approximates the resulting bacterial shape. AFM-based bacteria height measurements provide insights into *in situ* physiology, live-dead bacteria, and in situ phage-bacteria

interactions. This study refines the methodology for quantifying bacteria-mediated carbon fluxes and the role of bacteria in marine ecosystems as well as suggests the potential of AFM for individual cell physiological interrogations in the natural marine assemblages.

INTRODUCTION

Marine bacteria are important players in oceanic biogeochemical cycles (Pomeroy et al. 2007). Through their action they control the fate of the fixed carbon in the ecosystem (Azam et al. 1994). Their role is variable and the strength of coupling between primary carbon production and bacterial carbon demand is a critical factor in dictating the net trophic state of the system (Azam & Malfatti 2007). We gained this knowledge over the last three decades when scientists started measuring respiration rates (del Giorgio & Williams 2005) and growth rates (Fuhrman & Azam 1980, 1982) and visualizing marine bacteria by epifluorescence microscopy, EFM (Hobbie et al. 1977) and by electron microscopy (Sieburth 1975, Johnson & Sieburth 1982). The visualization of marine bacteria, the majority being dominated by diminutive cells, can be considered a capstone event in marine microbial ecology (Hobbie et al. 1977). The introduction of EFM investigation using a nucleic acid specific stain, acridine orange, on a black polycarbonate filter by Hobbie and coworkers (1977) has made broadly accessible to the scientific community imaging marine bacteria form different oceanic environments. After the discovery of large populations of bacteria (and more recently archaea as well) the next challenge has been to size the cells and compute the biovolume in order to quantify the flux of carbon though the microbial compartment. Since the late ’70 many studies have addressed this challenge to estimate correctly the size of marine bacteria (for a

review see (Fuhrman 1981, Sieracki et al. 1985, Suzuki et al. 1993)). There are two main steps in sample preparation: fixation procedures and the staining dyes. We know that fixatives such as formaldehyde cross-link proteins and nucleic acid (Gustavson 1956, Nie et al. 2007) and consequently the cell shrinks. Different dyes might have more or less quantum yield (Cosa et al. 2001) and staining of the nucleic acid content might not be an optimal choice since the nucleoid does not represent the cell size as it shown in the transmission electron micrographs of seawater samples (Johnson & Sieburth 1982). It is important to have accurate measurements of cell size and bacterial biovolume in order to quantify how much carbon is taken up and becomes biomass and how much carbon is respired by marine bacteria in the ocean ecosystem.

Imaging technology has advance greatly in the past decades. More high-resolution instruments are available now that can be used to address many more questions about bacteria ecology at the microscale in the ocean. Live cell imaging is a good strategy to approach the study of marine bacteria. Laser scanning confocal microscopy with environmental chamber and Atomic Force Microscope (AFM) are versatile tools that allow high-resolution imaging *in vivo*, in natural liquid environmental conditions (Dufrene 2002, 2008). We used AFM in order to visualize the shape and the size (width, length, height) of marine bacteria from fixed and living specimens from different environments. AFM (Binning & Quate 1986) belongs to the family of scanning proximity probe microscope. It feels the 'near-field' physical interaction forces between the scanning probe and the surface sample. A cantilever carries at its end a sharp probe that is scanned over the sample. The continuous attraction-repulsion forces experienced during the scan cause probe deflection. The movement is then transmitted to the cantilever that is

monitored via interferometry in laser-photodector system. This constant attraction-repulsion movement of the cantilever creates a high-resolution 3D map of the surface of the specimen.

In this study we imaged by AFM marine bacteria from diverse pelagic oceanic provinces. We asked what were the shapes, the surface morphology, and size distribution of marine bacteria. We imaged living cells by AFM and formalin fixed cells to document whether biovolume estimates are influenced by sample treatment. We then compared AFM biovolume estimates with EFM estimates and we tested whether the use of different dyes, targeting nucleic acid or proteins or lipids, will affect measuring the size of marine bacteria.

MATERIAL AND METHODS

Sampling and processing. Seawater samples collected at different locations (Table 1) were fixed with 0.2-μm-filtered formaldehyde solution (2% final concentration) and kept at 4°C until further processing. Within 24 h a sample aliquot was filtered either on a 0.2 μm Isopore polycarbonate filter (Millipore Corp.) or a 0.02 μm aluminum oxide Anodisc filter (Whatman). Filters were rinsed with 0.02 μm filtered Milli-Q water (Millipore Corp.) and let dry, face-up, on a tissue paper while being covered by a Petri dish cover. Filters were then stored at -20°C until further analysis.

Epifluorescence Microscopy (EFM)

Staining Protocol. We compared different stains targeting specific cell component: DNA stains DAPI (4',6-diamidino-2- Phenylindole; H-1200, Vector

laboratories Inc.) and SYBRGold® (S-11494, Invitrogen Corp.); protein stain NanoOrange® (N-6666, Invitrogen Copr.); and lipid stain NAO (10-N-nonyl acridine orange; 74395, Sigma-Aldrich).

DAPI staining. The samples, prepared on polycarbonate or anodisc filters as above, mouned on a clean glass slide. A 5 µl drop of DAPI VECTASHIELD solution was spotted on the slide and the filter was placed on it face up. A cover slip with a 5 µl drop of DAPI VECTASHIELD was placed on the filter (Fuchs et al. 2007).

SYBRGold® staining. Anodisc filters were stained and mounted as in Noble and Fuhrman (Noble & Fuhrman 1988, Patel et al. 2007). The wet filter was placed on a drop of SYBRGold®, 2.5/1000 final concentration, for 15 min in the dark at RT. Then the filter was dried and mounted with an antifading solution. The dry filter was placed, face up, on a 5 µl drop of the moviol mounting medium on a slide and a cover slip with a drop of SYBRGold® and moviol mounting medium (1:15 final concentration) was then place on the filter (Lunau et al. 2005).

NanoOrange® staining. The polycarbonate filter, once dry, was placed on a drop of moviol on a glass slide. A 5 µl solution of moviol mounting medium and NanoOrange®, (Grossart et al. 2000) was spotted on a cover slip. The cover slip was put on the filter.

NAO staining. NAO is a vital dye; the seawater sample was incubated with 10 µl NAO per 1ml of sample (stock solution 1 mg ml^{-1} in 100% ethanol) in the dark for 5 minutes at RT. NAO can also stain fixed samples. The NAO solution, final concentration 2 µg ml^{-1}, was mixed with the mounting medium (moviol or SYBRGold® mounting

medium and DAPI VECTASHIELD) and subsequently applied to the cover slip as described in the previous staining protocols.

EFM. Once stained, the filters were visualized immediately at the epifluorescence microscope, Olympus BX51 at 1000x final magnification. DAPI is excited at 345 nm and emits at 458 nm. SYBRGold® is excited at 495 nm and emits at 539 nm. NanoOrange® is excited at 485 nm and emits at 590 nm. NAO is excited at 494 nm and emits at 519 nm. Pictures were taken and bacteria were sized with the freeware software Image J (http://rsbweb.nih.gov/ij/). The software was calibrated with a picture of the stage micrometer at 1000x magnification. From 50 to 100 cells were measured per sample.

Biovolume Estimation. We estimated cell biovolume by the formula $V=(\pi*W^2)/4 * (L-W/3)$ (where L is the length and W is the width) (Bratbak 1985). The assumption is that bacterial shape is either similar to a cylinder with two hemispheres at its ends, where W=Z or similar to a sphere where W=Z=L.

Another formula e.g. because of flattening during fixation and drying that can be applied to calculate biovolume, if the cell shape is thought to approximate a prolate solid, a 3D ellipse: $V=4/3\pi*a*b*c$ (with a,b,c the semi axes of the solid). This formula has recently been proposed in a study on marine bacteria with AFM by Nishino et al. (Nishino et al. 2004). It requires measuring W, L and Z.

Bacterial cultures. We streaked bacterial isolates from the -80°C stock pure cultures, on ZoBell solid medium (5 g peptone, 1 g yeast, 1 g agar in 1 liter GF/F filtered seawater). After 24 h, a colony was picked and inoculated into liquid ZoBell medium

overnight. Bacteria cells were centrifuged at 9000x g for 5 min and washed twice with 0.02 μm filtered autoclaved seawater (FASW) and resuspended in FASW. Bacteria cells were fixed, washed from the medium and filtered as described above for EFM and AFM.

Atomic Force Microscopy

Sample preparation.

Imaging in air. The sample was treated as above. With a sterile scissor a piece of filter was cut and was attached to a glass slide with double sided sticky tape or held in place with mini magnets (1/16"x1/32", AmazingMagnets.com). Additionally, for selected samples 50 μl of fixed seawater was spotted on freshly cleaved mica and let dry completely and rinsed. Then the mica was affixed to a slide with double sided sticky tape (Veeco Instruments, Santa Barbara). This set up allowed simultaneous EFM and AFM imaging so, a cell could be first identified by EFM then scanned with AFM (Malfatti and Azam, submitted).

Synechococcus epifluorescence microscopy (EFM)-identification. We used EFM prior to AFM imaging in order to make positive identification of *Synechococcus*. Freshly cleaved (0.2 μm thick) mica disc (# 50; Ted Pella Inc.; # 71856-01, Electron Microscopy Sciences), reduced in thickness with a clean razor blade, was affixed on a microscopy slide using double sided sticky tape. (Note that the tape is strongly autofluorescent, so it must be placed at the edges of mica disk in order to prevent excessive background fluorescence). Seawater was spotted on mica, dried and washed with HPLC water (W5-4; Fisher). On the mica we identified, at 400x, *Synechococcus* cells based on phycoerythrin

autofluorescence (filter set 51006; Chroma). We then acquired AFM scans in air of the EFM identified *Synechococcus* cells on mica (Malfatti and Azam, submitted).

Imaging in liquid. Seawater was collected and immediately filtered onto a 0.2 µm Anodisc filter (Whatman). The filter was then placed on a glass slide, held with mini magnets and overlaid with FASW.

AFM imaging. AFM imaging was performed with MFP-3D BIO (Asylum Research, Santa Barbara, USA). In this configuration the AFM is mounted on an inverted epifluorescence microscope (Olympus IX 51). The images were acquired in AC mode. The cantilever carries at its end a probe that interacts with the sample. The cantilever is acoustically driven to oscillate at its residence frequency. Once the probe approaches the sample, the lever oscillation amplitude is reduced proportionally to the sample topography. The scan rates were between 0.64 and 1 Hz. Image size was 256x256 or 512x512. In air, we used a silicon nitride cantilever (AC160TS; Olympus) with a spring constant of 42 N/m. In liquid, we used a Au/Cr coated silicon nitride cantilever (TR400PB; Olympus) with a spring constant of 0.02 N/m.

AFM image analysis. We recorded trace and retrace of height, amplitude, phase and Z sensor channels. Topography images were processed with Planfit and Flatten functions. Bacteria were sized with the measuring tool part of the Igor Pro 6.03A MFP3D 070111+830 software. Briefly, a ruler can be drawn on the object of interest to delineate the topographic profile and measure the three dimensions.

RESULTS

We imaged by AFM >950 individual bacteria and 27 *Synechococcus* cells off Scripps Pier (referred to as *coastal*), 350 bacteria were from Southern California Current System (referred to as *CCE*) and 450 from Southern Polar Ocean (referred to as *Antarctic*) in Austral winter (Table 1). (Additional data on AFM images was presented in Malfatti and Azam; submitted). We also imaged bacterial isolates BBFL7 (*Cytophaga-Flavobacteria*; genome sequenced), TW6 and TW7 (*Alteromonadales;* genome sequenced) and SWAT3 (*Vibrionacea;* genome sequenced).

Bacteria shape and size

In AFM images the heterotrophic bacteria were predominantly rods, cocci, C-shaped and S-shaped (Figure 1-2). We cannot rule out that other morphologies were present but could not be definitively distinguished from gels and colloids that are typically present abundantly in seawater samples. *Synechococcus* cells were either cocci or rods. The bacterial isolates BBFL7 and TW7 were rod shaped whereas TW6 was s-shape. The size of bacteria in the natural assemblages ranged from <0.2 μm to 2μm. It is noteworthy that very small and very large bacteria typically co-occurred in the same sample of seawater.

Cell volume comparison by AFM and EFM

Since standard EFM protocol requires fixed, filtered and dried samples we did AFM imaging also on parallel seawater samples treated similarly in order to assess the effect of technique. (Live cell were also imaged; below). EFM samples were stained with

DAPI since DAPI is the most commonly used fluorophores for counting and sizing pelagic bacteria (so, a large body of contextual data on DAPI-based cell volumes exists from around the World ocean). An advantage of AFM is that in addition to length (L) and width (W) it also enables height (Z) measurement. We calculated volume as $V = (\pi*W^2)/4 * (L-W/3)$, where L is the length and W is the width (Bratbak 1985). While we did measure Z for each AFM imaged cell our initial comparison assumes that Z =W (as is standard in EFM based calculation). Figure 3a compiles AFM and EFM based volume averages for all cells in each sample for 20 different sampling days and from the three study areas (coastal, CCE and Antarctic). Sample-average cell volume measured ranged 0.010-0.135 μm^3 by EFM and 0.027-0.855 μm^3 by AFM. Of the 20 samples 6 co-localized on 1:1 line, indicating perfect agreement between DAPI and AFM. However, 11/20 samples showed $V_{AFM} > V_{EFM}$ including 3 when V_{AFM} was ~2x to ~4 x $V_{EFM.}$ And 3 samples were on the right side of 1:1 line, indicating $V_{AFM} < V_{EFM}$. If we exclude the cell volumes <0.01 μm (see below for the rationale) then $V_{AFM} > V_{EFM}$ would apply to all but 4 samples (Fig. 3c). So, DAPI-based EFM would generally underestimate the assemblage-average cell volume when compared with AFM.

In order to understand whether the two analyses were detecting similar size class populations we computed the ratio, V_{AFM}/V_{EFM} (Figure 3b). V_{AFM} /V_{EFM} was highly variable in different volume-classes of bacteria. The ratio was >>1 in cells with volumes <0.01 μm^3, possibly because AFM detects some cells too small to be detected by DAPI or alternatively AFM detect objects similar to cells. We chose to exclude this size class given the uncertainty (Fig. 3c).

In the case of cultured bacteria AFM clearly yielded much higher cell volume than EFM; V_{AFM} /V_{EFM} was ~ 2 (TW7), ~5 (TW6) and ~7 (BBFL7) (data not presented). So, the choice of method would give a very different picture of the cell volumes. A likely explanation for very high V_{AFM} /V_{EFM} in cultured bacteria is that as the cell volume increases the DAPI stained nucleoid becomes a smaller fraction of the cell and it defines poorly the total cell volume.

Synechococcus cell volumes in the natural assemblage from coastal site were also measured for 27 individual cells by AFM. The average volume was 0.39 μm^3 with a very broad range of 0.06 -1.01 μm^3. Since *Synechococcus* is typically detected and sized by phycoerythrin autofluorescence we did not measure its cell volume by DAPI.

Stain comparison. We compared AFM-based cell volumes with those determined with EFM using four different fluorophores: DAPI and SybrGold® targeting nucleic acids, NanoOrange® targeting proteins and NAO® targeting lipids (Table 2). Comparisons of other stains with DAPI were also done since DAPI is the commonly used fluorophores for cell sizing. V_{Syber} was very high, 3.8 x V_{DAPI}, and SybrGold® caused intense halos and fluorophores bleeding; so, we did not test it further. V_{NO} (0.149 μm^3) was 2.9 x V_{DAPI}. However, it showed reasonable agreement with V_{AFM} (0.114 μm^3). So, using V_{AFM} as standard (but see below for caveats) NanoOrange® might be a good choice as a fluorophore for EFM-based cell volume quantification The lipid stain NAO yielded even lower volumes (V_{NAO}=0.034 μm^3) than V_{DAPI} (0.046 μm^3) and much lower than V_{AFM} for the corresponding experiment (0.069 μm^3).

Height by AFM. AFM records the displacement along the Z-axis of the probe thus allowing cell height (Z) to be measured. We measured Z for bacteria (Z_{bact}) and *Synechococcus* (Z_{syn}) at coastal site (Table 3). Z_{bact} was much lower than cell width (W) and this has important effect on volume calculations (below). Z_{bact} ranged very broadly, 11 nm to 369 nm, raising the question whether the very low Z bacteria might be dead (e.g. "ghosts", (Zweifel & Hagström 1995)). In our natural assemblage AFM images of bacteria the mode for height frequency distribution was 41-50 nm (Fig. 4a). The Z_{syn} range was less broad than for bacteria, 135nm to 474 nm, and peaks in height frequency distribution occurred at 201-300 and 301-400 nm (Fig. 4b). The cultured bacteria presented variable height range (Fig. 4c,d). On average the isolates were higher than bacteria in marine assemblages; the mode for height frequency distribution was 101-120 nm (Fig. 4c).

Height during phage infection. We ran two experiments with a phage-host system to test for a height difference in phage-infected cells *versus* uninfected cells. We examined two phage-host systems. We isolated one phage infecting a *Flavobacterium* BBFL7 from Scripps Pier (F. Malfatti, unpublished data) and a second phage, SIO2, infecting a *Vibrio* SWAT3 was isolated by A-C Baudoux at Scripps Pier (unpublished data). Uninfected BBFL7 Z-range was 54 nm -193 nm while the phage-infected cells were in a tighter but lower height range, 44-121 nm (Fig. 5a). Infected cells had a rougher surface than the control cells (Fig. 5b-d). In SWAT3-SIO2 system, Z for uninfected SWAT3 ranged 102-221 nm (Fig 6a). In phage-infected cells two different morphologies

were recognizable that could be attributed to lysed and unlysed cells (Fig. 16b, c). The height range of the lysed cells was 25-187 nm and their surface looked rough. The height range of phage exposed but unlysed cells was 171-345 nm (Fig. 6a). It appears that infected but unlysed cells swell taller before phage release. Alternatively, the higher Z cells were phage-resistant and growing actively (hence taller) at the expenses of dissolved organic matter derived from lysed cells.

Height-biovolume relationship. The cell volume calculated by the formula $V = (\pi * W^2)/4 * (L-W/3)$ is overestimated because it is assumed that Z=W, which is not true for dried and fixed cells recovered on a filter. Height reduction of marine bacteria due to sample processing was observed previously by Nishino et al. (2004) but its quantitative significance for estimates of bacterial biomass and carbon pools in the ocean has not been made. We propose to use the following formula: $V=4/3\pi*a*b*c$, where a,b,c are semi axes of the solid ellipse (a=L/2, b=W/2, c=Z/2) that consider $Z \neq W$ and uses AFM based measurements of Z and W. For coastal site samples we plotted bacteria biovolume computed by the two formulas (Fig. 7). The two assumptions lead to dramatically lower cell volumes for $Z \neq W$ on two sampling days; on a third day the effect was more complex.

In order to address the problem of artifacts due to fixation and drying we compared AFM- based biovolume for live versus formalin-fixed marine bacteria assemblages. The live bacteria were imaged in filtered autoclaved seawater while the formalin fixed cells were imaged in air. In both cases the bacteria were concentrated from seawater on 0.2-µm pore size Anodisc filters (Whatman). The live cells' average height

was 333 nm, with a range of 31-747 nm (Fig. 8 and Fig. 9a). The average height of fixed and dried cells was much lower, 99 nm, with a range of 58-150 nm (Fig. 8 and Fig.9b). The collapse of cell height in fixed/dried cells may also have change L and W. That the cell volume in fixed/filtered cells was not conserved can be seen from the calculation of the relative cell volumes.

If we compute cell volume by assuming Z=W the live cell average volume is 0.72 μm^3 (range: 0.07-2.22 μm^3) and for fixed/dried sample it is 0.85 μm^3 (range: 0.05-1.56 μm^3). Using the actual measured Z for each cell the live cell average biovolume is 0.235 μm^3 (range: 0.009-0.765μm^3) and for fixed/dried cells it is 0.076 μm^3 (range: 0.010-0.142 μm^3). Thus, assumption of Z=W overestimates the volume 3-folds for live and 11-folds for fixed/dried cells. The volume size distributions were different for live and fixed/dried cells and depending on the formula used (Fig. 10). Live cell volume had a mode in the <0.1 μm^3 class with a more tight volume distribution compared with volumes computed assuming Z=W (mode >1μm^3). EFM biovolume average using DAPI was 0.158 μm^3 with a range 0.011-0.609 μm^3. EFM values were 1.5x smaller than the real biovolume of live cells, 0.235 μm^3.

Filter comparison.We tested whether biovolume measurement was affected by two commonly used filter types (Table 3). We compared 0.2 µm Anodisc and 0.2 µm Isopore filters. We first used EFM with DAPI to estimate the volume of cells at SIO site. The average volume on Isopore was 0.042 μm^3 (range 0.008-0.188 μm^3; mode 0.011-0.03 μm^3) and on Anodisc it was 0.065 μm^3 (range 0.016-0.133 μm^3; mode 0.031-0.05 μm^3). The Isopore membrane is made of polycarbonate and only 1% of the surface has

pores. The pores are not evenly distributed and there are some double or triple pores (Fig. 1a). Anodisc filter is made of an homogenous layer of alumina oxide colloids that are compressed and the filter resembles a sand filter in AFM; there are no real pores (Fig. 1b). So, the filter properties appear to affect the measurement of cell size distribution. Anodisc might flatten bacteria more than Isopore yielding larger cell area in EFM.

DISCUSSION

Atomic Force Microscopy is potentially a powerful and versatile tool that offers high-resolution images with capabilities for environmental studies. However, imaging natural bacterial populations in liquid is still challenging. The major problem is that the cell being imaged must be firmly attached to the substrate, e.g. filter membrane or mica. At the distance of van der Waals forces cells not firmly attached to the substrate would be displaced by the repulsive forces of the scanning probe. We managed to image 26 cells in liquid by immobilizing them by filtering on Anodisc filters (while majority of cells became displaced). Chemistries, such as poly-L-lysine and PEI (Polyethyleneimmine), can be applied to the substrate to improve cell adhesion, and we are in the process of optimizing chemical coating of the substrate while minimizing the nanoscale environment of individual bacteria. Further, there are potential artifacts associated with probe size and sharpness. AFM resolution in XY depends on how thin and sharp is the probe and associated dilation effect causing AFM measurement to tend to overestimate XY (Wong et al. 2007). This point has been discussed for marine bacteria (Nishino et al., 2004) but the degree of overestimation for natural bacterial population is unknown. There is a need to establish size standards applicable to AFM imaging of marine bacteria.

Despite these and other challenges AFM can begin to provide powerful constraints on hypotheses in microbial biogeochemistry.

Bacterial surface and morphology. AFM has 2-3 orders of magnitude greater resolving power than EFM and thus allows nm exploration of natural bacterial populations. The "small blue dots" imaged by EFM become large bacteria in the AFM with visible surface features interacting with other microbes within the organic matter continuum (Malfatti and Azam, submitted). In AFM, cell surfaces of bacteria in our seawater samples were smooth or rough, and some smooth cells were covered with mucus (Fig. 1, 2). AFM allows physical manipulation of cell surface at the nm scale. We often see mucus on bacteria including *Synechococcus* and we asked whether the mucus on *Synechococcus* contributed substantially to the cell thickness and volume. We optimized a protocol for natural marine assemblages to gradually strip away the mucus on a *Synechococcus* cell by repetitive cycles of scanning (Fig. 2b). The first scan height was 424 nm (Fig. 2a) and this was reduced after 30 scans to 370 nm (Fig. 2 c,d). The cell then appeared mucus free. The mucus height was therefore 54 nm (a minimum estimate since imaging in air would have reduced the degree of hydration of mucus (Balnois & Wilkinson 2002)). We estimated the mucus layer volume to be 0.31 μm^3 and this represent 33% of the "clean" cell volume of 1.014 μm^3. Such large mucus layers have adaptive and biogeochemical implications e.g. size-dependent and surface-charge-dependent protistan grazing, digestion-resistance in protist food vacuoles (partially digestible mucus might "feed" the protist but save the prey bacterium). Mucus layers are known as potential defense against phage infection; and they may also play roles in trace

metal scavenging, reducing metal toxicity, as well as carbon and trace metal (e.g. iron) transfer to higher trophic level by *Synechococcus*.

Importantly, mucus may play a role in cell-cell recognition as documented by us in the case of conjoint cells (Malfatti and Azam, submitted). Remarkably, in some of our samples all imaged cells were covered with mucus (e,g, Fig. 11). We do not yet understand when and under what conditions in the ocean do bacteria express mucus layers. However, our experience in imaging natural assemblages over a period of two years, as well as populations exposed to varied productivity regimes in microcosms, show large variations in the patters of expression of cell surface architectures. AFM should help study the regulation of bacterial structural phenotypes such as nutrient status, interaction architectures and biochemical potential (enzymes, lectins, antibiotics, etc.) as well as their adaptive and biogeochemical functions under ecological conditions. While methodology for such "ocean exploration" is still in its infancy perturbation experiments could help test mechanistic hypotheses on bacteria- environment interplay.

In our phage-host systems the surface of the lysed SWAT3 and infected BBFL7 cells was rougher then the control cells (Fig. 5, Fig. 6). Such increase in roughness has also been reported for *E.coli* 057 and A157 phage-host system (Dubrovin et al. 2008). Further, AFM studies have shown that mechanical damage of cell surface results in increased roughness—including the damage caused by EDTA (Amro et al. 2000), detergents (Camesano et al. 2000), proteases (Malfatti unpubb.)(Camesano et al. 2000) and antibiotics (Braga & Ricci 1998, Meincken et al. 2005). Marine phage lyse ~50% of bacteria production in the upper ocean; and it would be interesting to see if phage

infected bacteria and archaea could be identified through a surface "signature". Interpreting the relative variation in cell surface structure between treatment and control cells is complicated by the effect of fixatives as we saw from our images of live and formalin fixed bacteria (Fig. 8a,b). Optimizing the conditions for rapid imaging of live marine bacterial assemblages is a highly desirable goal.

We have imaged >1700 marine bacteria cells over a period of two years. It is surprising then that we have encountered only four general shapes, cocci, rods, s-shape and c-shape (Fig. 1). (However, the cell size varied dramatically; e.g. Fig.1). *Synechococcus* cells were also either cocci or rods (Fig. 2, 12) (indicating pleiomorphism that might be related to difference in light regime (Ahlgren & Rocap 2006, Palenik et al. 2006) and or grazing pressure (Christaki et al. 1999, Christaki et al. 2005)). Previous SEM and TEM imaging of marine bacteria by Costerton (Costerton et al. 1981) and Siebruth (1972) and Heissenberger (Heissenberger et al. 1996) as well as recent AFM studies of marine bacteria by Nishino (2004) and Seo (Seo et al. 2007) reported similar shapes as we did. This is remarkable given the great diversity of species (Venter et al. 2004) and potentially wide range of physiological states (compare ghost cells (Zweifel & Hagström 1995) with actively growing bacteria (Fuhrman & Azam 1980)) of marine bacteria and archaea. Despite the fact that it is still unknown what is the total microbial diversity in the seawater (Whitman et al. 1998), many species coexist in a continuum of physiological states (del Giorgio P. & Gasol 2008). Bacteria represent the largest biological surface in the ocean (Pomeroy et al. 2007) and seek nutrients gradient transient that are in space and time (Azam 1998). Marine bacteria have evolved strategies to

exploit the continuum of organic matter (Verdugo et al. 2004) by the use of their biochemical attributes and strategies such as hydrolytic cleavage of complex molecules and efficient up-take systems. Cell shape has obvious adaptive value (Cabeen & Jacobs-Wagner 2005). One might speculate that despite their varied biogeochemical functions in ocean ecosystems pelagic bacteria maintained few common fundamental shapes that are optimized for survival in the environment. An alternative hypothesis is that pelagic bacteria have many other shapes but we miss them because they co-occur with a great morphological diversity of marine gels and colloids. In other words, we imposed the result by selecting bacteria with distinctive morphologies. Concurrent high resolution EFM (1,000x; currently not feasible in our AFM system) should help to search for bacteria with other shapes, and their adaptive value (e.g. bacteria in marine snow).

Biovolume--a matter of depth (or height). Microbial oceanographers use several different approaches to quantify bacterial volume and carbon content because of the fundamental ecological importance of these parameters. In addition to EFM, and recent use of AFM, electronic counters (flow cytometer and Coulter Counter (Kubitschek 1969)) have often been used. An advantage of electronic counters and FCM is that they interrogate individual particles/cells in the particle's native morphology--unless the protocol requires chemical fixation. Imaging-based techniques have the advantage that they can provide additional, sometime critical, information on bacteria e.g. their associations with other bacteria or with gels and colloids. A dramatic example is our AFM-based finding (Malfatti and Azam; submitted) that often a substantial but variable fraction (21-43%) of pelagic heterotrophic bacteria and *Synechococcus* cells occurred

conjoint with other bacteria (Fig. 12, showing *Synechococcus* cell conjoint with heterotrophic bacterium). FCM and Coulter Counter treat conjoint partners as a mega-cell. High and low DNA populations (Bouvier et al. 2007, Falcioni et al. 2008) detected by FCM in marine environments could also be affected by the presence of conjoint heterotrophic bacteria. Further, AFM can provide a wealth of information on the bacterium's microscale ecology that goes well beyond the initial intent to know the cell volume and carbon content.

In EFM cell width and length are measured and used to calculate $V = (\pi * W^2)/4 * (L-W/3)$. Two assumptions are made: 1) a bacterial cell can be approximated to a cylinder with hemispheres (W=Z) at its ends, or a sphere (W=L); and 2) a bacterial cell maintains its shape, size and volume on the filter. We have provided a quantitative context to the cautionary note of Nishino et al (2004). Since Z≠W, we compared live imaging as a reference where we could assume volume conservation. The EFM-based volume determinations of marine bacteria are likely in error. Nishino and colleagues compared filtered fixed cells with drop deposited fixed cells and found that the filtered cells had lower Z. We found that fixation and drying, standard practice in EFM, has a large contribution to the decrease in Z (Fig. 8) and its effect on *V*. Our findings are significant because they show that the error (often recognized but neglected) can indeed be very large. Therefore, the measurement error has biogeochemical implications.

Applying the 3D ellipse approximation to our measurements on live cells the average bacteria volume was 0.235 μm^3. This is 3-fold less than if we assumed W=Z (0.718 μm^3). Considering our AFM data on formalin-fixed cells the error was much

greater; the volume was 11-fold lower (0.076 μm^3 instead of 0.855 μm^3). It appears that in formalin fixed and dried cells on membrane filters W, L and Z all change —with a huge effect on the computed cell volume. EFM allows the measurement of W and L (that change due to fixation and filtration), and further assumes Z=W, but interestingly the result is often not too much in error—i.e. the calculated *V* can be right for wrong reason (mainly because the use of Z=W compensates for cell shrinkage due to fixation). However, our results show that the error is quite variable and dependent on the size frequency distribution of the assemblage. This has implications for EFM-based variability in bacterial assemblage carbon pool available for grazers as the size frequency distribution of bacteria changes in ocean space and in time.

Bacterial height. The height range by AFM for live cells on filter was 31 -747 nm. This large interval can be due to volume difference in different species or/and within-species volume differences in varied physiological states (possibly because of exposure to varied microniches). Both causes are likely to be operative. It is interesting to ask whether in the natural assemblage a certain range of height is characteristic of dying or dead cells. Zweifel and Hagström (1995) argued that a variable fraction, from 2 to 30%, of the total bacterial EFM count is comprised of cells that lack nucleoid ("ghosts") presumably lysed by phages. It should be possible to test this hypothesis by AFM by assuming that ghost cells have a smaller Z than the average metabolically active bacteria. In our study the average Z measured by AFM on formalin fixed cells was 41-50 nm. On the basis of our AFM-based Z measurements of phage lysed and formalin fixed (cultured) bacteria we suggest that dead cells <20 nm or perhaps <30 nm Z-class might be mainly

comprised of dead bacteria. The Z average measured by AFM for living bacteria was 333 nm, much higher than fixed cells, with a range of 31-747 nm. Based on these values we might constrain the height range for ghosts and dead cells as 10-30 nm when measured by "live" cells protocol (i.e. without fixation and in seawater). It should be possible to further explore this hypothesis by coupling AFM with stains for cell viability (e.g. LIVE/DEAD® stain; Invitrogen Corp.) or electron transport chain activity, e.g. CTC (5-Cyano-2,3-ditolyl tetrazolium chloride). Preliminary experiments with CTC are promising, and it is possible to AFM-image CTC crystals forming in association with bacteria (unpublished).

Bacteria mortality by viral attack is an important aspect in the marine carbon cycle. Phages are responsible for 10-50% of bacteria mortality in the upper ocean (reviewed in Fuhrman (Fuhrman 1999)) and up to 32% for the heterotrophic bacteria and 15% for the *Cyanobacteria* can be infected (Proctor & Fuhrman 1990). In our experiment with two phage-host systems we observed a difference in height and in surface topography of the lysed cells (Fig. 8, 10). In the SWAT3 experiment, the lysed cells presented Z range from 25-187 nm and the control cells Z range was 102-222 nm. The surface topography was rougher in the lysed cells and the cells appeared damaged and partially empty. The cell did not present clear margins and this did not allow us to reliably measure the cell dimensions. The wide Z-range for phage-lysed cells could be attributed to different degrees of cellular degradation of different cells. The Z-range of phage lysed SWAT3 cells was wider than natural bacterial community. We were hoping that we would be able to recognize phage-infected bacteria at the final stage before host

lysis (as can be done by TEM; visibly infected bacteria; (Steward et al. 1992, Wommack et al. 1992)). We did see in some instances phages surrounding seemingly lysed bacteria or phage attached to intact bacteria. In order for us to confidently identify phages it would be necessary to combine TEM and AFM imaging on parallel seawater samples. If we assume that bacteria lysis occurs mainly/only through phage attack then we could estimate phage lysis in terms of the concentration of cells with Z <30 nm. We hasten to add that this criterion needs to be refined with rigorous control experiments e.g. by using phage –host systems where the host has been acclimated in unenriched seawater to various physiological state representative of the natural assemblages.

Bacterial biovolume and its implication for the carbon cycle. Biovolume distribution is a function of community diversity (Starza et al., 2009), metabolic activity level (Mitchell 1991), grazing pressure (Simek & Chrzanowski 1992, Corno & Jurgens 2006) and phage infection (Dubrovin et al. 2008). Thus, we expect variations in the biovolume classes in natural mixed assemblage where potentially each cell has a different μ and lives in a specific microniche. Consequently, average values for cell biovolume should be used cautiously in conjunction with information on community size structure. This also has important implications for cell volume to carbon conversion. Simon and Azam (Simon & Azam 1989) determined that smaller cells contain more protein per volume than the larger cells in pelagic marine environments. They proposed the use of a power function $y=88.6x^{0.59}$ to convert volume to cell protein which is proportional to C (C=protein*0.86); y is the C content per cell and x is cell volume. By applying the power function we computed the C content per cell for the population of live cells imaged by

AFM (i.e. directly measuring all three dimensions) as well as DAPI stained cells (Fig.13). A substantial proportion of bacterial population as determined by AFM had large volumes and C content as large as 50-70 fg cell^{-1} (Fig. 13). (cf. *E. coli* carbon content =100 fg (Neidhardt et al. 1990)) This C cell^{-1} is unexpectedly large for pelagic bacteria and suggests that a larger fraction of bacteria is in a robust growth physiological state (Lee & Fuhrman 1987). Carbon content based on volume distribution has implication for carbon flow pathways from bacteria to protists in view of size selective grazing by protists on bacteria.

Further thymidine based C production estimates depend on the assumption of an average cell carbon of 11 fg C cell^{-1} (Garrison et al. 2000) or 20 fg C cell^{-1} (Simon & Azam 1989). Our AFM based C per cell estimates indicate that depending on size distribution of the assemblage thymidine based C production estimates could be substantially higher then the currently believed. Therefore the previous literature estimates of the strength of bacteria-organic matter coupling that have been based on thymidine incorporation may need to be reconsidered since a larger fraction of carbon may flow through bacteria than indicated in the previous studies.

CONCLUSIONS

Our findings suggest we should revise the methods used for estimating bacterial biovolumes and carbon content. There is a need to rethink the optimal methodology for measuring bacteria shapes and bacterial overall dimensions. Our study suggests AFM of live cells, under native conditions, is a suitable method; however it is currently not a practical method for high-throughput. However AFM could be considered as a reference

for the development of other more rapid methods. One possibility that might be explored is to develop a method based on LSCM. In order to prevent distortion of the morphology of bacteria the method should be based on live cells placed in a three-dimensional format in a material that would not affect cell shape. The choice of stain could include protein stains such as NanoOrange® because it gives a distinct resolution of the limit of the cell.

This study has important implications for microbial carbon budget and carbon cycling in the ocean. A re-examination of bacterial size distribution and dynamics has implications for remote sensing of the particle field in the ocean. Finally, AFM has the potential for interrogation of individual cell physiology and interaction with organic matter (Malfatti and Azam, submitted). Such approach could be informative on the response of pelagic bacteria and their microscale interaction to a changing ocean.

Acknowledgments: We thank Maura Manganelli, Jessica Ward and Anne-Clarie Baudoux for kindly providing the offshore samples: BWZ II cruise 2006 in Antarctica, CCE LTER Process Cruise 2007 and SWAT3 phage experiment. We thank Asylum Research folks for their help and support with AFM. Chlorophyll and temperature data were retrieved from SCCOOS data archive website (www.sccoos.org) supported by NOAA, from CCE LTER data archive website (http://oceaningormatics.ucsd.edu/datazoo/data) supported by the Division of Ocean Sciences, NSF Grant OCE-0417616 and from BWZ II website supported by NSF Grant ANT- 0444134 to F.A. We thank Anne-Claire Baudoux for valuable comments. The work was supported by grants from Gordon and Betty Moore Foundations and NSF to F.A.

Literature cited

Ahlgren NA, Rocap G (2006) Culture isolation and culture-independent clone libraries reveal new marine Synechococcus ecotypes with distinctive light and N physiologies. Appl. Environ. Microbiol. 72:7193-7204

Amro NA, Kotra LP, Wadu-Mesthrige K, Bulychev A, Mobashery S, Liu Gy (2000) High-Resolution Atomic Force Microscopy Studies of the Escherichia coli Outer Membrane: Structural Basis for Permeability. Langmuir 16:2789-2796

Azam F (1998) OCEANOGRAPHY: Microbial Control of Oceanic Carbon Flux: The Plot Thickens. Science 280:694-696

Azam F, Malfatti F (2007) Microbial structuring of marine ecosystems. Nat Rev Micro 5:782-791

Azam F, Smith DC, Steward GF, Hagström Å (1994) Bacteria-organic matter coupling and its significance for oceanic carbon cycling. Microbial Ecology 28:167-179

Balnois E, Wilkinson KJ (2002) Sample preparation techniques for the observation of environmental biopolymers by atomic force microscopy. Colloids and surfaces. A, Physicochemical and engineering aspects 207:229-242

Binning G, Quate CF (1986) Atomic force microscopy. Physical Review Letters 56:930-933

Bouvier T, del Giorgio P.A., Gasol JM (2007) A comparative study of the cytometric characteristics of high and low nucleic-acid bacterioplankton cells from different aquatic ecosystems. Environmental Microbiology 9:2050-2066

Braga PC, Ricci D (1998) Atomic force microscopy: application to investigation of Escherichia coli morphology before and after exposure to cefodizime. Antimicrob. Agents Chemother 42:18-22

Bratbak G (1985) Bacteria biovolume and biomass estimations. Appl. Environ. Microbiol. 49:1488-1493

Cabeen MT, Jacobs-Wagner C (2005) Bacterial cell shape. Nat. Rev. Microbiol. 3:601-610

Camesano AT, Natan MJ, Logan BE (2000) Observation of changes in bacterial cell morphology using tapping mode atomic force microscopy. Langmuir 16:4563-4572

Christaki U, Jacquet S, Dolan JR, Vaulot D, Rassoulzadegan F (1999) Differential grazing and growth on Prochlorococcus and Synechococcus by two contrasting ciliates. Limnology and Oceanography 44:52-61

Christaki U, Vazquez-DomÌnguez E, Courties C, Lebaron P (2005) Grazing impact of different heterotrophic nanoflagellates on eukaryotic Ostreococcus tauri and prokaryotic picoautotrophs Prochlorococcus and Synechococcus. Environmental Microbiology 7:1200-1210

Corno G, Jurgens K (2006) Direct and Indirect Effects of Protist Predation on Population Size Structure of a Bacterial Strain with High Phenotypic Plasticity. Appl. Environ. Microbiol. 72:78-86

Cosa G, Focsaneanu KS, McLean JRN, McNamee JP, Scaiano JC (2001) Photophysical Properties of Fluorescent DNA-dyes Bound to Single- and Double-stranded DNA in Aqueous Buffered Solution¬∂. Photochemistry and Photobiology 73:585-599

Costerton JW, Irvin RT, Cheng KJ (1981) The Bacterial Glycocalyx in Nature and Disease. Annual Review of Microbiology 35:299-324

del Giorgio P., Gasol JM (2008) Physiological structure and single-cell activity in marine bacterioplankton. In:

del Giorgio PA, Williams PJlB (2005) The global significance of respiration in aquatic ecosystems: From single cells to the biosphere. In: del Giorgio PA, Williams, P.J.l.B. (ed) Respiration in Aquatic Ecosystems. Oxford University Press, p 2667-2273

Dubrovin EV, Voloshin AG, Kraevsky SV, Ignatyuk TE, Abramchuk SS, Yaminsky IV, Ignatov SG (2008) Atomic Force Microscopy Investigation of Phage Infection of Bacteria. Langmuir 24:13068-13074

Dufrene YF (2002) Atomic force microscopy, a powerful tool in microbiology. J. Bacteriol. 184:5205-5213

Dufrene YF (2008) Atomic force microscopy and chemical force microscopy of microbial cells. Nat. Protocols 3:1132-1138

Falcioni T, Papa S, Gasol JM (2008) Evaluating the flow-cytometry nucleic acid double staining protocol in realistic situations of planktonic bacterial death. Appl. Environ. Microbiol. 74:1767-1779

Fuchs BM, Pernthaler J, Amann R (2007) Single cell identification by fluorescence in situ hybridization. In: Reddy CA, Beveridge TJ, Breznak JA, Marzluf G, Schmidt TM, Snyder LR (eds) Methods for general and molecular microbiology. ASM Press, Washington, D.C., p 886-896

Fuhrman JA (1981) Influence of method on the apparent size distribution of bacterioplankton cell: epifluorescence microscopy compared to scanning electron microscopy. Mar. Ecol. Prog. Ser. 5:103-106

Fuhrman JA (1999) Marine viruses and their biogeochemical and ecological effects. Nature 399:541-548

Fuhrman JA, Azam F (1980) Bacterioplankton Secondary Production Estimates for Coastal Waters of British Columbia, Antarctica and California. Appl. Environ. Microbiol. 39:1085-1095

Fuhrman JA, Azam F (1982) Thymidine incorporation as a measure of heterotrophic bacterioplankton production in marine surface waters: evaluation and fiels results. Mar. Biol. 66:109-120

Garrison DL, Gowing MM, Hughes MP, Campbell L, Caron DA, Dennett MR, Shalapyonok A, Olson RJ, Landry MR, Brown SL, Liu H-B, Azam F, Steward GF, Ducklow HW, Smith DC (2000) Microbial food web structure in the Arabian Sea: a US JGOFS study. Deep Sea Research Part II: Topical Studies in Oceanography 47:1387-1422

Grossart H-P, Steward GF, Martinez J, Azam F (2000) A Simple, Rapid Method for Demonstrating Bacterial Flagella. Appl. Environ. Microbiol. 66:3632-3636

Gustavson KH (1956) The Chemistry of Tanning Processes., Vol. Academi Press, New York

Heissenberger A, Leppard G, Herndl G (1996) Ultrastructure of marine snow. II. Microbiological considerations. Mar Ecol Prog Ser 135:299-308

Hobbie JE, Daley RJ, Jasper S (1977) Use of nuclepore filters for counting bacteria by fluorescence microscopy. Appl. Environ. Microbiol. 33:1225-1228

Johnson PW, Sieburth JM (1982) In-situ morphology and occurrence of eucaryotic phototrophs of bacterial size in the picoplankton of estuarine and oceanic waters. Journal of Phycology 18:318-327

Kubitschek HE (1969) Counting and sizing micro-organisms with the Coulter Counter. . Methods Microbiol. 1:593-610

Lee S, Fuhrman JA (1987) Relationships between Biovolume and Biomass of Naturally Derived Marine Bacterioplankton. Appl. Environ. Microbiol. 53:1298-1303

Lunau M, Lemke A, Walther K, Martnes-Habbena W, Simon M (2005) An improved method for counting bacteria from sediments and turbid environments by epifluorescence microscopy. Environmental Microbiology 7:961-968

Meincken M, Holroyd DL, Rautenbach M (2005) Atomic force microscopy study on the effect of antimicrobial peptides on the cell envelope of Escherichia coli. Antimicrob. Agents Chemother 49:4085-4092

Mitchell J (1991) The influence of cell size on marine bacterial motility and energetics. Microbial Ecology 22:227-238

Neidhardt FC, Ingraham JL, Schaechter M (1990) Physiology of the bacterial cell, Vol. Sinauer Associated, Inc., Sunderland

Nie CL, Yan Wei Y, Chen X, Liu YY, Dui W, Liu Y, Davies MC, Tendler SJB, He RG (2007) Formaldehyde at Low Concentration Induces Protein Tau into Globular Amyloid-Like Aggregates In Vitro and In Vivo. Plos ONE July:13

Nishino T, Ikemoto E, Kazuhiro K (2004) Application of atomic force microscopy to observation of marine bacteria. Journal of Oceanography 60:219-225

Noble TR, Fuhrman JA (1988) Use of SYBR Green I for rapis epifluorescence counts of marine viruses and bacteria. Aquatic Microbial Ecology 14:113-118

Palenik B, Ren Q, Dupont CL, Myers GS, Heidelberg JF, Badger JH, Madupu R, Nelson WC, Brinkac LM, Dodson RJ, Durkin AS, Daugherty SC, Sullivan SA, Khouri H, Mohamoud Y, Halpin R, Paulsen IT (2006) Genome sequence of Synechococcus CC9311: Insights into adaptation to a coastal environment. Proceedings of the National Academy of Sciences 103:13555-13559

Patel A, Noble TR, Steele JA, Schwalbach MA, Hewson I, Fuhrman JA (2007) Virus and prokaryote enumeration from planktonic aquatic environments by epifluourescence microscopy with SYBR Green I. Nature Protocols 2:269-276

Pomeroy LR, Williams PJL, Azam F, Hobbie JE (2007) The microbial loop. . Oceanography 20:28-33

Proctor LM, Fuhrman JA (1990) Viral mortality of marine bacteria and cyanobacteria. Nature 343:60-62

Seo Y, Eiko I, Akihiro Y, Kazuhiro K (2007) Particle capture by marine bacteria. Aquat Microb Ecol 49:243-253

Sieburth JM (1975) Microbial seascape. A pictorial essay on marine microorganisms and their environments., Vol. University Park Press, Baltimore

Sieracki ME, Johnson PW, Seiburth JM (1985) Detection, enumeration, and sizing of planktonic bacteria by image-analyzed epifluorescence microscopy. Appl. Environ. Microbiol. 49:799-810

Simek K, Chrzanowski TH (1992) Direct and Indirect Evidence of Size-Selective Grazing on Pelagic Bacteria by Freshwater Nanoflagellates. Appl. Environ. Microbiol. 58:3715-3720

Simon M, Azam F (1989) Protein content and protein synthesis rates of planktonic bacteria. . Mar Ecol Prog Ser 51:201-213

Steward GF, Wikner J, Smith DC, Cochlan WP, Azam F (1992) Estimation of virus production in the sea: I. Method development. Marine Microbial Food Webs 6:57-78

Suzuki MT, Sherr EB, Sherr BF (1993) DAPI Direct Counting Underestimates Bacterial Abundances and Average Cell Size Compared to AO Direct Counting. Limnology and Oceanography 38:1566-1570

Venter JC, Remington K, Heidelberg JF, Halpern AL, Rusch D, Eisen JA, Wu D, Paulsen I, Nelson KE, Nelson W, Fouts DE, Levy S, Knap AH, Lomas MW, Nealson K, White O, Peterson J, Hoffman J, Parsons R, Baden-Tillson H, Pfannkoch C, Rogers Y-H, Smith HO (2004) Environmental Genome Shotgun Sequencing of the Sargasso Sea. Science 304:66-74

Verdugo P, Alldredge AL, Azam F, Kirchman DL, Passow U, Santschi PH (2004) The oceanic gel phase: a bridge in the DOM-POM continuum. Marine Chemistry 92:67-85

Whitman WB, Coleman DC, Wiebe WJ (1998) Prokaryotes; the unseen majority. Proceedings of the National Academy of Sciences 95:65-78-6583

Wommack KE, Hill RT, Kesel M, Russek-Cohen E, Colwell R (1992) Distribution of viruses in the Chesapeacke Bay. Appl. Environ. Microbiol. 58:2965-2970

Wong C, West P, Olson K, Mecartney M, Starostina N (2007) Tip dilation and AFM capabilities in the characterization of nanoparticles. JOM Journal of the Minerals, Metals and Materials Society 59:12-16

Zweifel UL, Hagström A (1995) Total counts of marine bacteria include a large fraction of non-nucleoid-containing bacteria (Ghosts). Appl. Environ. Microbiol. 61:2180-2185

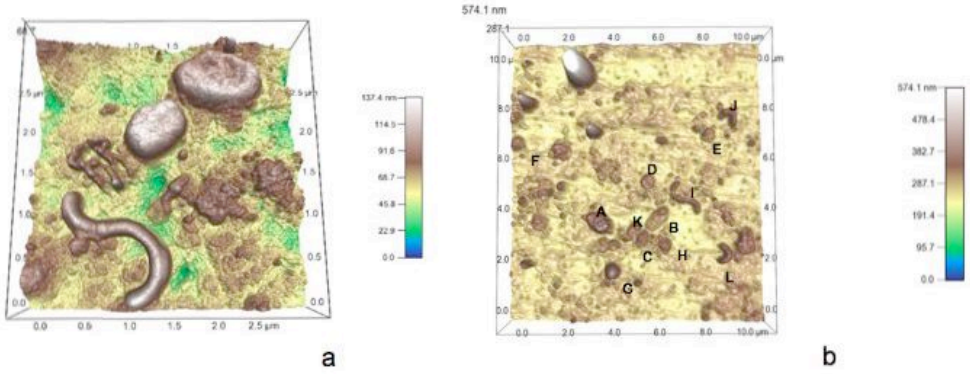

Figure 4.1: **AFM topographic images of natural bacterial community**. The color gradient (blue to brown) indicates the Z range. **a**) Sample from coastal site (SIO, 10 March, 2007) recovered onto Anodisc 0.2 µm pore size. Two rod shape cells and a s-shape cell are present. Surface of the rod cells is visibly rougher than the s-shape cell. Organic matter is present on the filter. **b**) Sample from CCE site (stn, 7 m) recovered onto Isopore 0.2 µm pore size. Three rod shape cells (A, B, C), five cocci (D, E, F, G, H), one s-shape cell (I) and 3 c-shape cells (J, K, L) are present. On the top left corner an higher cell is present, possibly a Cyanobacterium. Organic matter is present on the filter.

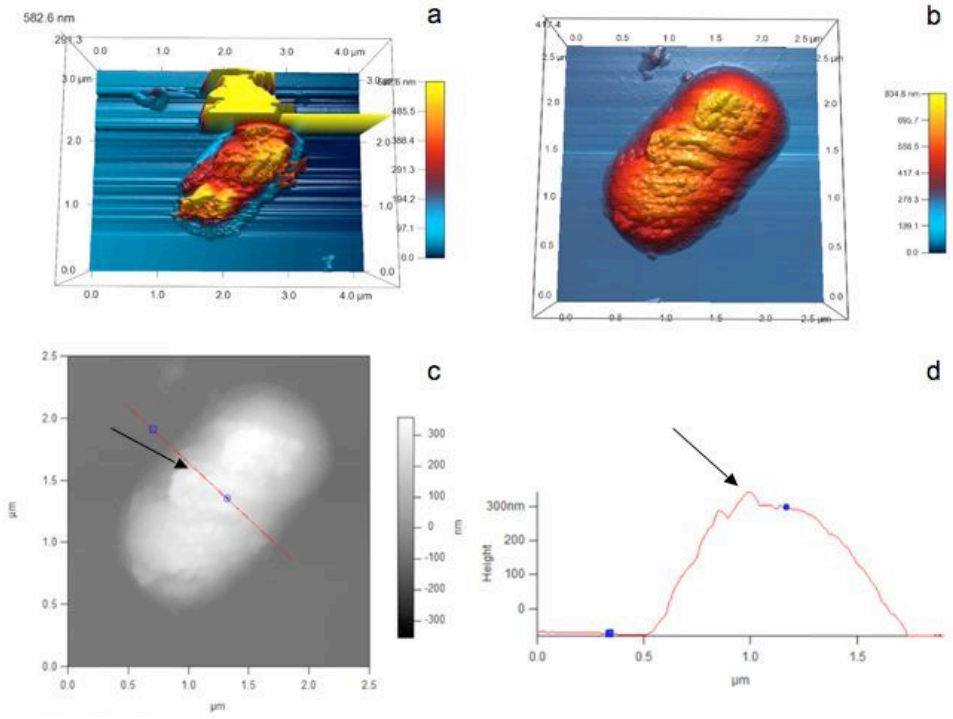

Figure 4.2: **AFM topographic images of *Synechococcus* cell drop deposited on mica.** Sample from coastal site. The color gradient (blue to red) indicates the Z range. **a**) This is the first scan of the cell; the AFM probe is interacting with the mucus layer that covers the cell creating interference stripes. The cell has been scanned for 30 min to remove by the AFM probe the mucus layer. The result is presented in the next figure (Figure. 2**b**); **b**) Cell in Figure 2**a** after removal of the mucus layer by the probe. During the 30 min scan, the scan rate was increased from 1 Hz to 3 Hz but the force was kept constant to prevent cell damage; **c)** AFM height image of *Synechococcus* cell in Figure 2**b**. The grey scale indicates the Z range. The red line is a ruler; **d)** Section graph of cell height. From the profile line it is possible to see that the surface was partially covered by mucus (arrow).

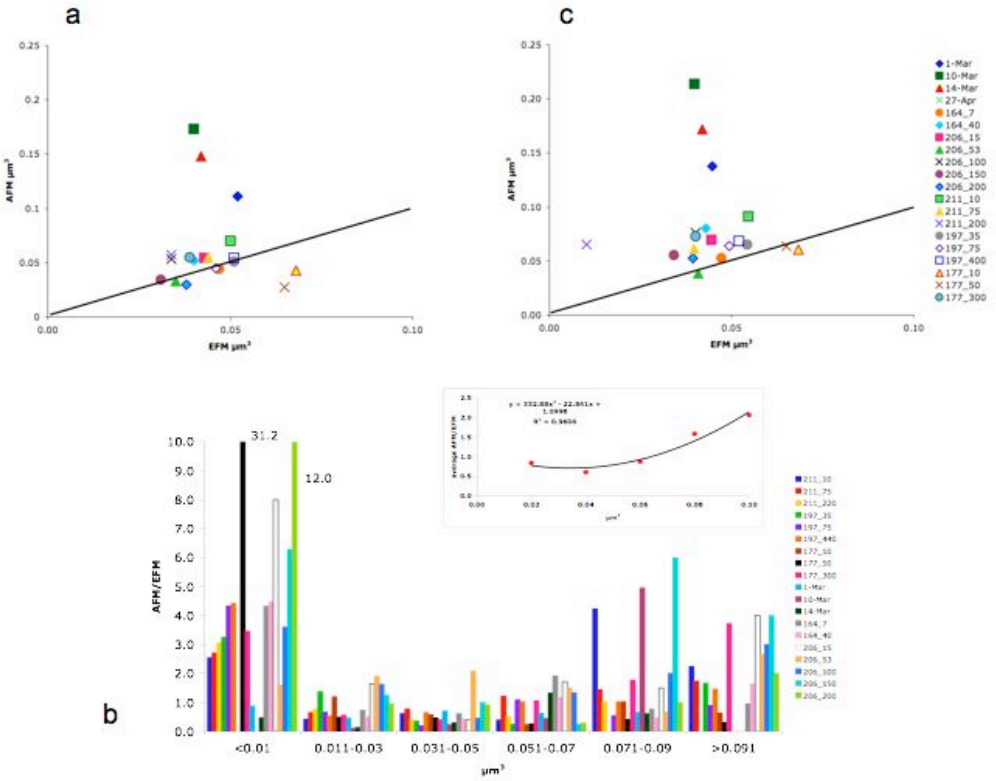

Figure 4.3: Average biovolume by EFM and AFM and biovolume ratio (AFM/EFM). Biovolume assumption is W=Z. **a**) The line is 1:1 line. Sample SIO 27-Apr is off scale (0.083; 0.855). All biovolume size classes are present; **b**) The AFM/EFM for each biovolume classes for SIO, CCE and Antarctica samples. In the insert: average ratio for each size class showing higher ratio towards the higher size class; < 0.01 class has been excluded; **c**) The biovolume size class <0.01 µm^3 has been excluded from the figure and the new average values are plotted.

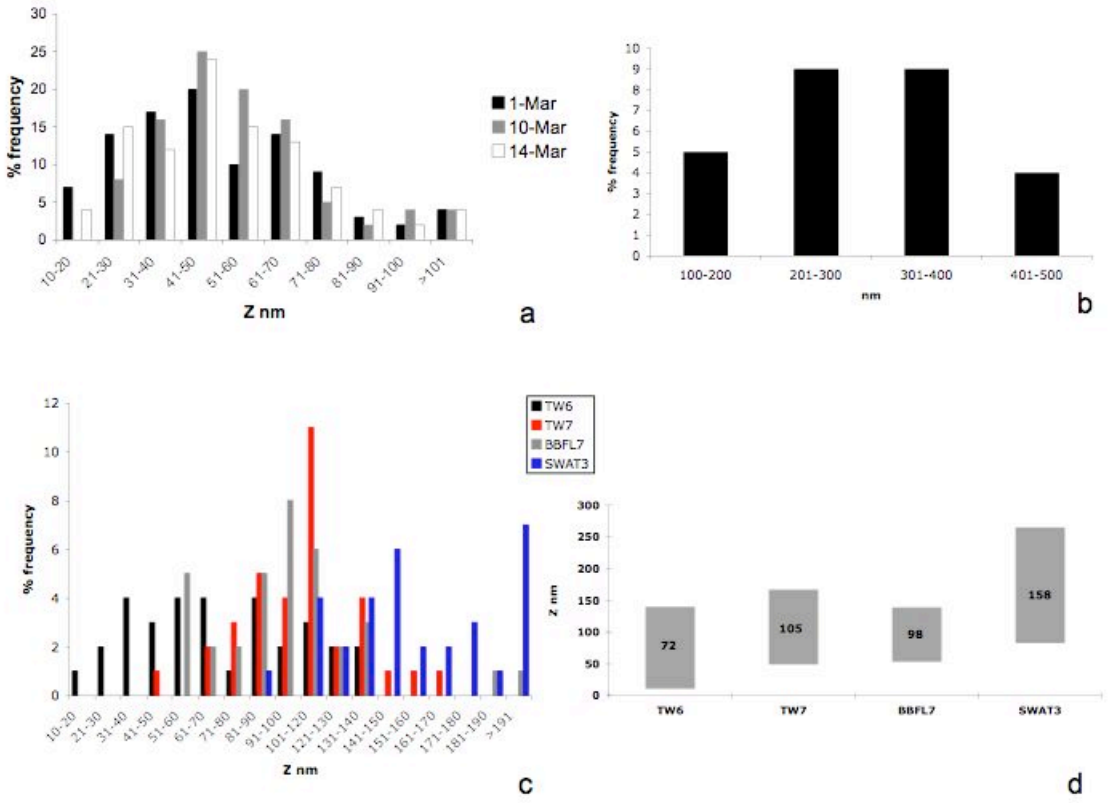

Figure 4.4: **Height frequency distribution for heterotrophic bacteria and bacterial isolates**. Height, Z, was measured by AFM for formalin fixed bacteria. **a**) Heterotrophic bacteria height distribution presented mode values in the 41-50 and 51-60 nm class; **b**) Height frequency distribution for *Synechococcus* cells. The mode values are in the 201-300 and 301-400 nm class; **c**) Mode values were higher for bacterial isolates in comparison with natural heterotrophic bacteria; **d)** Height range for each isolate, average Z is reported.

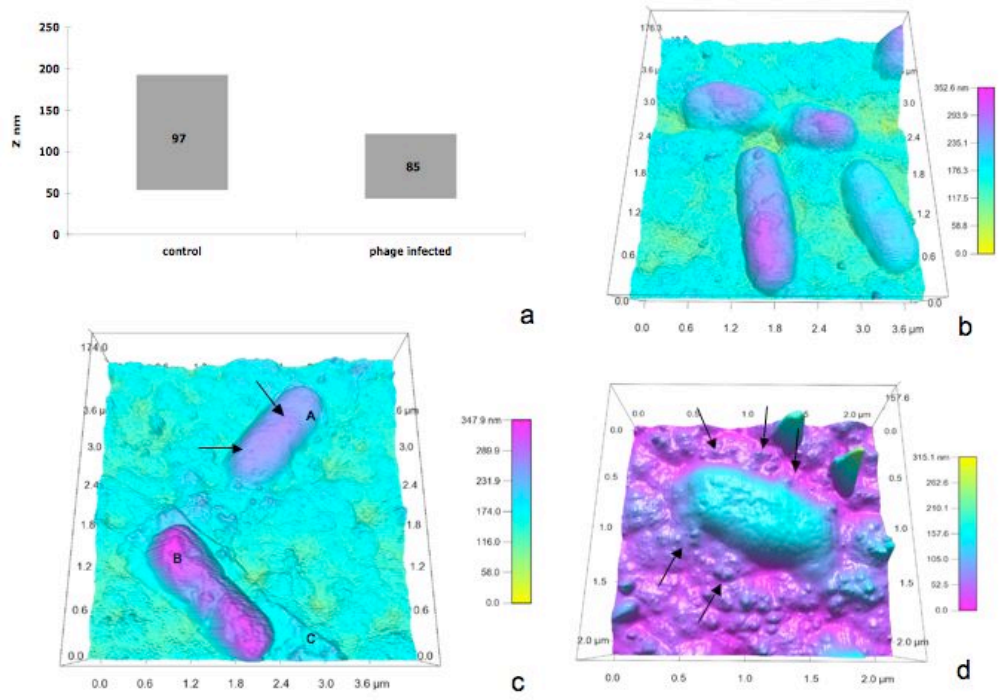

Figure 4.5: **BBFL7-phage experiment. a)** Height, Z was measured by AFM on formalin fixed cells. BBFL7 cells either were or were not exposed to the phage. Phage-infected cells decreased the Z. **b,c,d)** AFM topographic images from phage-host experiment with BBFL7 isolate. The cells have been recovered on Anodisc filter with 0.2 µm pore size. The color range (yellow to purple) indicates the Z range. Note that purple indicates higher Z in **b** and **c** but in **d** yellow indicates higher Z. **b**) BBFL7 cells not exposed to the phage. Three cells are present; the top cell is dividing. **c**) BBFL7 cells exposed to phage. A cell might have two phage particles adsorbed on the surface (arrow). Cell B, sitting on the remains of a lysed cell C, presents extremely rough surface. **d)** BBFL7 cells exposed to phage. The cell undergoing lysis is surrounded by phage particles (arrows).

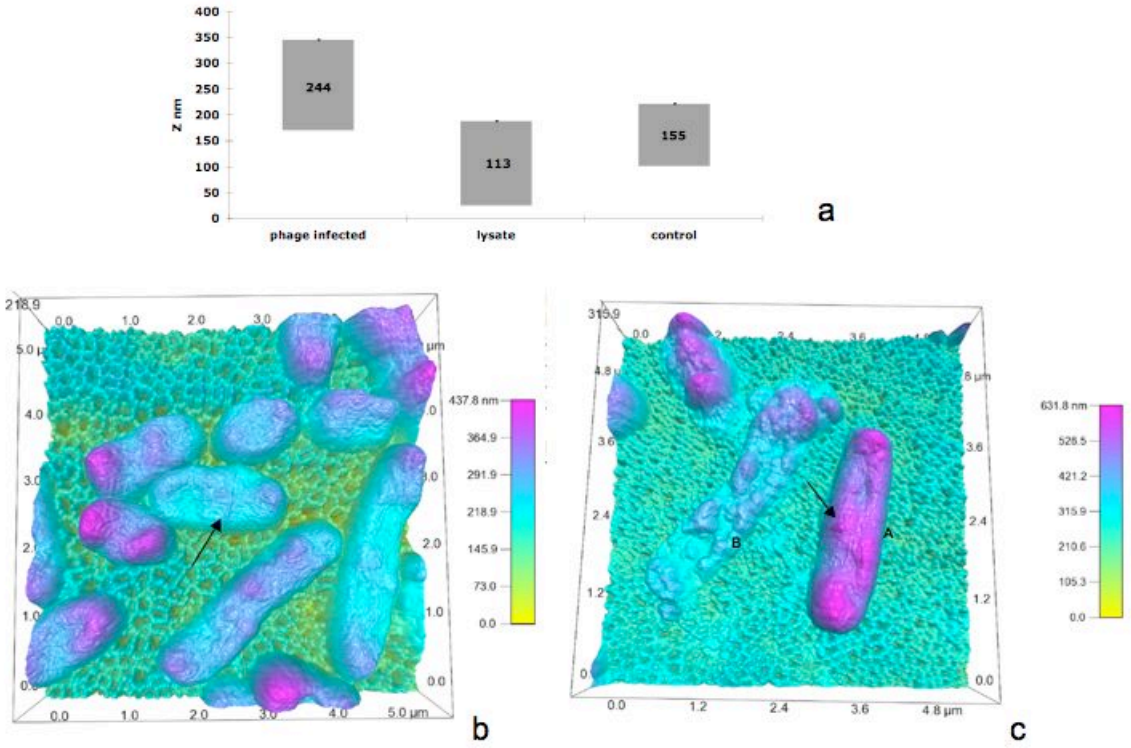

Figure 4.6: **SWAT3-phage experiment. a**) Z was measured by AFM on formalin fixed cells. SWAT3 cells were or were not exposed to the phage. **b,c**) AFM topographic images from phage-host experiment with SWAT3 isolate. The cells have been recovered on Anodisc filter with 0.2 µm pore size. The color range from yellow to purple indicates the Z range. **b)** SWAT3 cells not exposed to the phage. On the central cell, the flagellum is visible (arrow). **c)** SWAT3 cells exposed to phage. A cell appears to have one phage particle adsorbing on the surface (arrow). Cell B is lysed and presents extremely rough surface.

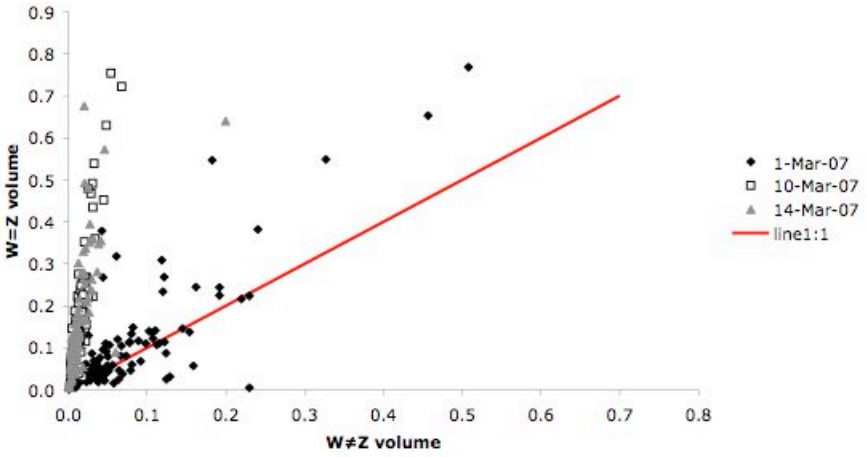

Figure 4.7: **AFM biovolume scatter plot for heterotrophic bacteria.** Samples are from the SIO coastal site. Biovolume values were computed assuming W=Z and W≠Z, W is width and Z is height.

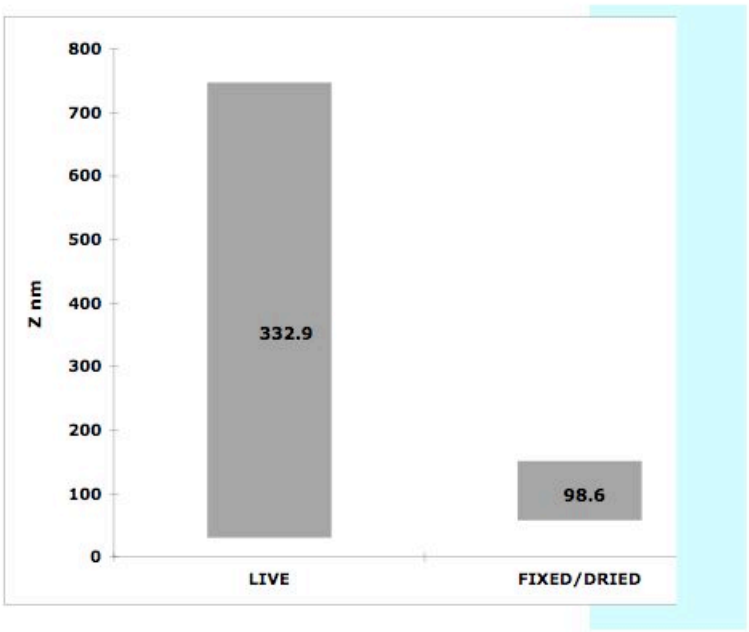

Figure 4.8: **Height, Z, for LIVE and formalin FIXED/DRIED heterotrophic bacteria.** The cells were recovered onto Anodisc 0.2 μm pore size. Z was measured by AFM. LIVE was measured under environmental conditions.

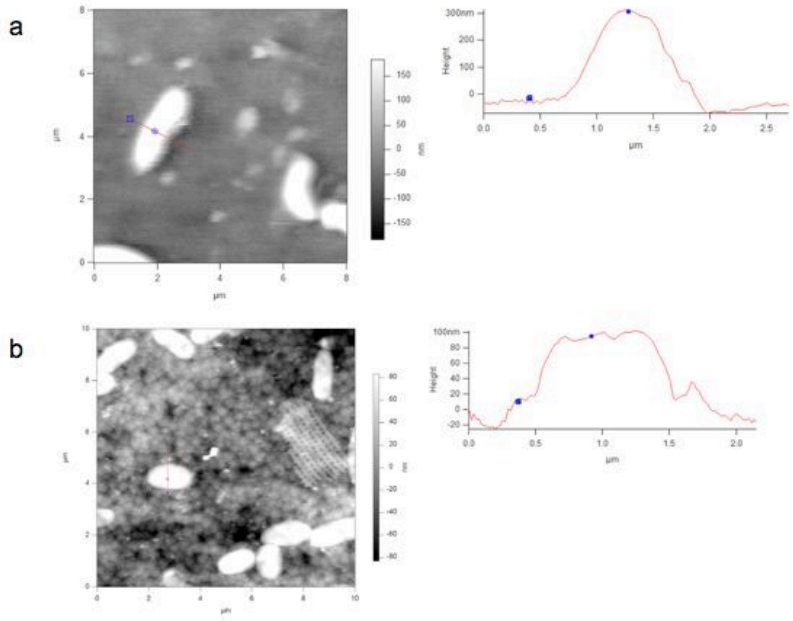

Figure 4.9: **LIVE and formalin FIXED/DRIED heterotrophic bacteria.** The grey scale indicates the Z range and the red line is a ruler. Bacteria from coastal site were recovered on Anodisc filter with 0.2 µm pore size. **a)** On the left: AFM height image of *living* (LIVE) heterotrophic marine bacteria. The imaged was acquired in liquid, there is a loss of details of the structure of the membrane. On the right: section graph of cell height. From the profile line it is possible to see that the cell presented smooth surface; **b)** On the left: AFM height image of *dead*, formalin FIXED/DRIED heterotrophic marine bacteria. On the right: section graph of cell height. From the profile line it is possible to see that the cell presented rough surface.

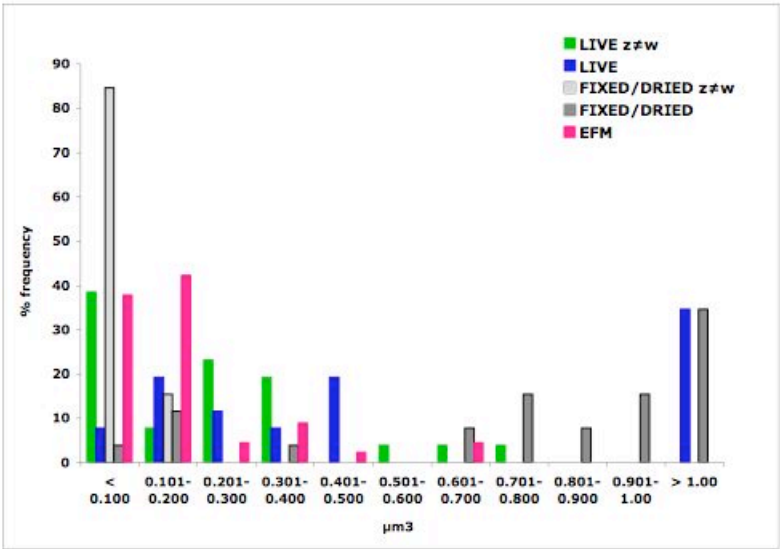

Figure 4.10: **Biovolume frequency distribution for LIVE and formalin FIXED/DRIED heterotrophic bacteria by AFM and EFM.** Bacteria were collected onto Anodisc with 0.2 µm pore size. LIVE was measured under environmental conditions. Biovolumes by AFM were computed assuming both W=Z (note labeled in graph) and Z≠W (labelled in the graph).

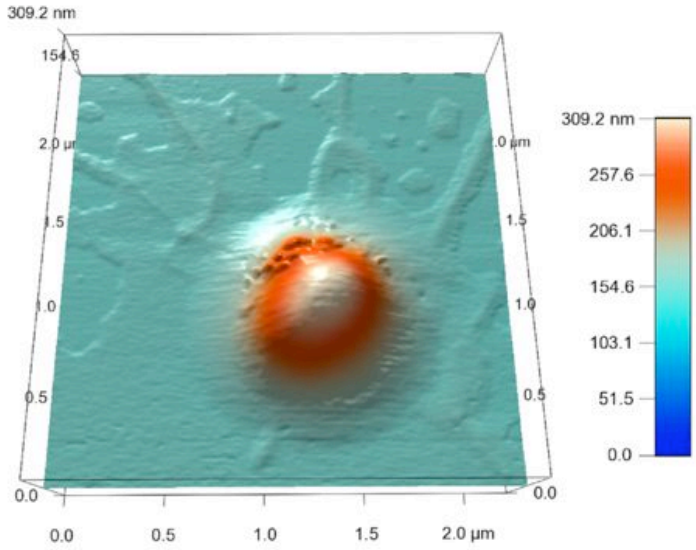

Figure 4.11: **AFM topographic image of a heterotrophic marine bacterium in a mucus layer.** The color gradient (blue to red) indicates the Z range. Sample is from costal site SIO.

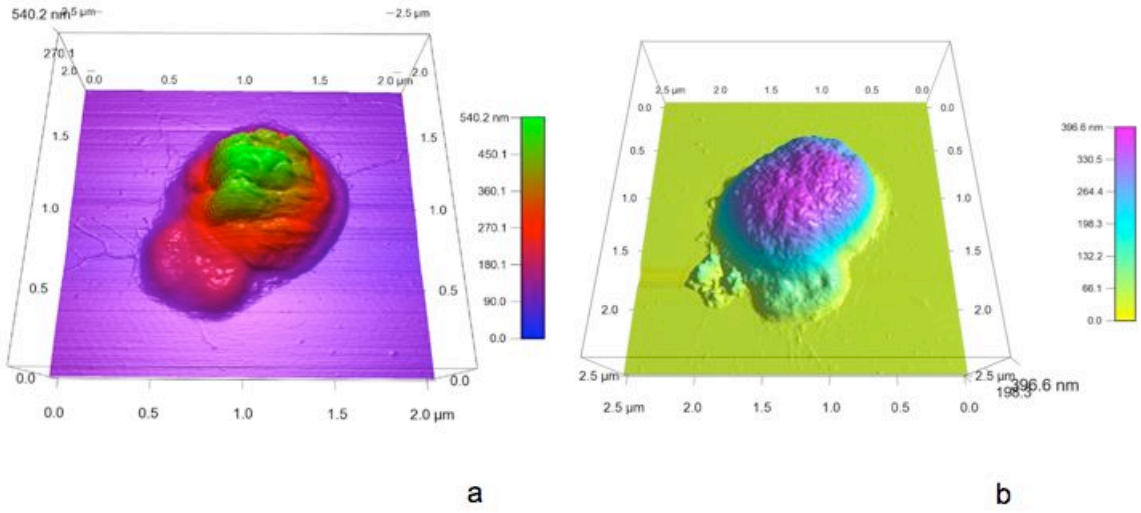

Figure 4.12: **AFM topographic images of *Synechococcus* cell and a conjoint heterotrophic bacterium on mica**. The color gradient indicates the Z range, in **a**) blue to green; in **b**) yellow to purple. *Synechococcus* cell was identified by EFM by autofluorescence of phycoerythrin prior of AFM scan. The *Synechococcus* is much larger than the conjoint heterotrophic bacterium. Samples are **a**) from costal site and **b**) from off-shore CCE 164 at 7m.

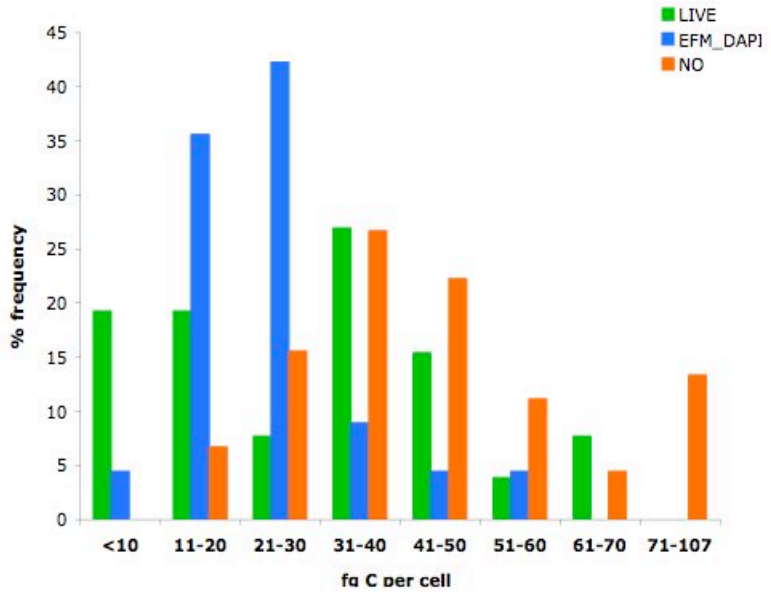

Figure 4.13: **Distribution of carbon content per cell for LIVE and formalin FIXED/DRIED heterotrophic bacteria by AFM and EFM.** LIVE was measured under environmental conditions by AFM, biovolume was measured assuming Z≠W. Biovolume of DAPI stained cells was measured by EFM assuming W=Z. The biovolumes for NanoOrange®, NO, were computed by multiplying the DAPI-based volume by 2.9 (see text for derivation of this volume factor). Carbon content was calculated by the power function $y=88.6x^{0.59}$, where x is the biovolume and y is the protein content (protein*0.86=C, see text).

Table 4.1: **Sampling sites.** Sampling site location, site category, collection date and environmental variables: temperature (°C), chlorophyll a (μgL^{-1}).

Site	Station	Coordinate	Depth m	Period	Chl a μgL^{-1}	Temperature °C
Coastal	SIO	32.867 N -117.257 W	1	1-Mar-07	5.8	14.1
				10-Mar-07	3.9	14
				14-Mar-07	3.1	15
				27-Mar-07	3.2	16
				29-Mar-07	3.5	15
				13-Jun-07	7.6	19.7
				11-Jul-08	2.14	19.7
				27-Aug-08	9.23	23.8
				31-Mar-09	3.3	14.6
CCE	164	35.358 N -121.075 W	7	7-Apr-07	1.2	12.5
			40		1.7	11.5
	206	33.659 N -123.133 W	15	9-Apr-07	0.18	14.4
			35		0.24	14.1
			100		0.11	12.3
			150		-	9.8
			200		-	9.4
Antarctica	177	-59.383 S -53.377 W	10	21-Jul-06	0.11	-0.7
			50		0.12	-0.73
			300		0.01	1.66
	197	-59.249 S -57.625 W	35	25-Jul-06	0.16	-0.95
			75		0.08	-1
			400		0.01	2.05
	211	-62.216 S -59.785 W	10	31-Jul-06	0.04	-1.27
			75		0.02	-1.32
			200		0.04	-1.43

Table 4.2: **Summary biovolume table for filter type and fluorophore tests.** Average biovolume estimated by AFM and EFM for filter type comparison (Isopore and Anodisc) and for fluorophore comparison (SYBRGold®, NanoOrange®, NAO and DAPI).

Site	Date	Experiment	# imaged cells	AFM biovolume average μm^3	EFM biovolume average μm^3
SIO	29-Mar-07	Isopore	50	NA	0.042
		Anodisc	50	NA	0.065
		SybrGold	50	NA	0.247
	13-Jun-07	NanoOrange	50	0.114	0.149
		DAPI	50		0.051
	21-Mar-09	NAO	50	0.069	0.034
		DAPI	50		0.046

Table 4.3: **Summary height table.** Height (Z) range and average height by AFM for heterotrophic bacteria (HB) and *Synechococcus* cells (S) at coastal site.

Site	Sample ID	Cells	Z range nm	Z average nm
SIO	1-Mar-07	HB	11-217	53
	10-Mar-07	HB	21-226	56
	14-Mar-07	HB	13-369	57
	27-Apr-07	HB	58-150	99
	11-Jul-08	S	146-387	261
	27-Aug-08	S	135-474	323

Chapter IV has been submitted to ISME Journal as: Malfatti, F., Samo, T.J., F. Azam - High-resolution imaging of pelagic bacteria by Atomic Force Microscopy and implications for carbon cycling.

V

Atomic Force Microscopy reveals microscale networks and apparent symbioses among pelagic marine bacteria

Atomic Force Microscopy reveals microscale networks and apparent symbioses among pelagic marine bacteria

Francesca Malfatti[1] and Farooq Azam[1*]

[1]*Marine Biology Research Division, 0202, Scripps Institution of Oceanography, University of California San Diego, La Jolla, California 92093, USA.*

** Corresponding author: fazam@ucsd.edu*

ABSTRACT: Marine bacteria and archaea ("bacteria") interact with upper ocean productivity to fundamentally influence its biogeochemical fate with consequences for ecosystems and global climate. Most bacteria-mediated carbon cycling is due to numerically dominant free-living bacteria but their adaptive strategies to interact with primary productivity are not fully understood. Using atomic force microscopy (AFM) we made the surprising discovery that a substantial, and variable, fraction (30%) of "free-living" bacteria in our samples from California coastal and open ocean environments were, in fact, intimately associated with other bacteria at nm-µm scale. Twenty-one percent to 43% bacteria, including *Synechococcus*, were conjoint, putatively symbionts (but could also be antagonistic and parasitic); and often a substantial fraction (4-55%) was connected by pili and gels into networks. We frequently observed nanoparticles associated with the networks, raising the question whether they were scavenged from seawater colloid pool by the networks or produced by the bacteria within the networks.

We also observed, in the networks, structures that morphologically resembled coccoliths and protist scales. These may impart ballast to sinking particles if the network coalesced to form larger, sinking, particles. Our finding of abundant bacteria-bacteria association and apparent microniche structuring by pelagic bacteria offers a novel context for bacterial ecology and diversity and models of ocean productivity and elemental cycling.

KEY WORDS: Carbon cycling, Attached bacteria, Free-living bacteria, *Synechococcus*-Bacteria association, Bacteria-bacteria association, Microscale biogeochemistry

INTRODUCTION

Bacteria and archaea comprise the majority of marine biomass and an enormous biodiversity, and mediate over one-half of the global ocean carbon cycling (Pomeroy et al. 2007). Their actions on the upper ocean primary productivity (PP) regulate system respiration and carbon flux to the ocean's interior (del Giorgio & Williams 2005, Nagata 2008). Therefore, the nature and the strength of bacteria-PP coupling is an important variable in predicting the response of the ocean's biogeochemical state to ecosystem perturbations (Azam & Malfatti 2007). Since most bacteria-mediated carbon flux is due to free-living bacteria a long-standing question is how the free-living heterotrophic bacteria achieve tight coupling with (largely particulate) PP (Azam & Hodson 1977, Fuhrman & Azam 1980, 1982, Ducklow 2002, Nagata 2008). An emergent view is that a variety of physiological and trophic interactions transform a substantial fraction of productivity into a size continuum of organic matter from monomers to colloids to

particles and to aggregates (Koike et al. 1990, Azam et al. 1994, Azam 1998, Chin et al. 1998, Verdugo et al. 2004). All these organic matter phases would then be direct or potential (e.g. after enzymatic attack by bacteria) substrates for the free-living bacteria.

This departure from the traditional dichotomy of particle attached versus free-living bacteria suggests that free-living bacteria assemblages interacting with organic matter continuum create a mosaic of biogeochemical activity hotspots in seemingly homogeneous seawater. It also emphasizes the significance of bacterial cell surface, the largest biotic surface in the ocean (Williams 2005), for the interactions with organic matter pool to transform its biogeochemical behavior. In view of the great physicochemical diversity of the organic matter phases with which bacteria interact in seawater we considered that high resolution imaging (Dufrene 2008b) could provide additional insights on bacteria organic matter interactions.

Electron microscopy (TEM and SEM) has long been used to investigate marine bacteria and their surface layers and appendages potentially involved in interactions with the environment. Studies by Sieburth, Costerton, Johnson (Sieburth 1975, Costerton et al. 1981, Johnson & Sieburth 1982) and Beveridge (Beveridge & Graham 1991) have illustrated in detail the variety of sizes, shapes and surface morphologies of environmental bacteria as well as their occurrence as free-living (planktonic) or particle attached bacteria. Sieburth (Sieburth 1979) has published extensive TEM and SEM images of pelagic bacteria including cyanobacteria (Johnson & Sieburth 1979). Heissenberger and coauthors (Heissenberger et al. 1996) addressed bacteria interactions in natural seawater samples by TEM, using a water-soluble embedding resin, Nanoplast^{R}, that preserves capsules and mucus layers in their hydrated forms (Leppard et al. 1996,

Lienemann et al. 1998). They showed the presence of mucus and bacterial capsular material bridging bacteria with diatom detritus as well as other bacteria. There is also recent literature based on genomic inferences that pelagic bacteria express surface polysaccharides and proteins for interaction with particles and organisms, and these data have been interpreted in terms of attached and free living life-styles of bacteria (Moran et al. 2007, Thomas 2008). However, it is recognized that the "real life" interactions are likely to be much more complex. Ideally, one would wish to observe *in situ* microbial interactions with the organic matter continuum; but given the technical challenges involved at this time, multiple constraints with imaging, tracer and genomic approaches could begin to progressively sharpen our understanding of the interactions and their mechanistic bases. We considered that exploration at the nanometer to micrometer scale of physical interactions of bacteria and their *in situ* environment would provide biogeochemical insights and generate new hypotheses.

Since its invention (Binning & Quate 1986) atomic force microscopy has rapidly evolved in instrumentation, sample preparation and image-recording capabilities (Dufrene 2004) offering a new tool that can generate sub-nanometer resolution images of biological samples including bacterial surface structures (Dufrene 2002, 2008b). AFM enables high resolution comparable to electron microscopy but without the need for embedding or metal coating (Dufrene 2004). AFM is a scanning-proximity probe microscope. It provides information on the local properties of the sample, such as topography, viscoelasticity, electric forces, magnetic forces and chemical bonding. The principle of AFM is based on measuring the inter-atomic van del Waals forces between

the scanning probe and the sample surface. The cantilever carries at its end a sharp tip, or probe that is rastered over the sample and the cantilever movement is monitored via interferometry by a laser-photodector system. The cantilever continuously bends due to the attraction-repulsion forces between tip and sample thus creating a high-resolution topographic map of the specimen surface. Moreover, AFM has the potential for physiochemical interrogation at the nm-μm scale (Dufrene 2008a) of living specimens.

In our case, an additional advantage was that we could concurrently use AFM and EFM (Epifluorescence Microscopy) (Mangold et al. 2008) in order e.g. to identify a cell as cyanobacteria before AFM imaging. Such prior interrogation, not intuitive in TEM or SEM, is very useful in studying microbial interactions. The use of AFM in microbial oceanography is recent and still limited. Pioneering studies of Santschi (Santschi et al., 1998), Svetlicic and Zutic (Svetlicic et al., 2005) and Balnois and Wilkinson (Santschi et al. 1998, Balnois & Wilkinson 2002, Svetlicic et al. 2005) addressed questions on the nanoscale structure of marine organic gels and fibrils. The use of AFM to address the ecology of marine bacteria has been made only by Kogure and his colleagues (2004). They used it to size marine bacteria (Nishino et al., 2004) and to test whether bacteria capture nanoparticles from seawater (Seo et al. (2007). Because so few studies have been made in the marine system it is both an exciting opportunity to explore seawater with AFM and a challenge, due to currently limited constraints, to interpret the images for ecological and biogeochemical insights. However, there is considerable literature on AFM imaging of laboratory cultures of bacteria and we can draw upon this literature for interpretation (see Dufrene, 2002, 2008 for a review).

Our AFM imaging of whole seawater samples surprisingly revealed that many "free" bacteria were in fact intimately associated with other bacteria, either conjoint or in tight networks. These intimate associations may be adaptive for pelagic bacteria as well as cyanobacteria—with major biogeochemical implications.

MATERIAL AND METHODS

Sampling. Seawater samples for AFM imaging were taken from three different environments designated "Coastal", "CCE" (California Current System, offshore locations) and "Antarctic" (Table 1). Most Coastal samples were collected at the surface off the Pier of the Scripps Institution of Oceanography (SIO). This location has been sampled for ~90 year for physical, biological and biogeochemical parameters. A comparably extensive (~60 y) time-series data set has also been collected from the California Current Ecosystem, CCE (CalCOFI data set), and we analyzed seawater from two CCE stations as well. Time-series analysis indicates strong coherence of biogeochemical variability at SIO and CCE (McGowan et al. 1998, Hey-Jin 2008). Two other coastal sites, EK and Sorcerer II, were sampled once. Our extensive sampling at the Scripps Pier together with limited sampling in other coastal and CCE waters may be expected to include biogeochemical variability applicable to a geographically broad area. CCE samples were taken during Cycle 1 and Cycle 2 of a California Current Ecosystem-LTER cruise in April 2007 at stations 164 and 206 (http://cce.lternet.edu/data/cruises/cce-p0704/). Antarctic samples were collected during austral winter 2006 at stations 178 and 197 during the BWZ cruise in the Drake Passage (coordinates in Table 1).

Chlorophyll *a* was measured fluorometrically in discrete samples after extraction (Holm-Hansen & Riemann 1978) and by an *in vivo* chlorophyll sensor. Seawater temperature (CTD) data were retrieved from SCCOOS data archive website (www.sccoos.org supported by NOAA), from CCE LTER data archive website (http://oceaningormatics.ucsd.edu/datazoo/data supported by the Division of Ocean Sciences, NSF Grant OCE-0417616) and from BWZ II website (supported by NSF Grant ANT- 0444134).

AFM Sample Preparation

Drop-deposition. Seawater samples were fixed with 0.02 μm filtered formaldehyde solution (Nishino et al. 2004) and stored for 1 h at 4°C before spotting on mica. Fixation was necessary to prevent cell lysis. A high quality mica disc (# 50; Ted Pella Inc.; # 71856-01, Electron Microscopy Sciences) was attached to a clean glass slide by double- sided sticky tape (Veeco Instruments, Santa Barbara). A 50-100 μL drop was deposited on a freshly cleaved mica disc (Amro et al. 2000, Balnois & Wilkinson 2002), let dry at 50°C and rinsed with autoclaved HPLC-grade water. We tested different rinse waters for particle background: Milli-Q water (Millipore Corp.), Milli-Q water permeate through a100 kDa centrifugal ultrafiltration cartridge (Microcon; Millipore Corp.) and HPLC-grade water (Fisher Scientific). HPLC-grade water had the lowest particles level, so it was chosen as rinse water. We tested whether formalin fixation or drying temperature (room temperature versus 50°C) affected the appearance of organic matter structures. In these tests we noticed no obvious treatment-dependent differences in the AFM images of the organic matter in terms of size and shape of colloids and fibrils.

Further, we determined the effect of formaldehyde fixation on the appearance of the surface of bacteria (*Vibrio cholerae* strain N16961). The unfixed cells appeared smooth while the fixed cells presented rough surface, in agreement with previous AFM studies (Vadillo-Rodriguez et al. 2004, Vadillo-Rodriguez et al. 2008).

Filtration and filter-transfer-freeze to mica. CCE and Antarctic cruise samples had been collected on polycarbonate membranes (Isopore; Millipore Corp.). The roughness of Isopore filters is too high, ~3 nm (Gueven et al. 1997), for visualization of finer features of bacterial architecture or networks. Mica has a very low roughness,< 0.2 nm (Namba et al. 2000). We transferred the filtered cells and particulate matter onto mica using the Filter-Transfer-Freeze technique, FTF (Hewes & Holm-Hansen 1983). Transfer efficiency of FTF is known to be high (82-95%) for phytoplankton but it not known for bacteria or nanometer-size material; hence the imaged bacteria-associated material in samples treated by FTF would represent minimum estimates. Seawater samples were collected with Niskin bottles. Samples were fixed with 0.2 μm filtered formaldehyde (2% final). They were vacuum filtered (-16 kPa) onto 0.2 μm white polycarbonate filter, rinsed with 0.2 μm filtered autoclaved Milli-Q water and the filters stored frozen at -20C until transferred to mica. A freshly cleaved mica disc was attached to a clean glass slide and the back of the slide was flash-frozen with a brief spray of tetrafluoroethane (Decon Lab, PA, USA). One filter quadrant was placed, face down, on the chilled mica for 10 sec then peeled off. The mica was let air-dry in a Petri dish then washed with autoclaved HPLC water.

AFM Imaging. AFM imaging was performed in our laboratory with MFP-3D (Asylum Research, Santa Barbara, USA) mounted on an inverted epifluorescence microscope (Olympus IX 51). Images were acquired in AC mode in air with a silicon nitride cantilever AC160TS (Olympus, k=42 N/m; tetrahedral shape). Scan rates were 0.8-1 Hz. Image size was 256x256 or 512x512. We recorded trace and retrace of height, amplitude, phase and Z sensor channels. Topography images were processed with Planfit and Flatten functions. Bacteria and organic matter were sized with the measuring tool part of the Igor Pro 6.03A MFP3D 070111+830 software. While AFM dilates the object shape because of tip geometry (Wong et al. 2007) progress in nanotechnology to build super-sharp cantilevers (<10 nm apex radius, used here) and the deconvolution algorithms (Ritter et al. 2002) now essentially cancel out the tip effect.

Epifluorescence microscopy. We used EFM prior to AFM imaging in order to identify autofluorescent *Synechococcus* and SYBRGold® stained heterotrophic bacteria. A freshly cleaved mica disc, reduced in thickness (to enable EFM through it) with a clean razor blade, was affixed on a microscopy slide using double-sided sticky tape. (Note that the tape is strongly autofluorescent, so it must be placed at the edges of mica disc in order to prevent excessive background fluorescence). Seawater was spotted on mica, dried and washed, as above, then stained with SYBRGold® (Invitrogen; 5x final) for 15 min in the dark. On mica we identified, at 400x magnification *Synechococcus* cells based on phycoerythrin autofluorescence using Chroma filter set 51006 (Fig. 3g) as well as heterotrophic bacteria based on SYBRGold® staining using Olympus filter U-MNIBR. We then acquired AFM scans of the EFM identified *Synechococcus* cells on mica. Our

AFM scan-head interrogates from the top of the sample, so fluorescence microscopy must be done through the slide (plus mica). The depth of focus of our microscope objective limited us to the use of 40X and not higher magnification objectives.

RESULTS AND DISCUSSION

Cell surface architecture. Although we studied whole seawater samples our focus was on bacteria—other organisms and organic matter were considered only in the context of their interactions with bacteria. We imaged over 500 bacteria, including *Synechococcus,* and any interacting material, in seawater samples from coastal and offshore California, CCE, and Antarctica (Table 2). The majority of bacteria in the natural assemblages displayed surface architecture, and this could be relevant to their ecophysiology and interactions with organic matter. Combining all data for each sampling region 85 % of bacteria in coastal, 74% in offshore and 29% in Antarctic samples displayed distinct cell surface architectures. These were highly variable in dimensions and patterns and could be interpreted as capsule (Stukalov et al. 2008), pili, gel matrix (Svetlicic et al. 2005) and nanogels (Verdugo et al. 2004) (Fig.1a-d). Pili were 6-56 nm thick and 0.1-1.9 nm tall.

Pili and gel matrix extended 0.1-6 μm from cell surface. Taking these dimensions of pili and gels on face value (while recognizing that they may have been affected by sample processing) they could greatly increase the interaction volume of bacteria (e.g. Fig. 1a,c). In Fig. 1a, the *coccus* has a diameter, D, of 336 nm and biovolume of 0.02 μm^3, whereas if we considered the cell and its cell surface architecture, D=2.27 μm, and the total interaction volume is 6.12 μm^3. The difference in volume is ~ 300x, this changes

how we think about the possible interaction volume of bacteria and its variability in the pelagic ocean. We identified *Synechococcus* sp. by phycoerythrin autofluorescence (Fig. 3f,g). *Synechococcus* cells displayed from unarticulated tight capsules to elaborate and extensive architectures. These features were present in 65 % of *Synechococcus* cells in costal and 28% *Synechococcus* cells in offshore samples (Fig. 1c,d). In Fig. 1c, the *Synechococcu*s cell, D=900 nm, has a biovolume of 0.38 μm^3; whereas the combined cell+surface architecture, D=2.32 μm, biovolume is 6.6 μm^3. In this case the difference in biovolume is ~17x, this shows that *Synechococcus* cells as well as heterotrophic cells have the potential to greatly extend their sphere of influence in the microenvironment.

We are limited in our ability to interpret the AFM images of marine natural bacterial assemblage because there are few published images of marine natural assemblages or physiochemical characterization of marine bacterial surfaces. It is possible to use AFM to characterize cell surface architecture with functionalized tips with lectins, antibodies or enzymes (Dupres et al. 2005, Dufrene 2008a) and also to determine the stickiness and the elasticity (Abu-Lail & Camesano 2002). However such investigations would require developing protocols for natural bacterial assemblages.

The diversity of surface architecture among bacteria could reflect genetic diversity e.g. genes for LPS, pili and surface proteins. For instance, the marine *Synechococcus* have been shown to swim using a unique mode of motility involving interaction of specific cell surface proteins with the environment (Brahamsha 1996, McCarren et al. 2005, Palenik et al. 2006). The observed differences in surface architecture could also reflect different physiological states or microspatial environmental

variability that bacteria had been experiencing (Moran et al. 2007, González et al. 2008). While the presence of surface structures on bacteria is not surprising the AFM images illustrate the potential of advanced microscopy to change how microbial oceanographers envision the microbes and their interactions with the ocean system. We hasten to add that the cell surface architectures might have been affected by formaldehyde fixation (it cross-links proteins; (Gustavson 1956, Nie et al. 2007)). AFM imaging of glutaraldehyde-fixed Gram-negative bacteria presented small corrugations on the cell surface, and the fixed cell's surface was more rigid (Vadillo-Rodriguez et al. 2004, Vadillo-Rodriguez et al. 2008). We cannot rule out that some of the nanometer size spherical objects that we here call nanogels and colloids (Fig. 1b,d) are artifacts of sample preparation. However, the spherical objects in our images are comparable in shapes and size-range of natural colloids in previous AFM and TEM studies (Leppard et al. 1997, Santschi et al. 1998, Balnois & Wilkinson 2002, De Momi & Lead 2008).

Conjoint bacteria (including *Synechococcus).* A remarkable finding was that in most samples a substantial fraction of bacteria, including *Synechococcus*, occurred conjoint as bacteria-bacteria (i.e. heterotrophic bacteria conjoint with heterotrophic bacteria) or *Synechococcus*-bacteria associations (Fig. 2; Table 2). Conjoint heterotrophic bacteria were detectable in all but two seawater samples; 16 out of 18 costal, 2 out of 2 offshore and 2 out of 2 Antarctic samples. Forty-two % *Synechococcus* were conjoint with one or more heterotrophic bacteria in costal and offshore samples (Table 2). Incredibly, the extensive EFM of seawater samples missed such associations during the last three decades!

Most partners were morphologically dissimilar, presumably phylogenetically distinct, e.g. some cells were diminutive in relation to their partner (e.g. Fig. 2b,d). We do not think conjoint bacteria are artifacts of sample processing (*e.g.* free cells falling randomly at the same spot). In one test to rule this out we filtered 0.2 ml or 2 ml seawater on 0.22 μm Isopore filters and counted at the EFM over 200 *Synechococcus* cells in random fields to determine the % *Synechococcus*-heterotrophic associations. *Synechococcus*-heterotrophic partners accounted for 17% (37/209) and 15% (30/200) in 2 ml and 0.2 ml, respectively. Thus, the abundance of % *Synechococcus* in *Synechococcus*-heterotrophic associations was essentially independent of cell density on filters, supporting that the associations were not artifacts of random co-localization due to filtration.

Occurrence of abundant symbionts in the upper ocean has profound ecological, biogeochemical and evolutionary implications--and leads to new hypotheses on their diversity, nature and functional significance. Syntrophic associations have been found in benthic marine systems (Boetius et al. 2000) (Pernthaler et al. 2008), and their occurrence in the pelagic realm has been predicted (Azam & Malfatti, 2007). We use "symbiosis" operationally to describe the associations here, while recognizing that diverse molecular mechanisms by the partners and ecological relationship such as commensalisms, antagonism or parasitism might be happening. These analyses were beyond the scope of this exploratory biogeochemical study. In our images we could not detect any gross morphological deterioration that might have indicated one cell degrading the other cell or

bacteria undergoing phage lysis, as has been shown in a AFM based study of cultured bacteria infected by viruses (Dubrovin et al. 2008). A first step towards characterizing the nature and diversity of these symbioses would be to identify the conjoint partners e.g. by developing a protocol combining FISH and AFM for marine assemblages. A biogeochemically relevant prediction is that the conjoint heterotrophs coordinately enlarge their metabolic repertoires for utilizing polymers, nanoparticles and complex organic matter--with implications for carbon cycling (Fig. 2a,b). The symbionts' genome sizes could be reduced where metabolic potentials are shared (Boetius et al. 2000, Huber et al. 2002). The enormous bacterial diversity in metagenomic surveys (Venter et al. 2004, Rusch et al. 2007) and microdiversity in *Vibrionacaea* (Thompson et al. 2005) raised the question of diversity maintenance, and microscale patchiness has been proposed as explanation. Such patchiness could in part be generated by symbioses (and bacterial networks; later).

To study on large spatial and temporal scales Fuhrman and collaborators (Fuhrman & Steele 2008)Fuhrman, 2009) (Ruan et al. 2006) used global ocean biogeographical data to model bacterial communities as interaction network. This allowed them to predict taxon-specific niche space and positive/negative relationships with other taxa and with environmental variable. They predicted the co-occurrence of specific taxa, possibly symbionts. Our finding supports their prediction and further suggests conjoint symbiosis as a mechanism of co-occurrence.

Synechococcus-bacteria association could fundamentally influence the symbionts' microspatial nutrient status and growth physiology, and cause tight bacteria-PP coupling

(particularly in mucus enveloped associations e.g. Fig. 2d). The heterotrophs would benefit by *Synechococcus* exudation, in turn supplying regenerated nutrients and growth factors. *Prochlorococcus marinus* growth is enhanced in co-culture with heterotrophic bacteria ("helper effect") as the heterotroph removes toxic reactive oxygen species (Morris et al. 2008). We predict that in addition the respiration of a conjoint heterotroph could lower the microspatial pO_2 and enable daytime N_2 fixation. This scenario is consistent with biochemical and genomic evidence of a major role of unicellular cyanobacteria in oceanic N_2 fixation (Montoya et al. 2004, Zehr et al. 2008). Such enhanced N_2 fixation is also consistent with regime shift from N to P limited productivity in the central north Pacific (Karl et al. 1997). As a broader observation, microbial biogeochemistry generally considers bacteria-phytoplankton interactions in the context of bacteria and algae but our finding suggest *Synechococcus* (and possibly *Prochlorococcus* as well) are also important microscale interaction loci for bacteria-phytoplankton interactions. Biogeochemical consequences of *Synechococcus-bacteria* associations are particularly interesting because *Synechococcus* are abundant and essentially non-sinking cells.

Bacterial networks. High resolution AFM further revealed another level of microspatial coupling. In most samples, substantial fractions of bacteria and *Synechococcus* cells, including some conjoint, were interconnected by fine pili or cell-surface gel matrix into networks of two to several cells (Table 2, Fig. 3). Thirty-five % of total bacteria imaged were within such networks (costal 36%, offshore 37%; Antarctic 0%). Networks were detected in most but not all seawater samples (costal 14/18, offshore

1/2, Antarctic 0/2). However, we cannot rule out that bacterial networks were in fact present at low abundances since we are limited in the number of AFM field that can practically be examined at high resolution.

Fibril-mediated connections between bacteria, algae and detritus were previously discovered by TEM in a study in north Adriatic coastal waters (Heissenberger et al. 1996). Our images suggest that generally bacteria themselves produced cell surface architectures that served as structural bases for the networks (rather than bacteria colonizing a preformed gel particle). In some instances, however, our images suggested that bacteria had colonized preformed microgels. Pelagic microgels (Svetlicic et al. 2005) are formed by algal exocytosis (Chin et al. 2004), bacterial extracellular polysaccharides (EPS) mediated polymer self organization of dissolved polymers (Ding et al. 2008) and organic matter self organization (Kerner et al. 2003, Engel et al. 2004). Bacterial expression of surface appendages as a strategy for association with surface or other organisms is well known. What is noteworthy here is that pelagic bacteria samples typically examined by EFM do not reveal the highly abundant association of the type that we observed with AFM; so, these bacteria are considered free-living. Our findings would therefore change how we think about the ecology of free and attached bacteria, and the role of bacteria in pelagic aggregation.

Do bacterial networks trap nanoparticles? Bacterial surface architecture can trap pelagic nanoparticles (Seo et al. 2007). One might predict that nanoparticles would be subjected to locally intense activities of multiple ectohydrolases to convert them into

directly usable substrates (Martinez et al. 1996). We considered that bacterial networks might also be a strategy of some pelagic bacteria to capture a broad section of organic matter continuum, thus exposing it to concerted metabolisms of network community in order to generate DOM hotspots for bacteria uptake. AFM images showed that bacterial networks (as well as bacterial surface architecture as observed by Seo et al. 2007) contained abundant 10s to 100s nm structures (Fig. 1d, 2a-c,e-f, 3a-e), unattached gels and 2-5 μm long fibrils (Santschi et al. 1998). Further, viruses (10^{10} l^{-1} by EFM; not sized) were present in our samples. We could not resolve viruses from nanogels at the AFM; so viruses were likely included in the nanoparticles that we observed. For example, in Fig. 1d, particles in the range of 50-300 nm are present throughout the *Synechococcus* cell surface architecture, these particles may well be viruses. Whether the cell has released these particles or they have been trapped into the network from the environmental pool cannot be determined. This situation applies also to Fig. 2e, where *Synechococcus* and the conjoint c-shape heterotrophic bacterium are surrounded by abundant particles that we estimated hundred in this size range of 50-200 nm. Also, the nanoparticles in bacterial networks could be a source or a sink of nanoparticles in seawater (i.e. whether nanoparticles were produced by bacteria and released into seawater or whether bacterial networks captured nanoparticles from seawater). Phage adsorption to their host, or phage release from the host, could also create scenarios of the type we observed.

While we need to have independent criteria to identify viruses, AFM provides a tool for exploring the spatial context for phage as well as nanoparticles production by bacteria. For instance in Fig. 3b, the particles that seem emanating from the top of the heterotrophic bacterium are in the range of 70-230 nm and they could be viruses since

they are within the range of marine viruses. Nevertheless, a hypothesis relevant to bacteria-organic-matter interactions is that bacterial networks are a strategy for organic matter acquisition. A prediction from this hypothesis is that the network matrix is permeated with bound or free hydrolases for organic matter processing to assist tightly coupled trans-membrane transport. The functions of bacterial networks may also be to regulate diffusion, local viscosity and pH of the microenvironments to enable bacteria-bacteria quorum sensing and other metabolic and regulative activities.

Bacterial networks may act as suspended biofilms; indeed, one might speculate that traditional biofilms are an extensive expression of networks that bacteria form when they encounter and interact with a surface in the pelagic ocean. Such interactions would most commonly be with nanogels and bacteria. Finally, the networks' fibrils might include nanowires (Reguera et al. 2005, Gorby et al. 2006). This should be testable by conductive AFM. The width of the fibrils was 10-120 nm generally smaller than the reported range for nanowires, 50-150 nm (but the two ranges overlap).

Coccoliths in bacterial networks? Interestingly, our AFM images frequently showed coccoliths (314 nm- 1.67μm; possibly derived from the family *Rhabdosphaeraceae* and the family *Noelaerhabdaceae*) as well as protist scales probably derived from the genus *Paraphysomonas* seemingly trapped in bacterial networks (Fig. 3d,e). They might have an affinity for bacterial networks (Fig. 2c) since we rarely saw them free (however, it was not practical to make a quantitative comparison of attached and free coccoliths by AFM imaging the required large number of random fields at high resolution). Coccoliths were also seen in larger aggregates that formed during a

microcosm phytoplankton bloom (not shown). Coccolith capture into bacterial networks would cause "ballast effect" (Ziveri et al. 2007, Iglesias-Rodriguez et al. 2008) due to high specific density (2.7 g cm^{-3}) of their calcite. Ballast materials e.g. opal, calcite and terrestrial dust are often seen in marine snow and they are important in accelerating export flux (Ploug et al. 2008).

Our observations suggest the hypothesis that because of their high abundance, large surface area and potential for aggregation bacterial networks efficiently scavenge ballast particles and serve as conduit for ballast acquisition by marine snow. Bacterial metabolism could modify network microenvironment (e.g. pH; also affected by ocean acidification) thus affecting coccolith dissolution. If ballast capture by bacterial networks is confirmed as a quantitatively significant process and found to occur widely in the ocean it could be a variable in particle rain rate and carbon export.

CONCLUSION

Spatially intimate ecological relationships, whether positive or negative, as well as bacteria-bacteria networks were common among pelagic bacteria previously considered by epifluorescence microscopy to be dominated by "solitary" free-living bacteria. This microspatial organization is a fundamentally new view of the environmental context in which pelagic bacteria act as a major biogeochemical force in the ocean. The discovery of abundant bacteria-bacteria and bacteria-*Synechococcus* symbioses opens up exciting research avenues on phylogenetic specificities, biochemical and molecular bases, adaptive significance, and biogeochemical influences of the symbioses. Future studies on biogeochemical activity and adaptive biology (González et

al. 2008) of pelagic bacteria need to deviate from the classical dichotomy of particle-attached and free-living lifestyles and towards a unifying microspatial framework of genetically diverse assemblages dynamically interacting with organisms (most are microbes) and the organic matter continuum. Climate change and ocean acidification could alter the microspatial architecture and bacterial interactions, with feedback to ocean carbon cycle. Predicting the outcomes requires a convergence of biochemical and genomic approaches with fundamental insights that can further be gained by the study of microbial biogeochemistry as a microspatial structural problem.

Acknowledgments. We thank Ty Samo, Maura Manganelli, Jessica Ward, Eddie Kisfaludy and Chris Dupont for kindly providing the offshore samples: BWZ II cruise 2006 in Antarctica, CCE LTER Process Cruise 2007, EK 2008 and Socerer II 2008. We thank John McGowan for advice and insight on the coherence between SIO Pier and CCE biogeochemistry. We thank Asylum Research folks for their help and support with AFM. Chlorophyll and temperature data were retrieved from SCCOOS data archive website (www.sccoos.org) supported by NOAA, from CCE LTER data archive website (http://oceaningormatics.ucsd.edu/datazoo/data) supported by the Division of Ocean Sciences, NSF Grant OCE-0417616 and from BWZ II website supported by NSF Grant ANT- 0444134 to F.A. We thank Brian Palenik, Bianca Brahamsha and Stuart Sandin for their valuable comments and suggestions. The work was supported by grants from Gordon and Betty Moore Foundations and NSF to F.A.

Literature cited

Abu-Lail NI, Camesano TA (2002) Elasticity of Pseudomonas putida KT2442 Surface Polymers Probed with Single-Molecule Force Microscopy. Langmuir 18:4071-4081

Amro NA, Kotra LP, Wadu-Mesthrige K, Bulychev A, Mobashery S, Liu Gy (2000) High-Resolution Atomic Force Microscopy Studies of the Escherichia coli Outer Membrane: Structural Basis for Permeability. Langmuir 16:2789-2796

Azam F (1998) OCEANOGRAPHY: Microbial Control of Oceanic Carbon Flux: The Plot Thickens. Science 280:694-696

Azam F, Hodson RE (1977) Size distribution and activity of marine microheterotrophs. Limnology and Oceanography 22:492-501

Azam F, Malfatti F (2007) Microbial structuring of marine ecosystems. Nat Rev Micro 5:782-791

Azam F, Smith DC, Steward GF, Hagström Å (1994) Bacteria-organic matter coupling and its significance for oceanic carbon cycling. Microbial Ecology 28:167-179

Balnois E, Wilkinson KJ (2002) Sample preparation techniques for the observation of environmental biopolymers by atomic force microscopy. Colloids and surfaces. A, Physicochemical and engineering aspects 207:229-242

Beveridge TJ, Graham LL (1991) Surface layers of bacteria. Microbiol. Mol. Biol. Rev. 55:684-705

Binning G, Quate CF (1986) Atomic force microscopy. Physical Review Letters 56:930-933

Boetius A, Ravenschlag K, Schubert CJ, Rickert D, Widdel F, Gieseke A, Amann R, Jorgensen BB, Witte U, Pfannkuche O (2000) A marine microbial consortium apparently mediating anaerobic oxidation of methane. Nature 407:623-626

Brahamsha B (1996) An abundant cell-surface polypeptide is required for swimming by the nonflagellated marine cyanobacterium Synechococcus. Proceedings of the National Academy of Sciences of the United States of America 93:6504-6509

Chin W-C, Orellana MV, Quesada I, Verdugo P (2004) Secretion in Unicellular Marine Phytoplankton: Demonstration of Regulated Exocytosis in Phaeocystis globosa. Plant Cell Physiol. 45:535-542

Chin WC, Orellana MV, Verdugo P (1998) Spontaneous assembly of marine dissolved organic matter into polymer gels. Nature 391:568-572

Costerton JW, Irvin RT, Cheng KJ (1981) The Bacterial Glycocalyx in Nature and Disease. Annual Review of Microbiology 35:299-324

De Momi A, Lead JR (2008) Behaviour of environmental aquatic nanocolloids when separated by split-flow thin-cell fractionation (SPLITT). Science of total environment 405:317-323

del Giorgio PA, Williams PJlB (2005) The global significance of respiration in aquatic ecosystems: From single cells to the biosphere. In: del Giorgio PA, Williams, P.J.l.B. (ed) Respiration in Aquatic Ecosystems. Oxford University Press, p 2667-2273

Ding Y-X, Chin W-C, Rodriguez A, Hung C-C, Santschi PH, Verdugo P (2008) Amphiphilic exopolymers from Sagittula stellata induce DOM self-assembly and formation of marine microgels. Marine Chemistry 112:11-19

Dubrovin EV, Voloshin AG, Kraevsky SV, Ignatyuk TE, Abramchuk SS, Yaminsky IV, Ignatov SG (2008) Atomic Force Microscopy Investigation of Phage Infection of Bacteria. Langmuir 24:13068-13074

Ducklow HW (2002) Bacteria production and biomass in the oceans. In: Kirchman DL (ed) Microbial Ecology of the Oceans. Wiley-Liss, p 85-120

Dufrene YF (2002) Atomic force microscopy, a powerful tool in microbiology. J. Bacteriol. 184:5205-5213

Dufrene YF (2004) Using nanotechniques to explore microbial surfaces. Nat Rev Micro 2:451-460

Dufrene YF (2008a) Atomic force microscopy and chemical force microscopy of microbial cells. Nat. Protocols 3:1132-1138

Dufrene YF (2008b) Towards nanomicrobiology using atomic force microscopy. Nat Rev Micro 6:674-680

Dupres V, Menozzi FD, Locht C, Clare BH, Abbott NL, Cuenot S, Bompard C, Raze D, Dufrene YF (2005) Nanoscale mapping and functional analysis of individual adhesins on living bacteria. Nat Meth 2:515-520

Engel A, Thoms S, Riebesell U, Rochelle-Newall E, Zondervan I (2004) Polysaccharide aggregation as a potential sink of marine dissolved organic carbon. Nature 428:929-932

Fuhrman JA, Azam F (1980) Bacterioplankton Secondary Production Estimates for Coastal Waters of British Columbia, Antarctica and California. Appl. Environ. Microbiol. 39:1085-1095

Fuhrman JA, Azam F (1982) Thymidine incorporation as a measure of heterotrophic bacterioplankton production in marine surface waters: evaluation and fiels results. Mar. Biol. 66:109-120

Fuhrman JA, Steele JA (2008) Community structure of marine bacterioplankton: patterns, networks, and relationships to function. Aquat. Microb. Ecol. 53:69-81

González JM, Fernández-Gómez B, Fernández-Guerra A, Gómez-Consarnau L, Sanchez O, Coll-Lladó M, del Campo J, Escudero L, Rodríguez-Martínez R, Alonso-Sáez L, Latasa M, Paulsen I, Nedashkovskaya O, Lekunberri I, Pinhassi J, Pedrós-Alió C (2008) Genome analysis of the proteorhodopsin-containing marine bacterium Polaribacter sp. MED152 (Flavobacteria). Proceedings of the National Academy of Sciences 105:8724-8729

Gorby YA, Yanina S, McLean JS, Rosso KM, Moyles D, Dohnalkova A, Beveridge TJ, Chang IS, Kim BH, Kim KS, Culley DE, Reed SB, Romine MF, Saffarini DA, Hill EA, Shi L, Elias DA, Kennedy DW, Pinchuk G, Watanabe K, Ishii SÄ, Logan B, Nealson KH, Fredrickson JK (2006) Electrically conductive bacterial nanowires produced by Shewanella oneidensis strain MR-1 and other microorganisms. Proceedings of the National Academy of Sciences 103:11358-11363

Gueven O, Alacakir A, Tan E (1997) An atomic force microscopic study of the surfaces of polyethylene and polycarbonate films irradiated with gamma rays. Radiation Physics and Chemistry 50:165-170

Gustavson KH (1956) The Chemistry of Tanning Processes., Vol. Academi Press, New York

Heissenberger A, Leppard G, Herndl G (1996) Ultrastructure of marine snow. II. Microbiological considerations. Mar Ecol Prog Ser 135:299-308

Hewes CD, Holm-Hansen O (1983) A method for recovering nanoplankton from filters for identification with the microscope: the filter-transfer-freeze (FTF) techinique. Limnology and Oceanography 28:389-394

Hey-Jin K (2008) Climate impacts on the planktonic marine ecosystem in the Southern California current. UCSD

Holm-Hansen O, Riemann B (1978) Chlorophyll a Determination: Improvements in Methodology. Oikos 30:438-447

Huber H, Hohn MJ, Rachel R, Fuchs T, Wimmer VC, Stetter KO (2002) A new phylum of Archaea represented by a nanosized hyperthermophilic symbiont. Nature 417:63-67

Iglesias-Rodriguez MD, Halloran PR, Rickaby REM, Hall IR, Colmenero-Hidalgo E, Gittins JR, Green DRH, Tyrrell T, Gibbs SJ, von Dassow P, Rehm E, Armbrust EV, Boessenkool KP (2008) Phytoplankton Calcification in a High-CO2 World. Science 320:336-340

Johnson PW, Sieburth JM (1979) Chroococcoid cyanobacteria in the sea: a ubiquitous and diverse phototrophic biomass. Limnology and Oceanography 24:928-935

Johnson PW, Sieburth JM (1982) In-situ morphology and occurrence of eucaryotic phototrophs of bacterial size in the picoplankton of estuarine and oceanic waters. Journal of Phycology 18:318-327

Karl D, Letelier R, Tupas L, Dore J, Christian J, Hebel D (1997) The role of nitrogen fixation in biogeochemical cycling in the subtropical North Pacific Ocean. Nature 388:533-538

Kerner M, Hohenberg H, Ertl S, Reckermann M, Spitzy A (2003) Self-organization of dissolved organic matter to micelle-like microparticles in river water. Nature 422:150-154

Koike I, Hara S, Terauchi K, Kogure K (1990) The role of submicron particles in the ocean. Nature 345:242-244

Leppard G, Heissenberger A, Herndl G (1996) Ultrastructure of marine snow. I. Transmission electron microscopy methodology. Mar Ecol Prog Ser 135:289-298

Leppard GG, West MM, Flannigan DT, Carson J, Lott NAJ (1997) A classification scheme for marine organic colloids in the Adriatic Sea: colloid speciation by transmission electron microscopy. Can. J. Fish. Aquat. Sci. 54:2334–2349

Lienemann C-P, Heissenberger A, Leppard GG, Perret D (1998) Optimal preparation of water samples for the examination of colloidal material by transmission electron microscopy. Aquat Microb Ecol 14:205-213

Mangold S, Harneit K, Rohwerder T, Claus G, Sand W (2008) Novel Combination of Atomic Force Microscopy and Epifluorescence Microscopy for Visualization of Leaching Bacteria on Pyrite. Appl. Environ. Microbiol. 74:410-415

Martinez J, Smith D, Steward G, Azam F (1996) Variability in ectohydrolytic enzyme activities of pelagic marine bacteria and its significance for substrate processing in the sea. Aquat Microb Ecol 10:223-330

McCarren J, Heuser J, Roth R, Yamada N, Martone M, Brahamsha B (2005) Inactivation of swmA Results in the Loss of an Outer Cell Layer in a Swimming Synechococcus Strain. J. Bacteriol. 187:224-230

McGowan JA, Cayan DR, Dorman LM (1998) Climate-Ocean Variability and Ecosystem Response in the Northeast Pacific. Science 281:210-217

Montoya JP, Holl CM, Zehr JP, Hansen A, Villareal TA, Capone DG (2004) High rates of N2 fixation by unicellular diazotrophs in the oligotrophic Pacific Ocean. Nature 430:1027-1032

Moran MA, Belas R, Schell MA, Gonzalez JM, Sun F, Sun S, Binder BJ, Edmonds J, Ye W, Orcutt B, Howard EC, Meile C, Palefsky W, Goesmann A, Ren Q, Paulsen I, Ulrich LE, Thompson LS, Saunders E, Buchan A (2007) Ecological Genomics of Marine Roseobacters. Appl. Environ. Microbiol. 73:4559-4569

Morris JJ, Kirkegaard R, Szul MJ, Johnson ZI, Zinser ER (2008) Robust growth of Prochlorococcus colonies and dilute liquid cultures: facilitation by "helper" heterotrophic bacteria. Appl. Environ. Microbiol.:AEM.02479-02407

Nagata T (2008) Organic matter-bacteria interactions in seawater. In: Kirchman DL (ed) Microbial Ecology of the Oceans. Wiley-Blackwell, p 207-241

Namba Y, Yu J, Bennett JM, K Y (2000) Modeling and measurements of atomic surface roughness Applied Optice 39:2705-2718

Nie CL, Yan Wei Y, Chen X, Liu YY, Dui W, Liu Y, Davies MC, Tendler SJB, He RG (2007) Formaldehyde at Low Concentration Induces Protein Tau into Globular Amyloid-Like Aggregates In Vitro and In Vivo. Plos ONE July:13

Nishino T, Ikemoto E, Kazuhiro K (2004) Application of atomic force microscopy to observation of marine bacteria. Journal of Oceanography 60:219-225

Palenik B, Ren Q, Dupont CL, Myers GS, Heidelberg JF, Badger JH, Madupu R, Nelson WC, Brinkac LM, Dodson RJ, Durkin AS, Daugherty SC, Sullivan SA, Khouri H, Mohamoud Y, Halpin R, Paulsen IT (2006) Genome sequence of Synechococcus

CC9311: Insights into adaptation to a coastal environment. Proceedings of the National Academy of Sciences 103:13555-13559

Pernthaler A, Dekas AE, Brown CT, Goffredi SK, Embaye T, Orphan VJ (2008) Diverse syntrophic partnerships from deep-sea methane vents revealed by direct cell capture and metagenomics. Proceedings of the National Academy of Sciences 105:7052-7057

Ploug H, Iversen M, Koski M, Buitenhuis E (2008) Production, oxygen respiration rates, and sinking velocity of copepod fecal pellets: Direct measurements of ballasting by opal and calcite. Limnology and Oceanography 53:469-476

Pomeroy LR, Williams PJL, Azam F, Hobbie JE (2007) The microbial loop. . Oceanography 20:28-33

Reguera G, McCarthy KD, Mehta T, Nicoll JS, Tuominen MT, Lovley DR (2005) Extracellular electron transfer via microbial nanowires. Nature 435:1098-1101

Ritter C, Heyde M, Schwarz UD, Rademann K (2002) Controlled Translational Manipulation of Small Latex Spheres by Dynamic Force Microscopy. Langmuir 18:7798-7803

Ruan Q, Steele JA, Schwalbach MS, Fuhrman JA, Sun F (2006) A Dynamic Programming Algorithm for Binning Microbial Community Profiles. Bioinformatics 22:1508-1514

Rusch DB, Halpern AL, Sutton G, Heidelberg KB, Williamson S, Yooseph S, Wu D, Eisen JA, Hoffman JM, Remington K, Beeson K, Tran B, Smith H, Baden-Tillson H, Stewart C, Thorpe J, Freeman J, Andrews-Pfannkoch C, Venter JE, Li K, Kravitz S, Heidelberg JF, Utterback T, Rogers Y-H, Falc, n LI, Souza V, Bonilla-Rosso G, Eguiarte LE, Karl DM, Sathyendranath S, Platt T, Bermingham E, Gallardo V, Tamayo-Castillo G, Ferrari MR, Strausberg RL, Nealson K, Friedman R, Frazier M, Venter JC (2007) The Sorcerer II Global Ocean Sampling Expedition: Northwest Atlantic through Eastern Tropical Pacific. PLoS Biology 5:e77

Santschi PH, Balnois E, Wilkinson KJ, Zhang J, Buffle J, Guo L (1998) Fibrillar Polysaccharides in Marine Macromolecular Organic Matter as Imaged by Atomic Force Microscopy and Transmission Electron Microscopy. Limnology and Oceanography 43:896-908

Seo Y, Eiko I, Akihiro Y, Kazuhiro K (2007) Particle capture by marine bacteria. Aquat Microb Ecol 49:243-253

Sieburth JM (1975) Microbial seascape. A pictorial essay on marine microorganisms and their environments., Vol. University Park Press, Baltimore

Sieburth JM (1979) Sea Microbes, Vol. Oxford University Press, New York

Stukalov O, Korenevsky A, Beveridge TJ, Dutcher JR (2008) Use of Atomic Force Microscopy and Transmission Electron Microscopy for Correlative Studies of Bacterial Capsules. Appl. Environ. Microbiol. 74:5457-5465

Svetlicic V, Zutic V, Hozic Zimmermann A (2005) Biophysical Scenario of Giant Gel Formation in the Northern Adriatic Sea. Annals of the New York Academy of Sciences 1048:524-527

Thompson JR, Pacocha S, Pharino C, Klepac-Ceraj V, Hunt DE, Benoit J, Sarma-Rupavtarm R, Distel DL, Polz MF (2005) Genotypic Diversity Within a Natural Coastal Bacterioplankton Population. Science 307:1311-1313

Vadillo-Rodriguez V, Beveridge TJ, Dutcher JR (2008) Surface Viscoelasticity of Individual Gram-Negative Bacterial Cells Measured Using Atomic Force Microscopy. J. Bacteriol. 190:4225-4232

Vadillo-Rodriguez V, Busscher HJ, Norde W, de Vries J, Dijkstra RJB, Stokroos I, van der Mei HC (2004) Comparison of atomic force microscopy interaction forces between bacteria and silicon nitride substrata for three commonly used immobilization methods. Appl. Environ. Microbiol. 70:5441-5446

Venter JC, Remington K, Heidelberg JF, Halpern AL, Rusch D, Eisen JA, Wu D, Paulsen I, Nelson KE, Nelson W, Fouts DE, Levy S, Knap AH, Lomas MW, Nealson K, White O, Peterson J, Hoffman J, Parsons R, Baden-Tillson H, Pfannkoch C, Rogers Y-H, Smith HO (2004) Environmental Genome Shotgun Sequencing of the Sargasso Sea. Science 304:66-74

Verdugo P, Alldredge AL, Azam F, Kirchman DL, Passow U, Santschi PH (2004) The oceanic gel phase: a bridge in the DOM-POM continuum. Marine Chemistry 92:67-85

Williams PJlB (2005) Chapter 3. In: Kaiser D, Attrill, M., Jennings, S., Thomas D. N., Williams, P.J. le B. (ed) Microbial production and the decomposition of organic material. Oxford Univ. Press

Wong C, West P, Olson K, Mecartney M, Starostina N (2007) Tip dilation and AFM capabilities in the characterization of nanoparticles. JOM Journal of the Minerals, Metals and Materials Society 59:12-16

Zehr JP, Bench SR, Carter BJ, Hewson I, Niazi F, Shi T, Tripp HJ, Affourtit JP (2008) Globally Distributed Uncultivated Oceanic N2-Fixing Cyanobacteria Lack Oxygenic Photosystem II. Science 322:1110-1112

Ziveri P, de Bernardi B, Baumann K-H, Stoll HM, Mortyn PG (2007) Sinking of coccolith carbonate and potential contribution to organic carbon ballasting in the deep ocean. Deep Sea Research Part II: Topical Studies in Oceanography 54:659-675

Figure 5.1. **AFM topographic images of bacteria and *Synechococcus* cell surface architecture.** Seawater samples were collected from costal site, at the SIO station, in May and July 2008 (details in Table 1). Increase in height, Z, is indicated by warmer colors. **a)** A *coccus* with a diameter of 307 nm and the height of 54 nm, surrounded symmetrically by extensive pili 0.8-1 μm in length; **b)** A *coccus* (Z=203 nm) with extensive capsule and gel matrix with height range of 1-4 nm; **c)** A *Synechococcus* cell (Z=259 nm) with elaborate architecture and tightly knit fibrils in the range of 480-800 700 nm in length; **d)** A *Synechococcus* cell (Z=732 nm) with intricate asymmetrical architecture 14.5 μm long, on the upper end. (The architecture extends beyond the picture frame; shown partially). Cell height is purposely flattened, with loss of detail, to highlight the architecture that has a height range of 200-400 pm. Nanometer size particle in the range of 50-300 nm are highly abundant and associated with fibrils.

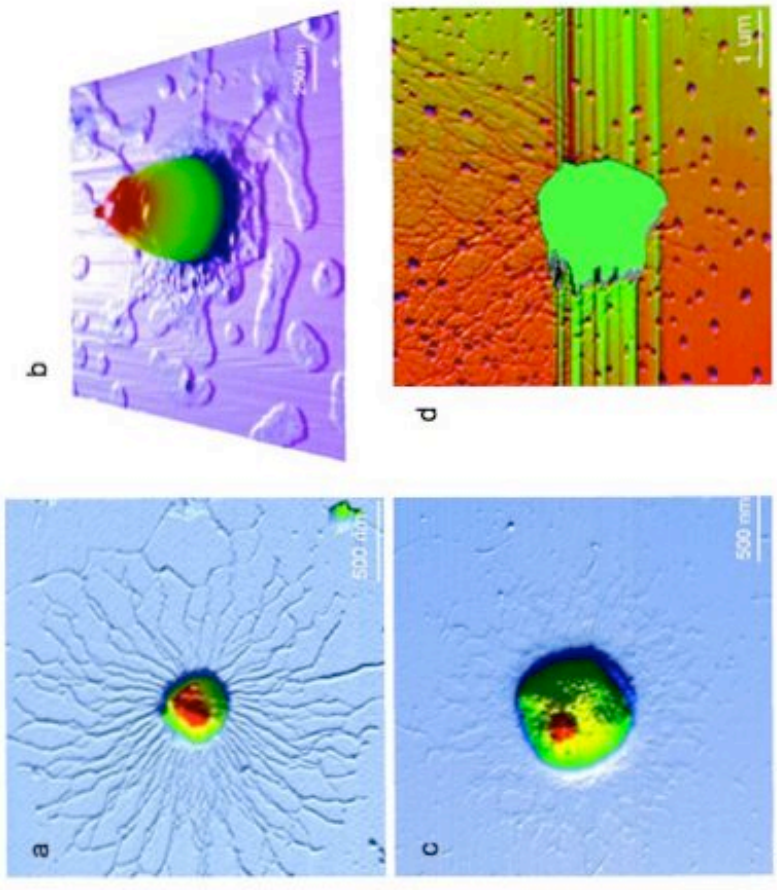

Figure 5.1

Figure 5.2. **AFM topographic images of conjoint bacteria and *Synechococcus*.** Seawater samples were collected from costal site, at the SIO, in May 2008 (details in Table 1). Increase in height, Z, is indicated by warmer colors. **a)** A *coccus* (Z=130 nm), and a larger rod (Z=144 nm) intimately conjoint. Nanometer size particles (green) in the range of 70-270 nm are present in the cell matrix; **b)** A conjoint pair of heterotrophic bacteria. Here, increase in height is indicated by cooler colors. The long s-shaped cell (Z=175 nm) embraces the tiny c-shaped cell (Z=122 nm). The conjoint pair is surrounded by gel architecture with nanometer size particles in the range of 30-230 nm. White arrow points to the c-shaped cell; **c)** A conjoint pair of rods. The upper cells is 194 nm tall, the lower cell is 179 nm tall. The cells are surrounded by a gel matrix. A coccolith, (D=1.12 μm) and nanometer size particles, in the range of 45-280nm, are present in the gel matrix; **d)** A *Synechococcus* cell conjoint with two diminutive bacteria, embedded in mucus layer. In the pictures there are 3 other heterotrophic bacteria not conjoint, two are in the upper part and one in the lower part of the picture. The *Synechococcus* cell has a diameter of 840 nm and an height of 374 nm; the left conjoint heterotrophic bacterium is 174 nm long, 143 nm wide and 42 nm tall; the right conjoint heterotrophic bacterium is 211 nm long, 133 nm wide and 43 nm tall; **e)** A *Synechococcus* cell (Z=712 nm) associated with a c-shaped cell (Z=115 nm), surrounded by numerous particles in the range of 50-200 nm. White arrow points to the c-shaped cell; **f)** A dividing *Synechococcus* cell (top cell) 427 nm tall is conjoint with a 1.2 μm-long and 119 nm tall heterotrophic bacterium. The conjoint pair is surrounded by a thin capsule and nanometer size particles in a range of 20-80 nm.

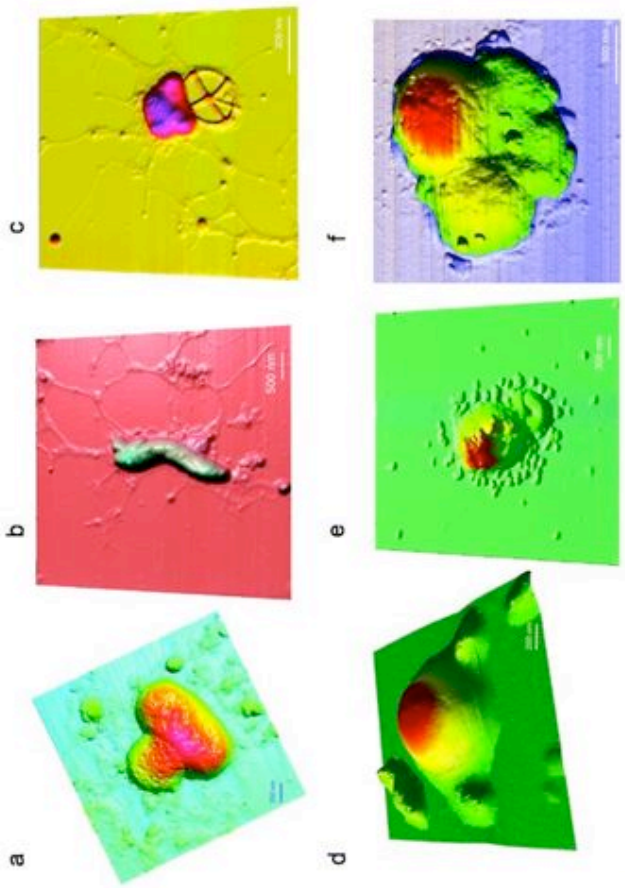

Figure 5.2

Figure 5.3. **AFM images of bacterial networks.** Seawater samples were collected from costal site, at the SIO station, in April and August 2008 and from off-shore site during the CCE cruise at 53 m at station 206 in April 2007 (details in Table1). Increase in height, Z, is indicated by warmer colors. **a)** An image with 2-cell network that covers an area of ~5x10 μm. The image has been acquired in the Amplitude channel that lacks height information. The network is characterized by extensive branching long fibrils not seen in this low-resolution image; **b)** Topographic close-up of the upper long rod cell in Fig. 3a. The cell is surrounded by extensive network fibrils. Nanometer size particles in the range of 70-230 nm seem to emanate from the cell. Cell's height is 140 nm; **c)** Topographic close-up of the lower rod cell in Fig. 3a. The cell is within the extensive network that connects it with the upper cell in Fig. 3b. Cell's height was 139 nm; **d)** Topographic image of two heterotrophic bacteria connected by an extensive network. The upper cell is 62 nm tall, the lower cell is 104 nm tall. The network occupies an area ~ 5x5 μm. A coccolith (D=589 nm; lower left) and nanometer size gel particles, in the range of 60-300 nm are present in the network; **e)** Topographic image of a 5-cell network. One large dividing cell (red, Z=200 nm) conjoint with a much smaller dividing cell (green, Z=92 nm; arrow #1). Also present in the network a tiny cell (lower right, Z=94 nm; arrow #2). The network covers an area of ~7x7 μm. Fibrils are departing from both the dividing pairs. A coccolith (D=1 μm) and a diatom fragment appeared within the network; **f)** Transmitted light micrograph of *Synechococcus* cells (circled) on mica from off-shore site (details in Table 1). The large pointed shadow is the cantilever that carries the probe at a 90° angle into the picture (therefore the probe is not visible here). Picture magnification is 400 x; **g)** Epifluorescence micrograph of two *Synechococcus* cells

(circled) from Fig. 3f. Under 480 nm excitation phycoerythrin autofluoresces, thus allows the visualization of the *Synechococcus* cells. Picture magnification is 400 x; **h)** Topographic image of the cells in Fig. 3f and 3g. The two *Synechococcus* cells are connected with fibrils (Z=1 nm) and are associated with 3 conjoint heterotrophic bacteria (arrow #1, #2, #3). The upper *Synechococcus* cell is 281 nm tall, the lower *Synechococcus* cell is 284 nm tall. From the top, the c-shaped heterotrophic bacterium is 85 nm tall (arrow #1), the *coccus*, conjoint with the upper *Synechococcus* cell, is 92 nm tall (arrow #2) and the *coccus* conjoint with the lower *Synechococcus* cell is 44 nm tall (arrow #3).

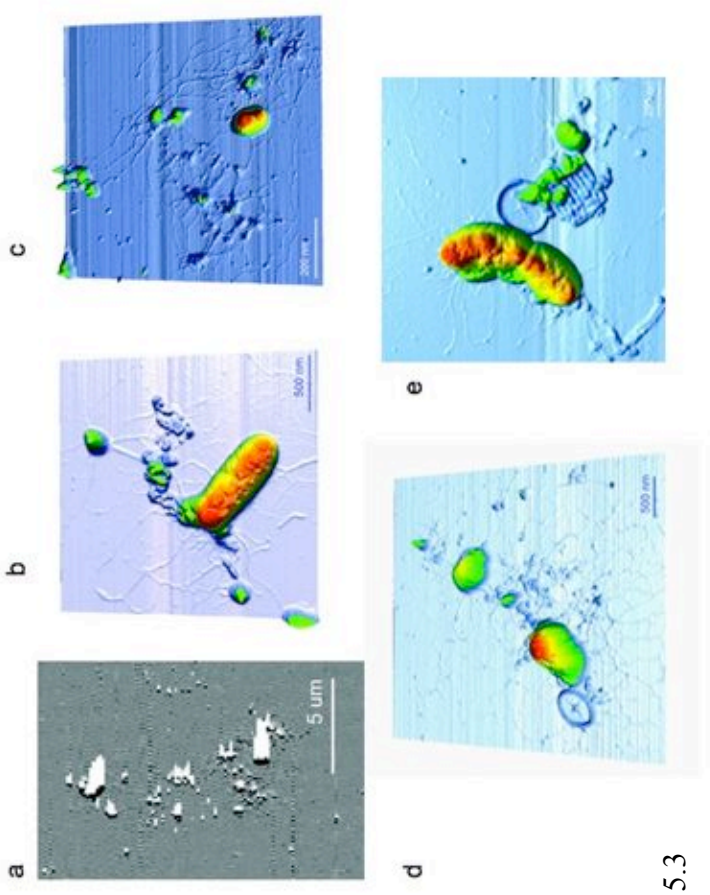

Figure 5.3

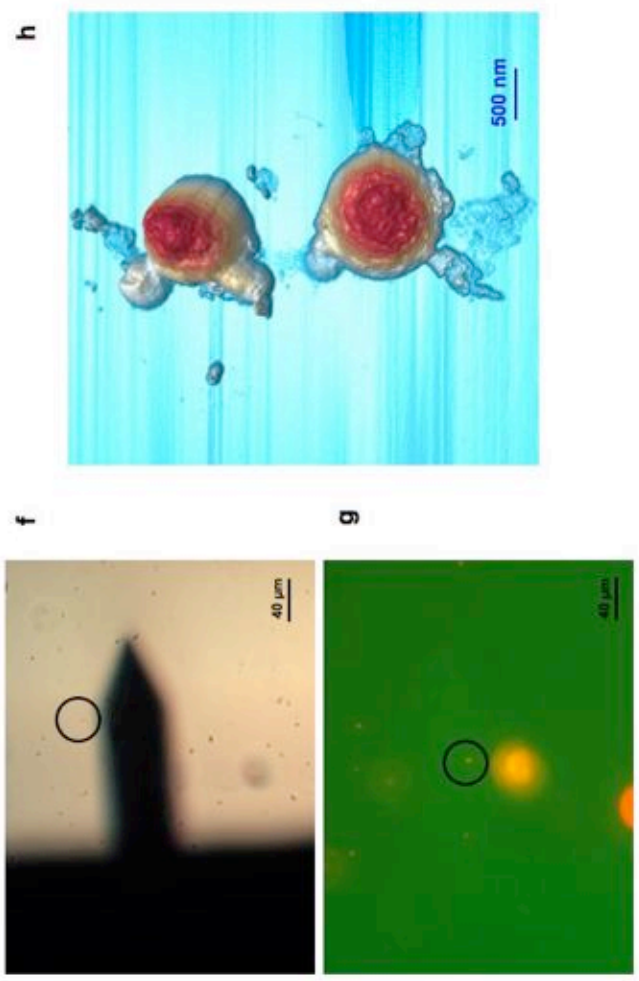

Figure 5.3 continued

Table 5.1. **Sampling sites.** The table shows sampling site location, site category, collection date and environmental variables.

Site	Station	Coordinate	Depth	Chl a	Temperature	Period	Number of samplings**
			m	$\mu g l^{-1}$	°C		
Coastal	SIO	32.867 N -117.257 W	1	0.38-14.7	10.4-24.4	Apr-Aug 08	16
	EK	32.523 N -117.165 W	1	-	18	15-May-08	1
	Sorcerer II	32.465 N -117.241 W	30	13	20	10-Sep-08	1
CCE	164	35.358 N -121.075 W	7	0.18	12.4	7-Apr-07	1
	206	33.659 N -123.133 W	15 (53)*	1.18	14.4	9-Apr-07	1
Antarctica	178	60.370 S -54.318 W	10	0.11	-0.96	21-Jul-06	1
	197	60.450 S -58.225 W	35	0.14	-0.66	25-Jul-06	1

**Synechococcus* sample was collected at 53 m
** Heterotrophic bacteria were samples at every station; *Synechococcus* cells were sampled 5 times at SIO coastal site and at CCE, off-shore site.

Table 5.2. **Summary table for heterotrophic bacteria and *Synechococcus* cells. a) Heterotrophic bacteria.** Cell abundance and percentages for bacteria presenting cell surface architecture, conjoint bacteria and bacteria in network for each site category are shown. **b) *Synechococcus* cells**. Cell abundance and percentages for bacteria presenting cell surface architecture, conjoint bacteria and bacteria in network for each site category are shown.

	Heterotrophic bacteria				
Site	Cell abundance	Number of	Surface architecture	Conjoint cells	Bacteria in networks
	10^9cell l^{-1}	cells imaged	% cells imaged	% cells imaged	% cells imaged
Coastal	0.22-3.14	321	85	21	26
Off-shore	1.22; 0.83	107	74	43	37
Antarctica	0.19; 0.11	24	29	38	0

Table 5.2a. **Heterotrophic bacteria.**

	Synechococcus cells				
Site	Cell abundance	Number of	Surface architecture	Conjoint cells	Bacteria in network
	10^8cell l^{-1}	cells imaged	% cells imaged	% cells imaged	% cells imaged
Coastal	0.13-1.15	85	65	42	55
Off-shore	0.13; 0.11	50	28	42	4

Table 5.2b. ***Synechococcus* cells.**

Chapter V has been submitted to Aquatic Microbial Ecology as: Malfatti, F. and Azam, F. - Atomic Force Microscopy reveals microscale networks and apparent symbioses among pelagic marine bacteria

VI

Conclusions

VI

Conclusions

Bacteria and Archaea dominate the ocean in abundance, diversity and metabolic activity. The hydrolysis and uptake of organic matter by microbes represent a major carbon-flow pathway. The variability and the strength of coupling between producers of organic matter and microbes, seen as consumers, can change the overall flux of carbon in the ocean. At the scale at which bacteria exert their "engineering" activities, the organic matter can be viewed as a continuum of size, constantly changing in space and time according to the sources of production and the microbial activity that causes dissolution or aggregation.

It is important to consider the dual nature of the research in marine microbial ecology and microbial oceanography. The nature of the problem is comparable to a photon that exhibits properties of both wave and particles. One must consider this dual nature in order to predict exactly the photon behavior. Marine microbial ecology and microbial oceanography should be addressed by merging the knowledge we gain from microbial processes at the microscale as well as from ocean system scale processes (Azam & Malfatti 2007). This dissertation has attempted to address the dual "scale" aspect of the carbon biogeochemical cycle bacteria mediated.

The results from the ocean basin scale study reported in this dissertation highlighted the active role of the microbial loop in the Southern Ocean, during two seasons in an area that is characterized by strong iron and chlorophyll gradients in the summer. We observed significant level of coupling in the summer between bacteria and phytoplankton productions, suggesting a dynamic microbial loop. In same area during the long austral winter, when primary production is negligible, the microbial loop was active and it was sustained by the excess of summer dissolved organic carbon produced. We observed that during the winter Bacteria and Archaea were the major producers of biogenic particles that fuel the microbial food web.

Parts of the Southern Ocean are High Nutrient Low Chlorophyll (HNLC) areas, mostly caused by the intermittent supply of iron that limits phytoplankton growth. Many perturbation experiments have been performed during the long summer in order to sequester carbon dioxide by increasing primary production upon iron stimulation followed by the downward flux of particles into the deep ocean (as reviewed in (Smetacek & Naqvi 2008)). Despite the fact that we cannot predict with absolute certainty what would be the net carbon dioxide sequestration and the response to the microbial loop; such perturbations could alter the natural coupling between the primary producers and bacteria in the summer with consequences for the system during the winter. Higher coupling values might preclude slow-to-degrade dissolved organic matter accumulation in the summer that is critical for fueling the microbial loop in the winter. Lower coupling values might allow dissolved organic matter to over accumulate and

potentially aggregate overtime forming an extensive mucilage layer as it happens in the Northern Adriatic Sea.

As future direction it would be rather important to understand the variation in the strength and degree of coupling between primary producers and bacteria and its signature on the dissolved organic matter pool in terms of percentage of more or less recalcitrant fraction during the perturbation experiment with the purpose of predicting the effect on the microbial compartment and on the carbon cycle in low primary productivity regimes such as the austral winter.

Our investigation at the nanometer to micrometer scale using Atomic Force Microscopy, let to the important discovery that pelagic bacteria and *Synechococcus* cells can for association among each other. This finding change how we think about the free-living and particle-attached life style of marine bacteria. Physically close association and organic matter mediated association, that here we called networks are important nanometer- micrometer hotspots in the pelagic ocean where tight coupling might be achieved by the synergic activities of the partners. We found bacteria-bacteria and bacteria-*Synechococcus* association in coastal, off-shore sites in the California Current System and in the winter Antarctic water. These putative symbioses possibly are widespread in any ocean province and trophic regime.

In the future we will identify the partners and will study the dynamic of the associations. For instance it would be interesting to explore whether *Archaea*,

Prochlorococcus and *Ostreococcus* occur in such symbioses. The dynamic of symbiosis might be variable according to the physiological state of the partners and the metabolic capability for instance day-night cycle and nitrogen fixation and dinitrification processes. The pair can be sorted by flowcytometer and by micromanipulation of the sample and the their 16SrRNA genes can be amplified using multidisplacement amplification technique (MDA, (Stepanauskas & Sieracki 2007, Lasken 2009)). On other technique, Fluorescence In Situ Hybridization (FISH) coupled with AFM visualization would allow to see and identify the partners in the organic matter network.

It is quite important to describe and quantify the fluxes of elements among the partners; high-resolution secondary ion mass spectrometry (nanoSIMS) would be a useful instrument to use coupled with stable isotopes incubation experiments ((Fike et al. 2008, Pernthaler et al. 2008)) to map at the nanoscale level the exchange of nutrients in the partneship.

Atomic Force Microscopy live imaging is a powerful tool that needs to be further develop in the future. Investigations on topography change at the small scale in real time of marine bacteria would be possible to perform. Perturbation experiments offer a useful approach to assess the effect of the changes on bacterial surface and volume when cells are exposed to high dissolved organic matter levels comparable to phytoplankton bloom and for instance the change in morphology during a phage attack. Genomic predictions from the sequenced bacterial isolates could be tested with the aim to assess gene

activation for hydrolytic enzyme production and uptake based on volume increase and surface changes.

The effect of phage attack could be monitored in SWAT3-SIO2 host-phage system. We predict that the infected cell will increase the volume just before lysing due to the presence of the phage progeny and autolysis process in the host cell to liberate the viruses and on the contrary we do not expect any volume change in the resistant cells during the infection process. Surface topography should vary over time in the infected cells becoming rougher over time, possibly due to the disassemblies of the outer and inner membrane.

Visualizing live cells from different ocean environments and trophic systems would allowed us compute a more realistic cell volume in order to correct the quantification of bacteria-mediated carbon fluxes and the strength and degree of coupling with primary productivity in the global ocean.

To conclude, it urges the need to integrate across scale bacterial action on organic matter continuum in order to have a quantitative and mechanics view of the biogeochemical cycle of carbon in the ocean.

Literature cited

Azam F, Malfatti F (2007) Microbial structuring of marine ecosystems. Nat Rev Micro 5:782-791

Fike DA, Gammon CL, Ziebis W, Orphan VJ (2008) Micron-scale mapping of sulfur cycling across the oxycline of a cyanobacterial mat: a paired nanoSIMS and CARD-FISH approach. ISME J 2:749-759

Lasken RS (2009) Genomic DNA amplification by the multiple displacement amplification (MDA) method. Biochemical Society Transactions 037:450-453

Pernthaler A, Dekas AE, Brown CT, Goffredi SK, Embaye T, Orphan VJ (2008) Diverse syntrophic partnerships from deep-sea methane vents revealed by direct cell capture and metagenomics. Proceedings of the National Academy of Sciences 105:7052-7057

Smetacek V, Naqvi SWA (2008) The next generation of iron fertilization experiments in the Southern Ocean. Philosophical Transactions of the Royal Society A: Mathematical, Physical and Engineering Sciences 366:3947-3967

Stepanauskas R, Sieracki ME (2007) Matching phylogeny and metabolism in the uncultured marine bacteria, one cell at a time. Proceedings of the National Academy of Sciences 104:9052-9057